Novel Aspects of Insulin Signaling underlying Growth and Development in *Drosophila melanogaster*

Dissertation

zur Erlangung des akademischen Grades

Doctor Rerum Naturalium
(Dr. rer. nat.)

vorgelegt
der Fakultät Mathematik und Naturwissenschaften
der Technischen Universität Dresden
von

SUHRID SUNDAR GHOSH
geboren am 14. März 1991 in Kalkutta, Indien

Eingereicht Juni 2020
Die Dissertation wurde in der Zeit von Januar 2016 bis Juni 2020
im **Max-Planck-Institut für molekulare Zellbiologie und Genetik**
angefertigt.

1.Gutachter: Prof. Dr. Christian Dahmann, TU Dresden

2.Gutachter: Dr. Pierre Leopold, Institut Curie

asato mā sadgamaya,	*Lead us from unreal to the real,*
tamaso mā jyotirgamaya,	*Lead us from darkness unto light,*
mṛtyor mā'mṛtaṃ gamaya	*Lead us from death to immortality.*

- Brihadaranyaka Upanishads (1.3.28)

For ***Suzanne...***

And

To ***Ma*** *and* ***Baba.***

Declaration according to §5.5 of the doctorate regulations

I herewith declare that I have produced this paper without the prohibited assistance of third parties and without making use of aids other than those specified; notions taken over directly or indirectly from other sources have been identified as such. This paper has not previously been presented in identical or similar form to any other German or foreign examination board.
The thesis work was conducted from **07.01.2016** to **01.06.2020** under the supervision of **Late Prof. Dr. Suzanne Eaton** at **Max Planck Institute of Molecular Cell Biology and Genetics**, Dresden.
I declare that I have not undertaken any previous unsuccessful doctorate proceedings.
I declare that I recognize the doctorate regulations of the Fakultät für Mathematik und Naturwissenschaften of the Technische Universität Dresden.

Erklärung entsprechend §5.5 der Promotionsordnung

Hiermit versichere ich, dass ich die vorliegende Arbeit ohne unzulässige Hilfe Dritter und ohne Benutzung anderer als der angegebenen Hilfsmittel angefertigt habe; die aus fremden Quellen direkt oder indirekt übernommenen Gedanken sind als solche kenntlich gemacht. Die Arbeit wurde bisher weder im Inland noch im Ausland in gleicher oder ähnlicher Form einer anderen Prüfungsbehörde vorgelegt.
Die Dissertation wurde im Zeitraum vom **07.01.2016** bis **01.06.2020** verfasst und von **Prof. Dr. Suzanne Eaton (verstorben)** am **Max-Planck-Institut für molekulare Zellbiologie und Genetik**, Dresden, betreut.
Meine Person betreffend erkläre ich hiermit, dass keine früheren erfolglosen Promotionsverfahren stattgefunden haben.
Ich erkenne die Promotionsordnung der Fakultät für Mathematik und Naturwissenschaften, Technische Universität Dresden an.

Dresden, 01. Juni 2020

Suhrid Sundar Ghosh

Table of contents

Figure Index

Acknowledgements

I am eternally grateful to Suzanne for believing in me. Her enthusiasm and generosity made me look up during difficult times. Even in Suzanne's absence, her indomitable spirit continues to inspire me and will continue to do so all my life.

I am thankful to Dr. Pierre Leopold for readily agreeing to supervise me after Suzanne's passing. I would also like to thank our lab alumna, Dr. Valentina Greco for motivating me, especially during those tough few months. I express my gratitude to Prof. Christian Dahmann for taking up the official responsibilities of supervision.

I thank Dr. Natalie Dye for being my scientific confidante and leading our group. My thesis committee members Dr. Teymuras Kurzchalia and Dr. Ünal Coskun, and Dr. Jochen Rink were extremely helpful through their suggestions and criticisms on my thesis work.

All the facilities at the MPI-CBG, especially the light microscopy and the electron microscopy facility, have always been forthcoming with assistance.

The hardships of scientific research have been manageable, thanks to my comrades in arms – Alex, Ivona, Shady, Ali, Coleman, Shamba, Akansha, Nico, Michal, Pepe, Persephone and Byung-Ho.

My great lab members, past and present- Franz, Ioannis, Steffi, Tomek, Vanessa, Sonja, Romina, Salma, Jana, Venky, Abhijeet, Allison, Anika and Paula. Also, our amazing fly-keepers- Sven and Conny.

I am indebted to Devika, for being there. I am grateful for the continuous support of my parents, Nitai and Meera, my brother, Sumit and my sister-in-law, Devika and their two little ones- Nina and Masha. My love for my late grandmother Bhaloma, who left this world as I was writing this thesis.

Abbreviations

AEL – After egg laying
AKH – Adipo-kinetic hormone
AKHR - Adipo-kinetic hormone receptor
AKT – AK thymoma/ Protein kinase B
AMP – Adenosine monophosphate
ANF – Atrial natriuretic factor
ANOVA – Analysis of variance
BBB – Blood-brain barrier
BSA – Bovine serum albumin
CA – Corpora allata
CBG – Molecular cell biology and genetics
CC - Corpora cardiaca
CCK – Cholecystokinin
CD8 – Cluster of differentiation 8
CLEM – Correlative light and electron microscopy
CME – Clathrin-mediated endocytosis
CNS – Central nervous system
d (prefix) - *Drosophila*
DAPI - 4,6-diamidino-2-phenylindole
DCV – Dense-core vesicles
DILP – *Drosophila* Insulin-like peptide
DN – Dominant negative
DSHB – Developmental studies hybridoma bank
EM – Electron microscopy
FBS – Fetal bovine serum
FOXO - Forkhead box factor O
GDM – Gestational diabetes mellitus
GFP – Green fluorescent protein
GPCR – G-protein coupled receptor
HEK – Human embryonic kidney
HGH – Human growth hormone
HRP – Horse radish peroxidase

IF – Immuno-fluorescence
IGF – Insulin-like growth factor
IIS – Insulin/insulin-like signaling
IPC – Insulin-producing cells
InR – Insulin receptor
IRS – Insulin receptor substrate
m (prefix) - mammalian
MPI – Max Planck Institute
NGS – Normal goat serum
PAGE – Polyacrylamide gel electrophoresis
PBS – Phosphate-buffered saline
PBST - Phosphate-buffered saline with Triton-X100/Tween20
PF – Plant-lipid food
PFA - Paraformaldehyde
PG – Prothoracic gland
PI - Phosphoinositide
PTEN – Phosphatase and tensin homolog
PTTH – Prothoracicotropic hormone
RG – Ring gland
RIPA – Radioimmunoprecipitation assay
RTK – Receptor tyrosine kinase
SDS – Sodium dodecyl sulphate
TOR – Target of rapamycin
WB – Western blot
WT – Wild type
YF – Yeast lipid food

Summary

Complexity in multi-cellular life arises from the ability of tissues to communicate with each other; tissue cross-talk during development coordinates growth and ultimately gives rise to organs with appropriate form and function. *Drosophila* larvae use systemic signaling mediated by endocrine factors and hormones to successfully grow and transition through developmental stages.

Larvae sense nutrition primarily through the secretion of *Drosophila* insulin-like peptides (DILPs) 2 and 5 produced in the larval brain. Secreted DILPs bind to receptors in target tissues and activate the insulin/insulin-like signaling (IIS) pathway, which in imaginal tissues like the wing disc regulate adult wing size and cell number. The IIS pathway also directly regulates timing of developmental transitions through the production of the molting hormone ecdysone. Upon nutritional deprivation, growth is repressed but larvae manage to transition to pupal stages. This robust physiological adaptation allows *Drosophila* to successfully develop when grown on inadequate nutrient sources. However, the role of IIS in development under starvation is not clearly understood. In the first part of the thesis, I show that DILPs 2 and 5 are taken up in the corpora cardiaca (CC). No protein apart from the *Drosophila* insulin receptor (dInR) has been previously implicated in cellular uptake of DILPs in any tissue. I demonstrate that DILPs bind to non-canonical insulin-binding protein IMPL2 and are endocytosed in a clathrin-dependent manner. The CC produce adipo-kinetic hormone (AKH), a functional analog of glucagon. I show that up-taken DILPs are co-packaged with AKH in secretory vesicles. CC is known to secrete AKH upon larval starvation. I find that upon starvation, CC cells also secrete stored DILPs to the prothoracic gland(PG) in a paracrine fashion, through neuronal projections running along the 'lumen' of the latter. DILP secretion from CC to PG reveals a novel type of hormonal signaling and provides a mechanism to ensure the insulin-dependent ecdysone production in the PG cells under nutritional deprivation. Based on this mechanism, I propose a model for how successful larval development may be achieved in the absence of sufficient nutrition; the model is further supported by the absence of ecdysone-mediated growth repression during starvation.

Rearing temperature affects body size in all ectotherms including *Drosophila*. Previous work in the lab suggested a role for nutrient-dependent DILPs 2 and 5 in mediating body and tissue size changes with increased rearing temperature. In the

second part of my thesis, I demonstrate that temperature does not have an effect on tissue IIS activity. I further show that it is not the absence of DILPs 2 and 5, but the abundance of DILP2 that abrogates temperature-dependent body size change. Upon closer inspection, I find that DILP2 up-regulation increases IIS activity specifically in the PG. I hypothesize that the observed growth inhibition in DILP2 over-expressing larvae might be due to an increase in ecdysone production by the PG cells.

In a previously-published study from our group, dietary lipids derived from yeast (compared to those derived from plants) were shown to better facilitate high-temperature survival of *Drosophila* larvae, and acted by secreting higher levels of DILP2, followed by up-regulation of IIS activity in target tissues. In the third part of my thesis, I demonstrate that neither diet nor DILP2 level dictate larval survival at high temperatures. Using a wing disc explant culture system, I show that dietary lipids do however have an effect on tissue insulin sensitivity.

1. Introduction

Cellular interactions underlying the development of a multi-cellular organism from a single fertilized egg are diverse and complex. One key aspect of development includes growth – the process by which an organism efficiently converts available resources into biomass. Growth must be coordinated between various tissues so that body parts develop with correct form and function, and do so repeatedly over multiple generations. At the same time, coordination of growth is resilient and adaptable to environmental challenges like changes in temperature, poor nutrition, etc. Such plasticity in development forms the basis of natural selection and is responsible for the diversity of life we see around us today.

I have been fascinated by various methods of communication employed by tissues to coordinate growth. **For this thesis, I have chosen to explore how nutrition is sensed and allocated between different tissues and organs during development, as well as the inter-organ signals involved in mediating growth in the face of nutritional deprivation.**

1.1 Sensing nutrition is key for growth and development

Organisms from all species in the animal kingdom – from worms to humans - convey nutritional information through systemic signals. The worm *C. elegans* forms a dormant 'dauer' state to combat unfavorable growth conditions such as nutritional deprivation. The formation of this state is absolutely essential for its survival and maturation to a reproducing adult. Some of the genes necessary for 'dauer' formation in worms are those in the insulin signaling pathway (Gottlieb & Ruvkun, 1994; Malone & Thomas, 1994). In humans and other mammals, multiple systemic factors convey nutritional information and regulate metabolism (reviewed in detail in Karsenty & Olson, 2016; Liu, Alexander, & Lee, 2014).

1.1.1 Role of metabolic hormones - insulin and glucagon

Insulin- and glucagon-like metabolic hormones are widespread across the animal kingdom. In mammals, both insulin and glucagon, are produced and released from specialized cells (beta and alpha cells respectively) located in the pancreatic islets (Figure 1A). Insulin is secreted in a blood glucose-dependent way and is normally

coupled to feeding. Some research has shown that even external stimuli such as the sight or smell of food induces insulin secretion in humans (Johnson & Wildman, 1983), revealing the physiological importance of this peptide. Systemically circulating insulin binds to multiple target tissues across the body through the insulin receptor, a receptor tyrosine kinase. Binding of insulin to the receptor sets into motion a chain of intracellular signaling events that has diverse metabolic effects depending on the tissue type (Figure 1B). For example, muscles and adipose tissue take up glucose and convert it into triglycerides (Dimitriadis, Mitron, Lambadiari, Maratou, & Raptis, 2011). Overall lipolysis is decreased in adipose tissue. Glycogen synthesis is induced in liver cells along with a decrease in levels of gluconeogenesis. Glucagon, on the other hand, is secreted during the non-feeding state when blood glucose levels are low. Glucagon binding to the glucagon receptor (a G protein-coupled receptor) has effects opposite to insulin - it induces breakdown of glycogen and upregulates gluconeogenesis. Glucagon also induces hepatic ketogenesis in order to maintain metabolism in tissues during starvation (Weinstein 1973). Other signaling molecules such as GLP1 (glucagon-like peptide), IGF1 (insulin-like growth factor), ghrelin, CCK (cholecystokinin), leptin,etc. also relay nutritional information between different organ systems (Silverthorn 2009; c-lo 2011). The experiments in this thesis focus on the roles of insulin and glucagon in *Drosophila* growth and development.

1.1.2 Absence of nutrition sensing

Impairing insulin function has severe developmental consequences in humans. For example, gestational diabetes mellitus (GDM) can lead to birth defects resulting in stillbirth (Kjos 1999; Loeken, 2005). Additionally, GDM in mothers is linked to juvenile obesity (Huang, Lee, & Lu, 2007) and even adult metabolic syndrome (Moore, 2010). Type 2 diabetes mellitus (T2DM) during juvenile stages also affects growth and development. Evidence shows both skeletal defects and neuropsychological dysfunction in children with T2DM (Bussiah 2013; Rosenbloom 1974). Glucagon secretion by the alpha-cells depends on beta-cell insulin production (Cryer 2001), and hypoglycemia (low plasma glucose) develops due to complete loss of endogenous insulin caused by Type 1 diabetes mellitus (T1DM) or advanced stages of T2DM (Cryer, 2012). Neonatal hypoglycemia has been shown to impair physical growth and neuronal development (Duvanel, Fawer, Colling, Hohlfeld, & Matthieu, 1999). Additionally, low plasma glucose levels affect growth and development

through dysregulation of other hormones. Excessive human growth hormone (HGH) secretion, a hallmark of severe hypoglycemia, causes growth retardation in children (Kaplan 1968). Taken together, this collection of research shows that **insulin and glucagon affect growth and development** not just through direct uptake of nutrients but also by **relaying nutritional information** to other important tissues.

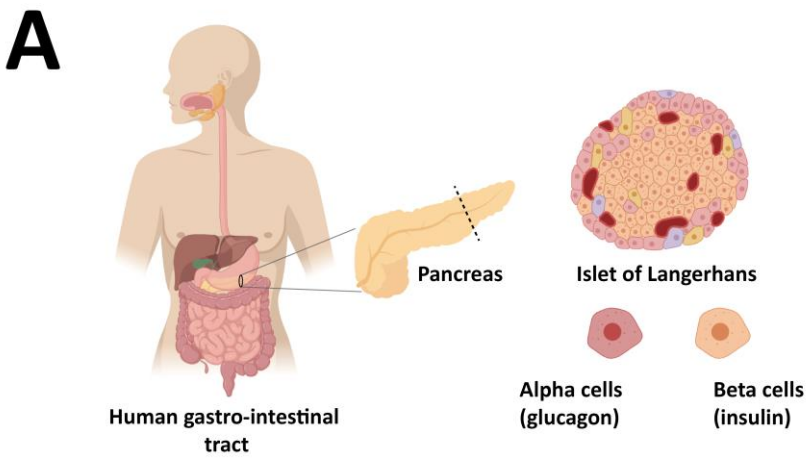

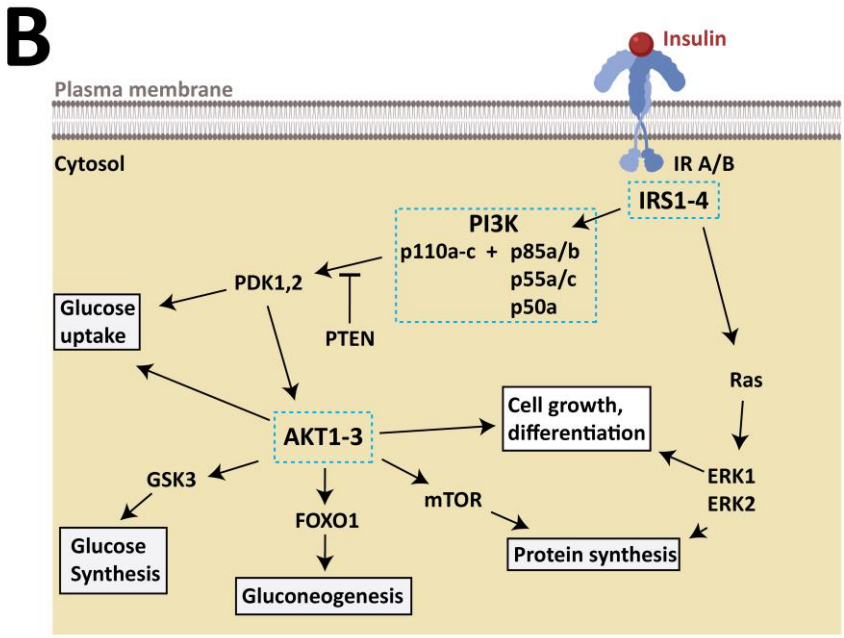

Figure 1. Insulin secretion and cellular action in humans.

(A) Alpha and beta cells located in pancreatic islets secrete glucagon and insulin respectively.
(B) Downstream insulin signaling (black arrows) is activated when insulin binds to the insulin receptor(IR). Multiple isoforms of insulin receptor substrate (IRS), phosphatidylinositol-3-kinase (PI3k) and protein kinase B (AKT) form the critical signaling nodes (dashed cyan box) in the pathway. Phosphatase and tensin homologue (PTEN) inhibit the function of PI3K. Proteins such as Ras, extracellular signal-regulated kinase 1 and 2 (ERK1, ERK2), forkhead box O1(FOXO1), mammalian target of rapamycin(mTOR), glycogen synthase kinase 3 (GSK3) and phosphoinositide-dependent kinase 1 and 2 (PDK1,2) mediate insulin action by regulating various cellular processes (white boxes). **Figure adapted from (Taniguchi, Emanuelli, & Kahn, 2006)**.

1.2 Studying inter-organ communication in *Drosophila melanogaster*

Drosophila melanogaster is made up of well-differentiated organ systems which are similar to mammals in function and structural organization. In the last century, extensive studies in *Drosophila* have helped in the development of sophisticated genetic tools. Using these tools, scientists have identified multiple inter-organ signaling factors involved in growth and development. Factors mediating inter-organ communication in flies have been excellently summarized by Droujinine and Perrimon (Droujinine & Perrimon, 2016a). In the next sections I will introduce the *Drosophila* signaling components that are functionally equivalent to the mammalian insulin-glucagon signaling axis.

1.2.1 *Drosophila* life-cycle

Drosophila develops through embryonic, larval and pupal stages before forming the adult (Figure 2). Adults organs are present in larval stages in the form of 'imaginal' tissues, whose growth in the larva dictate organ size and shape in the adult fly. Signals regulating metabolism and growth are similar in the larvae and adults. Thus, the larva is an appropriate model to study growth and development, whereas the adult is more suited for studying metabolic homeostasis, reproduction and aging. In my thesis, I have chosen *Drosophila* larval development as a model to study the role of insulin in supporting growth primarily in the face of external challenges such as nutrient deprivation, high temperature and change in dietary composition.

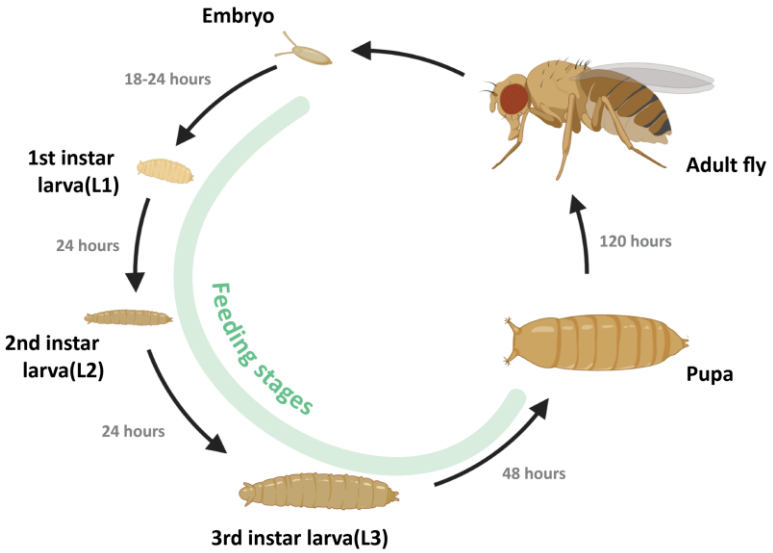

Figure 2. Schematic representation of the *Drosophila* life cycle.

Developmental time under laboratory conditions on standard food and temperature (25˚C). Feeding stages during development are shown in green.

1.2.2 *Drosophila* insulin-like peptides

Seven ***Drosophila* insulin-like peptides** (DILPs 1-7) are expressed in a tissue- and stage-specific manner and bind to a single ***Drosophila* insulin receptor (dInR)** (Brogiolo et al., 2001; Grönke, Clarke, Broughton, Andrews, & Partridge, 2010). Unlike the more complex mammalian system (Figure 1B), flies have one dInR, **one insulin receptor substrate (*chico*)** and one downstream **forkhead box O transcription factor (dFOXO)** (Puig, Marr, Ruhf, & Tjian, 2003b). Since their discovery, these components have been known to affect fly growth and development through the insulin/insulin-like signaling (IIS) pathway (Figure 3). Thus, although relatively simple in design compared to the mammalian system, the IIS pathway in flies is equally as essential.

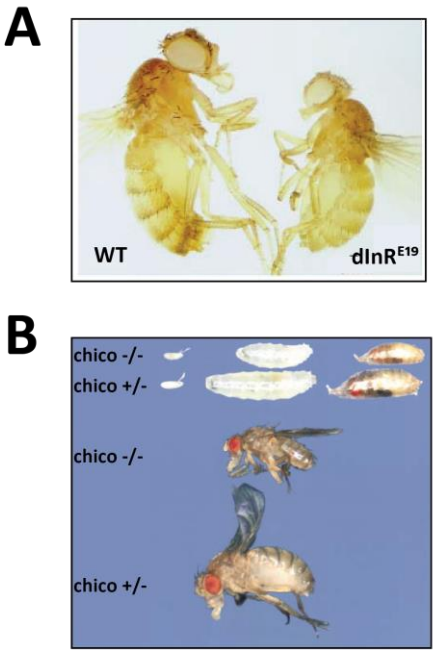

Figure 3. Growth effects of impaired insulin signaling in *Drosophila*.

Perturbation of insulin signaling reduces body size. **(A)** Adult wild type (WT) flies and insulin receptor hypomorphs ($dInR^{E19}$). **Image modified from (Brogiolo et al., 2001)**.

(B) Embryo, larva, pupa and adults of heterologous (+/-) and homologous (-/-) insulin receptor substrate (*chico*) mutants. **Image modified from (Böhni et al., 1999).**

Nutrient-sensing is primarily carried out by a group of 14 neuro-secretory cells called the insulin-producing cells (IPCs), located in the pars intercerebralis of the brain (Figure 4). They share common evolutionary origins and developmental progression with vertebrate endocrine beta-cells (Wang, Tulina, Carlin, & Rulifson, 2007). IPCs express DILPs 1, 2, 3 and 5. Of these DILP1 is expressed only in the pupal (non-feeding) stages and during adult reproductive diapause (Post et al., 2018). **DILPs 2 and 5 are highly expressed throughout larval feeding stages**, when the majority of biomass accumulation occurs. In contrast, DILP3 is expressed briefly just before puparium formation and its expression overlaps with a minor increase in larval size (Ikeya et al., 2002; Okamoto & Yamanaka, 2015). The IPCs also integrate signals from other tissues during development and have been discussed in section 1.2.5.

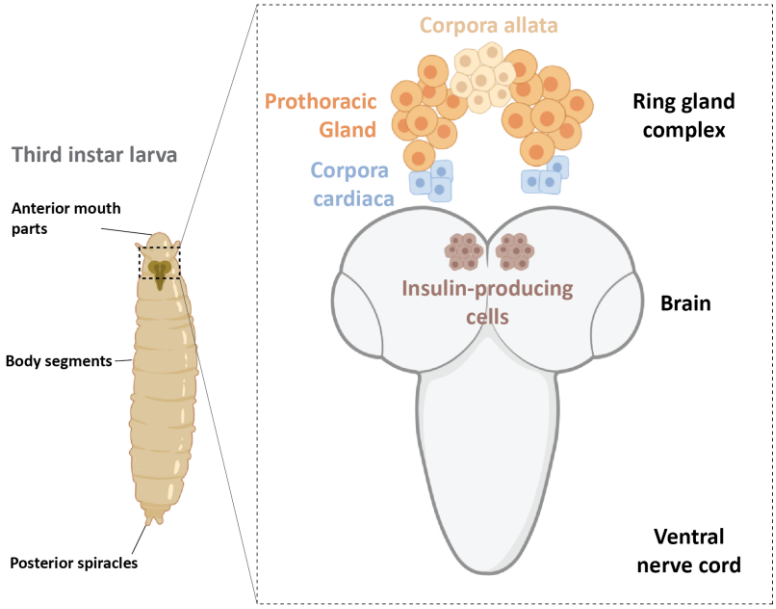

Figure 4. *Drosophila* larval brain and ring gland.

Major larval endocrine tissues depicted in the magnified image (dashed box) of the central nervous system.

In larvae, **IPC DILPs are secreted in response to diet**. Diets rich in amino acids and sugar facilitate the release of DILPs from IPCs, whereas poor diets or starvation cause retention of DILPs (Géminard, Rulifson, & Léopold, 2009). Moreover, ablation of the IPCs results in high circulating sugar levels, reminiscent of diabetes mellitus in humans (Rulifson, 2002). Larvae with ablated IPCs further develop into flies with reduced tissue size and low fecundity (Ikeya et al., 2002; Rulifson, 2002). Thus, IPCs play an important role in coupling nutrition to larval growth by regulating DILP secretion.

1.2.3 Adipo-kinetic hormone

Adipo-kinetic hormone (AKH) is the insect homolog of mammalian glucagon. It is produced throughout all life stages in *Drosophila*. Spatial expression of AKH is limited to a symmetrical cluster of neurosecretory cells called the corpora cardiaca (CC) located in the ring gland (RG) complex (Figure 4). Similar to mammals, AKH binds to a GPCR called **AKH receptor (AKHR)**. AKHR is primarily expressed in the larval fat body, which functions as a storage organ for lipids and glycogen (Ziegler, Jasensky, & Morimoto, 1995). Like other GPCRs, AKH binding to AKHR

induces downstream signaling through cyclic-AMP(cAMP) and Ca^{2+} secondary messengers (Arrese, Flowers, Gazard, & Wells, 1999; Vroemen, Van Marrewijk, Schepers, & Van Der Horst, 1995). These signals result in lipid release through upregulation of lipolytic *brummer* (*bmm*) gene (Baumbach, Xu, Hehlert, & Kühnlein, 2014; Grönke et al., 2007).

AKH maintains circulating levels of sugars such as glucose and trehalose in the larvae. Loss of AKH by CC ablation causes severe hypoglycemia in larvae (G. Lee & Park, 2004). Surprisingly, ablating CCs or knocking out AKH and AKHR makes flies starvation resistant (Galikova et al., 2015; G. Lee & Park, 2004), possibly due to the elevated sugar levels in circulation coupled with slow utilization of stored resources upon starvation. Starvation-induced hyperactivity, a trait associated with successfully finding alternative food sources, is completely absent in flies without AKH (Galikova et al., 2015; G. Lee & Park, 2004). However, no effect on growth and development was observed in AKH and AKHR mutants under well-fed conditions (Galikova et al., 2015), suggesting that AKH might not be as essential as IPC DILPs during larval feeding.

1.2.4 Ecdysone

Ecdysone is the master regulator of development in most insects including *Drosophila melanogaster*. It is a steroid hormone which is produced in the larval prothoracic gland (PG), a group of endocrine cells within the RG located anterior to the CC (Figure 4). Ecdysone is secreted into circulation and subsequently converted into its active form 20-hydroxyecdysone (20E) by peripheral tissues such as fat body and malpighian tubules (Petryk et al., 2003). In the course of this thesis, I will refer to both of these forms using the umbrella term “ecdysone”. 20E binds to the ecdysone receptor (EcR) in larval tissues and sets into motion gene expression changes which ultimately lead to molting and metamorphosis. The EcR is a nuclear hormone receptor that acts as a ligand-dependent transcription factor (Uyehara et al., 2019). Recent evidence suggests that neuronal cells may respond to ecdysone via the ecdysone importer (EcI) (Okamoto & Yamanaka, 2020). Cellular action of ecdysone in peripheral tissues has been reviewed in detail by Yamanaka and colleagues (Yamanaka, Rewitz, & O’Connor, 2013).

Ecdysone is produced at basal levels during larval feeding and pulses at instar transitions. In the late third-instar stage, **peaking of ecdysone levels initiates**

formation of the pupa (Figure 5), while a delay in the ecdysone peak postpones the onset of metamorphosis.

1.2.5 Tissue cross-talk coordinates growth and development

Nutrition-sensing is essential for metamorphosis. *Drosophila* larvae pass through a developmental checkpoint in order to ensure adequate nutrient storage during pupal stages. This stage, called '**critical weight**', is attained during the L3 larval phase (Figure 5). Beyond this point, larval starvation does not have an effect on pupariation timing, but instead produces smaller flies (Figure 5). Pre-critical weight starvation results in delay of pupariation until an alternative food source is found. In the absence of re-feeding, larvae usually fail to transition into pupariation and subsequently die.

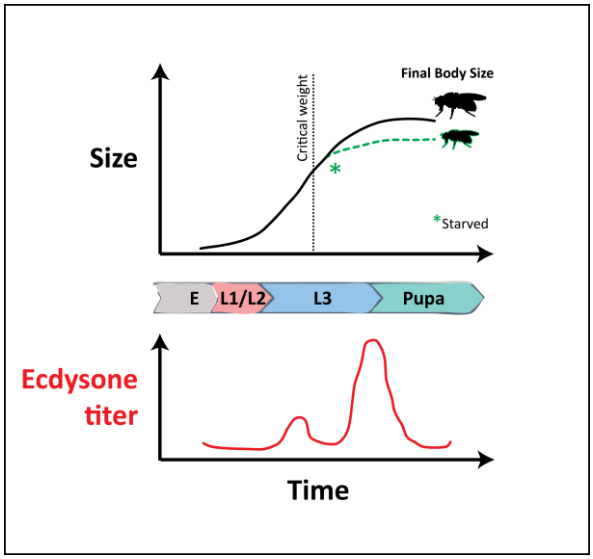

Figure 5. *Drosophila* larval growth curve.

Schematic representation of size increase during larval development. Starvation point (green asterisk) after critical weight (black dashed line) and subsequent growth (green dashed curve). Ecdysone levels (red) during developmental stages.

Attainment of critical weight is sensed by the PG through IIS activity. Ectopic upregulation of IIS pathway components in PG cells results in 'mis-sensing' of nutritional status, leading to higher ecdysone production, which ultimately translates into early pupariation and growth repression (Colombani, 2005; C. Mirth, Truman, & Riddiford, 2005). Moreover, IIS pathway transcription factor *Drosophila* forkhead box-O (dFOXO) has been implicated in the prevention of pupariation in pre-critical weight larvae through direct interaction with *ultraspiracle* (Usp), a gene involved in ecdysone biosynthesis (Koyama, Rodrigues, Athanasiadis,

Shingleton, & Mirth, 2014). In addition to IIS, PG cells also sense nutrition through the well-known target-of-rapamycin (TOR) pathway. Time-course analysis show that the final ecdysone peak responsible for pupariation depends on up-regulation of TOR pathway components post critical weight (Layalle, Arquier, & Léopold, 2008).

The IPCs sense poor nutritional state through the action of AKH (Kim & Neufeld, 2015). Under poor nutrition (no proteins), larval hemolymph trehalose stimulates AKH secretion from the CC which in turn instructs the IPCs to secrete DILP 3. DILP 3 further activates TOR signaling in the fat body, which then suppresses autophagy and allows larval growth under suboptimal nutritional conditions (Kim & Neufeld, 2015). However, it is still not clear how the CCs sense hemolymph sugar levels. Recent evidence points towards a specific glucose-sensing neuron which directly stimulates both, the CCs and the IPCs (Oh et al., 2019).

The interactions between DILP-producing IPCs and the AKH-producing CCs are not well characterized. Multiple studies have noted innervation between these tissues but no direct interactions have been recorded (Ikeya et al., 2002; Rulifson, 2002; Siegmund & Korge, 2001).

2. Aims of the thesis

Drosophila is an outstanding model organism in which to study integration of growth and development. Nutritional information in the growing larva is sensed by specific tissues, which in turn coordinate developmental transitions through secreted signals. These signals are highly conserved from flies to humans. The aim of my thesis is to understand the relationship between nutrition and insulin signaling in *Drosophila* growth and development.

Nutrient-dependent *Drosophila* insulin-like peptides (DILPs) govern larval growth through endocrine signaling. Although the influence of insulin signaling on development has been extensively studied in the last decade, many aspects remain poorly understood. The localization of DILPs to the larval corpora cardiaca is one such aspect, primarily because the corpora cardiaca produces glucagon-like adipokinetic hormone which is functionally antagonistic to DILPs. **In the first part of my thesis, I address the underlying mechanism responsible for insulin localization in the corpora cardiaca using tissue-specific gene knockdown and electron microscopy. I search for the intracellular compartments storing DILPs in corpora cardiaca cells and test if this phenomenon is relevant for growth and development.**

Previous work from our lab showed the essentiality of nutrient-dependent DILPs for growth and development at high rearing temperatures. **In the second part of my thesis, I test if temperature brings about tissue and body size change through the regulation of systemic DILP secretion and IIS activity in target tissues.**

A published study from our group demonstrated the importance of dietary lipids for enabling larvae to survive at high rearing temperatures. **In the third part of the thesis, I retest the hypothesis suggesting that insulin signaling is involved in mediating the effects of dietary lipids and test the temperature-independent effects of dietary lipids on tissue insulin sensitivity.**

3. Results

3.1 Role of non-canonical insulin secretion in *Drosophila* growth and development.

In order for *Drosophila* larvae to enter the pupal stages of development they must attain a critical body size (C. K. Mirth & Riddiford, 2007; C. Mirth et al., 2005). To do this, larvae must grow, efficiently converting available nutrition into biomass. Anabolic growth in the larvae is primarily mediated through the **insulin/insulin-like signaling(IIS)** pathway.

Similar to humans, *Drosophila* produces seven ***Drosophila* insulin-like peptides (DILPs)** which regulate body size and growth (Ikeya et al., 2002). Of the seven, DILPs 2 and 5 are produced during the entire period of larval growth (Ikeya et al., 2002; Okamoto & Nishimura, 2015a; Rulifson, 2002). Analogous to human insulin, DILP2 and 5 secretion depends on nutrition (Géminard et al., 2006, 2009; Okamoto & Nishimura, 2015a). However, while human insulin is produced in the pancreas, DILP2 and DILP5 are produced by **insulin producing cells(IPCs)** located in the pars intercerebralis (PI) of the larval brain. *Drosophila* also produce **adipo-kinetic hormone (AKH)**, a functional analog of human glucagon. AKH is a neuropeptide that controls sugar homeostasis through breakdown of stored fat and supports growth during bouts of larval starvation (Bharucha, Tarr, & Zipursky, 2008; Braco, Gillespie, Alberto, Brenman, & Johnson, 2012; Grönke et al., 2007). It is synthesized and secreted by **corpora cardiaca (CC)** neurons located in the larval **ring gland (RG)** (G. Lee & Park, 2004). Similar to the relationship between human insulin and glucagon, the metabolic effects of DILPs 2 and 5 , and AKH are distinct and antagonistic in nature (Buch, Melcher, Bauer, Katzenberger, & Pankratz, 2008; Choi, Lim, & Chung, 2015; Kim & Neufeld, 2015; Oh et al., 2019). This antagonism enables DILP2 and 5 and AKH to maintain metabolic homeostasis and tightly control allocation of nutrition between growth and storage in the developing larva.

IPCs are neuro-endocrine cells which project axonal processes out of the larval brain to form contacts with the larval aorta and the CC cells of the RG (Ikeya et al., 2002; Rulifson, 2002). The aorta surface forms a site of DILP release into the open circulatory system of the larva, enabling systemic insulin action. However, the functional relevance of CC contacts is not well understood. Rulifson and colleagues provided first clues when they reported results of **DILP2 staining in the AKH-producing CC cells:** based on the perinuclear localization of DILP2 inside

membrane-bound structures and the absence of *dilp2* mRNA expression in CC cells, they hypothesized that **CC** cells **take up DILP2**. At the time they did not look into the mechanism of uptake or the function DILP2 within the CC cells. While more studies have focused on the individual roles of DILP2 and AKH in larval growth and homeostasis, none have addressed the function of DILP2 in the CC cells. **The antagonistic nature of DILP2 (insulin) and AKH (glucagon) function in *Drosophila* (and other organisms) poses important questions: How does a hormone like insulin localize to the source tissue of a functionally opposite hormone like glucagon? What might be the physiological implications of this localization?** In this section, I explore the mechanism and physiological role of the CC pool of DILP2 in *Drosophila* larval growth and development.

3.1.1 *Drosophila* insulin-like peptides localize to the corpora cardiaca and are derived from the insulin-producing cells.

I began by replicating the experiments performed by Rulifson and colleagues (Rulifson, 2002) to confirm that CC cells contain DILP2. I dissected and fixed 96-hour larval brains with ring glands attached in larvae where I marked the IPCs by expressing CD8::GFP from an IPC-specific driver (dilp2-GAL4). I took extra care to prevent damage to neuronal processes extending from brain, and also removed all other tissues in proximity (eye discs and esophagus) to gain a clear view of the CC. I stained the cells for DILP2 and observed substantial amounts of DILP2 localization in the CC cells (Figure 6A). The CC cells are located posterior to the prothoracic gland (PG) in the RG complex, and IPC-derived processes containing DILP2 can be seen in close proximity to the CC cells (Figure 6A). These results confirm that CC cells contain DILP2. IPCs are also reported to secrete DILP5 during larval growth (Ikeya et al., 2002), so I next asked if CC cells also contain DILP5. I stained 96-hour wild-type (w1118) larvae for both DILP2 and DILP5 and used a higher magnification objective to collect images with better resolution. Images of the CC cells marked with a neuronal membrane marker (Figure 6B.i) show positive staining for both DILP2 (Figure 6B.ii) and DILP 5 (Figure 6B.iii). Because the staining patterns of the DILP2 and DILP5 channels were very similar (Figure 6B.ii and 6B.iii), I performed a pixel-based intensity colocalization between them. DILP2 and DILP5 show significant colocalization (Figure 6B.iv) with a high correlation of R= 0.94 (Spearman's

correlation coefficient). Taken together, my results show that CC cells contain both DILP5 and DILP2, and that these proteins colocalize within the CC cells. However, there is no direct evidence that the DILP2 and DILP5 pool in the CC is IPC-derived. Rulifson and colleagues showed the absence of DILP2 mRNA expression, but did not conclusively show the source of DILP2 in the CC.

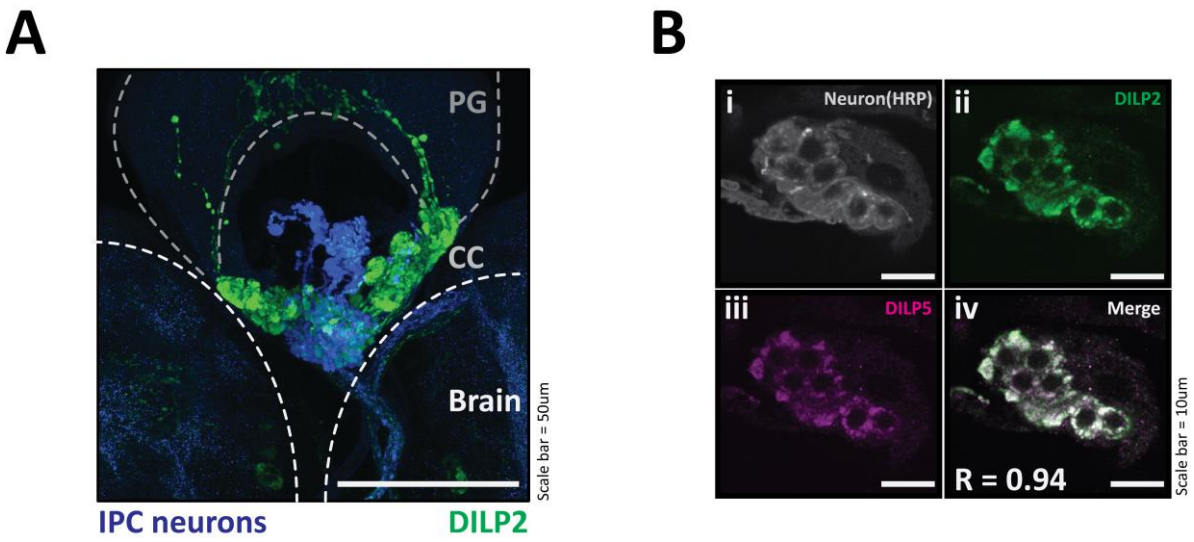

Figure 6. DILP2 and DILP5 localization in the Corpora Cardiaca.

(A) Maximum z-projection of confocal stack of larval (dilp2>GFP) CNS and ring gland (Scale bar = 50um). Individual tissues are marked with adjoining initials and/or dashed lines – **brain** (white) , prothoracic gland (**PG**, gray) and corpora cardiaca (**CC**) – and stained for **DILP2(green)** and **GFP(blue)**.
(B) Single medial plane of a corpora cardiaca cell body (Scale = 10um) stained for **(i)**neuronal marker **HRP** (grayscale), **(ii) DILP2** (green) and **(iii) DILP5** (magenta). **(iv)** is a **merged** image of DILP2 and DILP2 channels showing co-localization (white)**; R** = pixel-based correlation coefficient (Spearman) between DILP2 and DILP5 channels.

I next asked if DILP2 and DILP5 in the CC are derived from the IPCs. To do this, I performed an IPC-specific (dilp2-GAL4) RNAi-mediated knock-down of either DILP2 or DILP5. IPCs with DILP5 knocked down showed significant loss of DILP5 in CC cells (Figure 7A.i and 7A.ii) compared to controls (dilp2>w1118; Figure 7A.iii and 7A.iv). Quantification of DILP5 intensity in single CC cells shown in the adjoining boxplot shows a significant decrease in DILP5 knock-down larvae (Figure 7A). None of the available DILP2 RNAi lines proved to be efficient in knocking down DILP2 in the IPCs (data not shown). As an alternative, I ablated the IPCs by specifically expressing apoptotic cell marker *reaper* (rpr) in the CC. IPC ablation (dilp2>rpr) shows a loss of DILP2 in the CC cells (Figure 7B.i and 7B.ii) compared to the controls

(*dilp2*>w1118; Figure 7B.iii and 7B.iv). The quantitative decrease in DILP2 intensity in ablated versus control CC cells is shown in the adjoining boxplot (Figure 7B). Together, my results show that the DILP2 and DILP5 in the CC cells are not produced locally and are derived from the IPCs. This suggests that there might be an active or passive form of uptake responsible for the localization of DILPs to the CC.

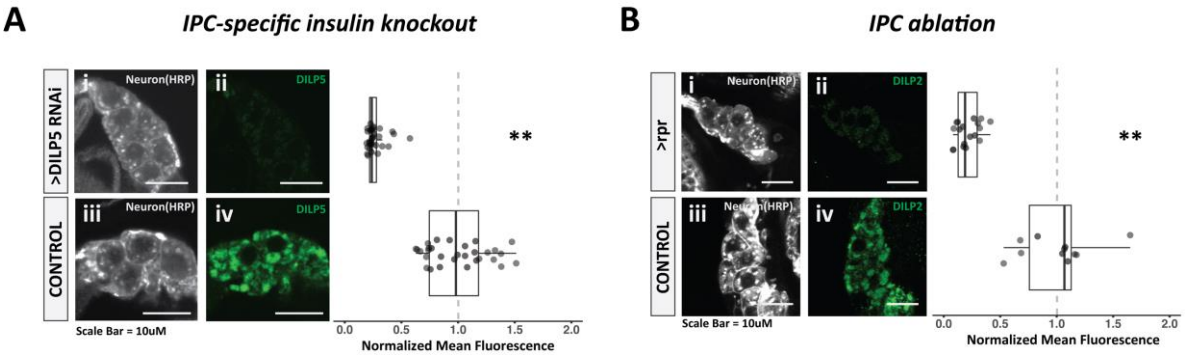

Figure 7.Source of Corpora Cardiaca pool of DILP2 and DILP5.

Representative images show single medial plane of corpora cardiaca cell bodies (Scale bar = 10um).
(A) IPC-specific DILP5 knock-down **(i, ii)** dilp2>dilp5-RNAi and **(iii, iv)** dilp2>w1118, stained for **(i, iii)** neurons (HRP, gray) and **(ii, iv)** DILP5 (green).
(B) IPC-ablation through *reaper* expression **(i, ii)** dilp2>reaper and **(iii, iv)** dilp2>w1118, stained for **(i, iii)** neuronal marker **HRP** (gray) and **(ii, iv) DILP2** (green).
Box plots (right side) show **(A)DILP5 /(B)DILP2** average fluorescence intensity values normalized to respective controls **(A.iv , B.iv)**. Each data point represents a single cell body. Multiple larvae (n>=3) were used from each treatment and control (**=p<0.01, Mann-Whitney U test).

3.1.2 Mechanism of DILP uptake in the corpora cardiaca

Cellular uptake - or endocytosis - is mediated through both clathrin-dependent and independent mechanisms. Across all organisms, including *Drosophila,* receptor tyrosine kinases (RTK) like the insulin receptor undergo clathrin-mediated endocytosis (CME) (Doherty & McMahon, 2009). CME is known to be a major endocytic mechanism in *Drosophila* neurons as it controls uptake of synaptic vesicles (Chanaday & Kavalali, 2018; Van Der Bliek & Meyerowrtz, 1991). Thus, I next asked if CME is the mechanism by which DILP2 and DILP5 are taken up in CC cells.

CME is regulated by the action of dynamin – a GTPase expressed by the *shibire* gene in *Drosophila* (Van Der Bliek & Meyerowrtz, 1991). I used a temperature-sensitive dominant-negative version of dynamin (*shibire^{TS1};* Kelly & Suzuki, 1974) to disrupt CME specifically in the CC (akh-GAL4) using the UAS/GAL4 system. I achieved temporal control of CME inhibition by rearing L3 feeding larvae at 18˚C and subsequently shifting them to a temperature of 29˚C for 2 hours and 4 hours respectively. I used unshifted larvae (0 hours) as controls. I fixed and stained

CC cells from the respective shifts and controls for DILP5. A short temperature shift of 2 hours increases the amount of DILP5 in CC cells compared to 0-hour control (middle panel, Figure 8A and 8B), yet the longer shift of 4 hours caused a significant reduction in DILP5 in CC cells compared to the controls (Figure 8A and 8B, left panel). The initial increase can be explained by jamming of endocytic vesicles at the membrane due to the inhibition of dynamin. This is because dynamin enables vesicle endocytosis by pinching off clathrin-coated invaginations from the membrane (De Camilli, Takei, & McPherson, 1995). Previous reports show that when the temperature of *shibire*^{TS1}

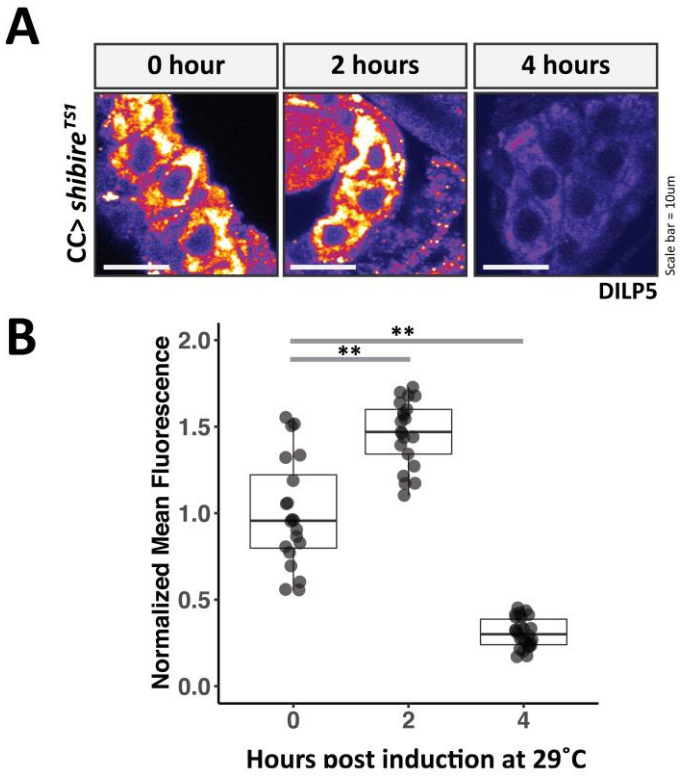

Figure 8. Effect of dynamin inhibition on Corpora Cardiaca DILP5 uptake.

Corpora cardiaca-specific expression of temperature-sensitive *shibire* protein (akh>shibireTS1)
(A) Representative images showing **DILP 5** intensities in single medial plane of corpora cardiaca cell bodies (Scale bar = 10um). Panels indicate the **duration of the high-temperature shift (29˚C)**.
(B) Box plots show **DILP5** average fluorescence intensity values normalized to control (0 hour); each data point represents a single cell body. Multiple larvae (n>=3) used from each time point.(**=p<0.01, Mann-Whitney U test)

mutant flies is elevated, the density of synaptic vesicles in neurons increased instantly (Estes et al., 1996; Ramaswami, Krishnan, & Kelly, 1994). The observed reduction of DILP5 levels at the longer (4 hour) timepoint of temperature increase (and dynamin inhibition) might be due to exocytosis (Koenig & Ikeda, 1996) or subsequent degradation of endocytic vesicles (Van De Goor, Ramaswami, & Kelly, 1995). Taken

together, these results suggest that disruption of CME prevents localization of DILP5 in the CC. I assume a similar outcome in case of DILP2.

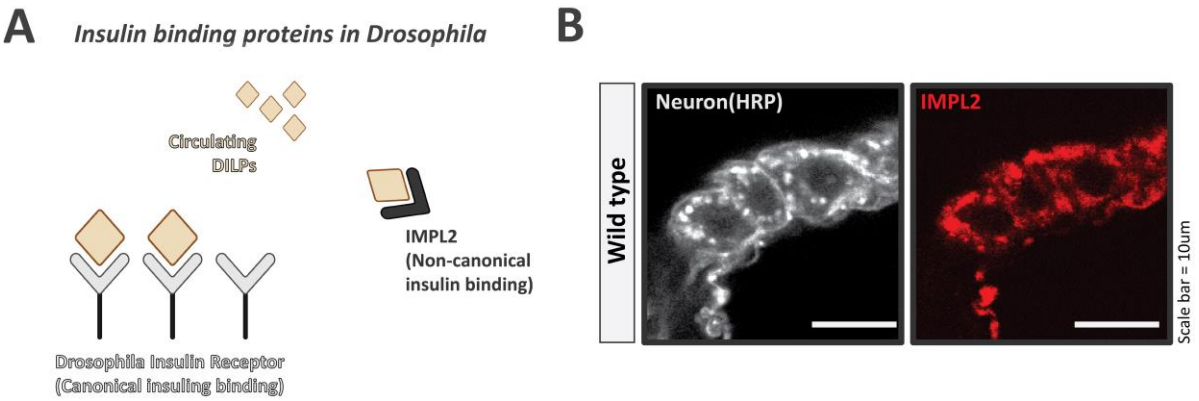

Figure 9.Expression of IMPL2 in the Corpora Cardiaca.

(A) Schematic representation of **canonical** and **non-canonical** insulin-binding proteins in *Drosophila*.
(B) Single medial plane of a corpora cardiaca cell body (Scale bar = 10um) stained for neuronal marker **HRP** (gray, left panel) and **IMPL2** (red, right panel).

CME-dependent uptake of DILP 5 suggests that a DILP binding receptor may be expressed in CC cells. Apart from the canonical *Drosophila* insulin receptor (dInR), imaginal morphogenesis protein late-2 (IMPL2) is the only other protein known to bind to DILPs 2 and 5 (Figure 9A) (Andersen, Hansen, Schäffer, & Kristensen, 2000; Roed et al., 2018). While dInR is ubiquitously expressed in *Drosophila* larvae (Garofalo & Rosen, 1988), expression of IMPL2 is limited to wing imaginal discs and few neurons in the larval brain (Honegger et al., 2008; Osterbur, Fristrom, Natzle, Tojo, & Fristrom, 1988); I asked if it is expressed in CC cells. I stained the CC cells with a specific antibody and observed significant levels of IMPL2 (Figure 9B), suggesting that CC cells might use both IMPL2 and dInR to take up DILP2 and DILP5. To test this, I carried out RNAi-mediated knock-down of dInR or IMPL2 specifically in CC cells with wild-type outcrossed larvae (akh>w1118) as controls and analyzed fixed cells for the presence of DILP2 and DILP5 by staining. Surprisingly, knocking down dInR did not reduce the amount of DILP2 (Figure 10A, middle row and quantification) or DILP5 (Figure 10B, only quantification shown) in the CC compared to controls (Figure 10A, top row and 10B). In contrast, the IMPL2 knock-down showed significant reduction in both DILP2 (Figure 10A, bottom row) and DILP5 (Figure 10B). Taken together these results suggest that IMPL2, but not dInR, is used by the CC to take up DILPs 2 and 5.

IMPL2 was first identified in *Drosophila* wing imaginal discs as target of 20-hydroxy-ecdysone (Osterbur et al., 1988). Since then it has been characterized as a

secreted protein that inhibits DILP activity through direct binding (Honegger et al., 2008; Okamoto & Nishimura, 2015a; Roed et al., 2018), though its role in the source tissue has not been studied in depth. One study, by Bader and colleagues, implicated

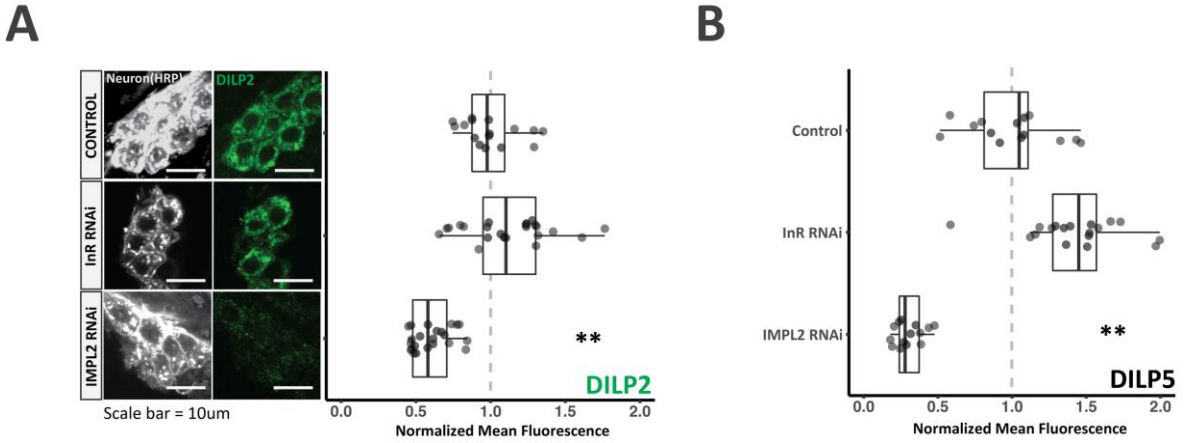

Figure 10. Effect of IMPL2 knock-down on Corpora Cardiaca DILP2 and DILP5 uptake.

(A) Representative images showing single medial plane of corpora cardiaca cell bodies (Scale bar = 10um) of **controls** (akh>w1118), RNAi-mediated insulin receptor knock-down (akh>**InR-RNAi**) and RNAi-mediated IMPL2 knock-down (akh>**IMPL2-RNAi**), stained for neuronal marker **HRP** (gray) and **DILP2** (green). Box plots (right of images) show **DILP2** average fluorescence intensity values normalized to control (akh>w1118); each data point represents a single cell body. Multiple larvae (n>=3) used for each knock-down and control (**=p<0.01, Mann-Whitney U test).
(B) Box plots show **DILP5** average fluorescence intensity values of insulin-receptor RNAi-mediated knock-down(akh>**InR-RNAi**) and IMPL2 RNAi-mediated knock-down (akh>**IMPL2-RNAi**), normalized to **controls** (akh>w1118). Each data point represents a single cell body. Multiple larvae (n>=3) used for each knock-down and control (**=p<0.01, Mann-Whitney U test).

IMPL2-dependent regulation of insulin signaling in the same subset of brain neurons where IMPL2 is produced. Given that the CCs are located adjacent to the PG in the ring gland complex (Figure 4), I asked whether expression of IMPL2 is induced by ecdysone signaling from the PG. Ecdysone signaling is mediated through the binding of ecdysone to ecdysone receptor (EcR) isoforms (Talbot, Swyryd, & Hogness, 1993) (Figure 11A). EcR is a ubiquitously-expressed nuclear receptor in that ecdysone target genes (like IMPL2) are expressed when the ligand-bound, activated form of EcR moves to the nucleus (Figure 11A). In order to inhibit ecdysone signaling in the CC, I knocked down all isoforms of EcR using RNAi. I then stained knock-down and control ring glands for DILP2 as a proxy for IMPL2 expression. EcR knock-down did not change DILP2 levels (Figure 11B, bottom) in the CC compared to controls (akh>w1118) (Figure 11B, top), suggesting that that IMPL2 production in the CC might be EcR-independent. However, there may be compensatory regulation involved; low levels of EcR could upregulate other activators of ecdysone target genes (Parvy et al., 2014).

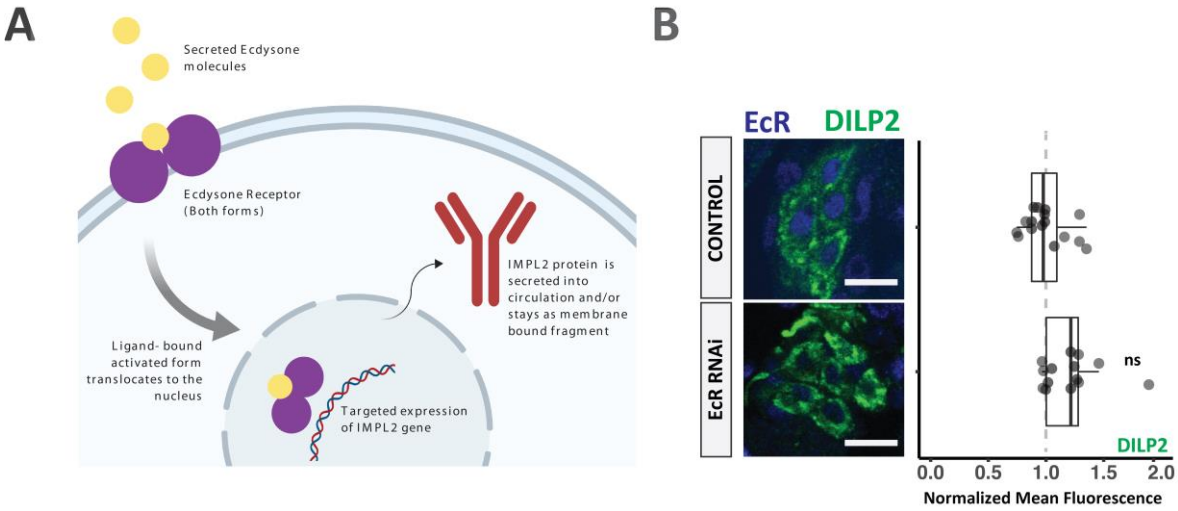

Figure 11. Effect of Ecdysone Receptor knock-down on Corpora Cardiaca DILP2 uptake.

(A) Outline of ecdysone signaling pathway and expression of IMPL2.
(B) Representative images showing single medial plane of corpora cardiaca cell bodies (Scale bar = 10um) of **controls** (akh>w1118) and RNAi-mediated ecdysone receptor(akh>**EcR-RNAi**) knock-down receptor stained for neuronal marker **HRP** (gray) and **DILP2** (green). Box plots show **DILP2** average fluorescence intensity values normalized to control (akh>w1118). Each data point represents a single cell body. Multiple larvae (n>=3) used for each knock-down and control (**=p<0.01, Mann-Whitney U test).

3.1.3 Ultra-structural analysis of DILP localization in the corpora cardiaca

In the mammalian pancreas, alpha cells store glucagon and beta cells store insulin in large dense-core vesicles (DCVs) (Bussolati, Capella, Vassallo, & Solcia, 1971; Westgaard, 1973) and secrete them from their respective endocrine cells in a calcium-dependent way (Gustavsson et al., 2009; Lang, 1999). Based on evidence from other insects, *Drosophila* is assumed to store neurohormones like DILPs and AKH in similar vesicle structures (Willey, 1960; Johnson and Bowers, 1963), however, there is no direct evidence for DILP or AKH-containing secretory granules in *Drosophila* IPCs or CC. I was curious to determine the cellular compartments in which DILPs 2 and 5 are stored in the CC. To do this, I first had to determine the ultra-structure of the *Drosophila* CC.

I collaborated with Dr.Michaela Wilsch-Brauninger and Dr.Weihua Leng from the electron microscopy facility at the MPI-CBG to generate an ultrastructure of the *Drosophila* CC. We fixed and embedded intact ring glands from 96-hour larvae in epon, then cut 70nm thin sections for imaging on a FEI electron microscope at 80kV. We then generated a high-resolution image of the horseshoe-shaped ring gland (RG) by stitching multiple regions of interests from each section using a Fiji plugin: the PG

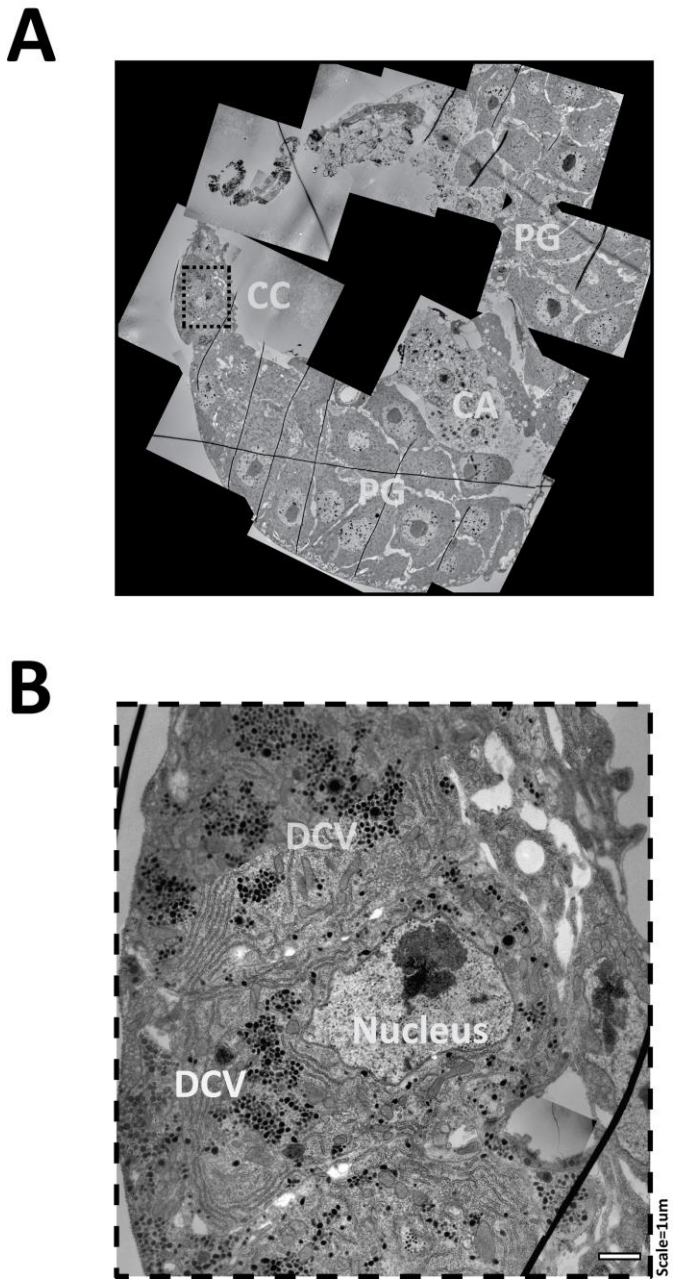

Figure 12. Ultrastructure of the *Drosophila* larval Corpora Cardiaca.

Electron micrographs obtained from ring gland sections (70nm) of wild-type control (akh>w1118) larvae.
(A) Macro-scale reconstruction of the entire ring gland from multiple micrographs; initials marking prothoracic gland (**PG**), corpora cardiaca (**black dashed box, CC**) and corpora allata (**CA**).
(B) High-resolution image of a single corpora cardiaca cell body, **black dashed box** area in **(A). Nucleus** and dense-core vesicles (**DCV**) are marked (Scale bar= 1um).

on either side can be distinguished by the large polyploid nuclei; the CA, located between

the two PG, has a different tissue density and nuclei size (Figure 12A); the CC form the posterior tip of the RG (Figure 12A, black dashed box). Multiple cellular structures such as endoplasmic reticulum, golgi and mitochondrion can be clearly

seen in the magnified image of the CC cell body region (Figure 12B). Importantly, the CC cell body shows an abundance of DCVs in both in the perinuclear space as well as the periphery (Figure 12B). Thus, electron microscopy thus reveals that, like in other insects, CC cells in *Drosophila* contain high number of DCVs in the cytoplasm.

Having determined the ultrastructure of the CC cells, we wanted to know which of the cellular structures contained DILP2 and 5. In order to do this, we performed correlative light and electron microscopy (CLEM) on Tokayasu cryo-sections of 108-
hour larval (akh>w1118) ring gland. Additionally, we performed immune-gold labelling of DILP2 and DILP5 with 10nm and 5nm particles respectively. We used low resolution fluorescent images to define regions of interest in each section. Only DCV regions in the CC cells showed positive staining for gold particles of both sizes (Figure 13A, white dashed outline); the rest of the cytoplasm and membrane regions of the CC were free of gold particle staining (Figure 13A). This indicates that DILP2 and DILP5 localize to DCVs in the CC. Higher-magnification images (Figure 13B) reveal that DILP2 and DILP5 co-localize in individual DCVs with diameters between 100-300nm (Figure 13B.i and 13B.ii). DILP2 and DILP5 were also found together in larger (>350nm) multi-vesicular bodies (MVBs) (Figure 13B.iii and 13b.iv) which are characterized by multiple smaller internal membranes. This suggests that up-taken DILPs are sorted for degradation, recycling or exocytosis (Corrigan et al., 2014; Krämer, 2002). No DCVs containing exclusively DILP2 or DILP5 were observed. Taken together, these results suggest that DILP2 and DILP5 co-localize to DCVs in the CC cell body and that CC cells possess the capability to re-secrete DILPs.

It has long been known that, in response to dietary stimuli, CC cells secrete AKH stored in the DCVs (G. Lee & Park, 2004; Scharrer, 1967). We asked if CC DCVs containing DILPs 2 and 5 also contain AKH. Using the same experimental setup described above, we stained DILP2 and AKH with 10nm and 5nm gold particles respectively. Similar to the results in Figure 13A, only DCV regions showed positive gold staining (data not shown). DILP2 and AKH co-localize in DCVs sized between 100-300nm in diameter (Figure 14.i-iv). Taken together, these results not only indicate re-secretion of DILPs 2 and 5, but also raise the possibility of their co-secretion with AKH from the CC. However, the physiological circumstances under which DILPs and AKH might be co-secreted from the CC are not clearly understood, primarily because the nutritional conditions which activate the CC cells are also the

ones which inactivate IPCs- the site of DILP2 and 5 secretion (Kim & Neufeld, 2015; Oh et al., 2019).

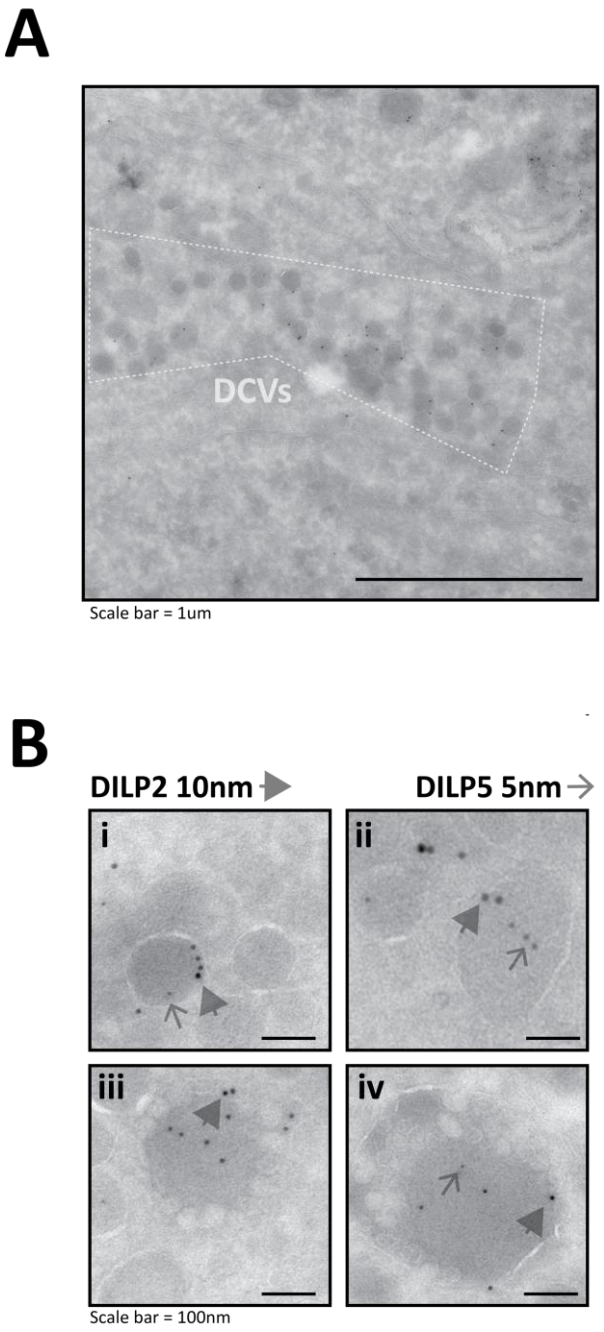

Figure 13. Subcellular localization of DILP2 and DILP5 in the Corpora Cardiaca.

Electron micrographs of immuno-gold staining of corpora cardiaca sections(70nm) of wild-type control (akh>w1118) larvae.
(A) Low-magnification image showing gold particle immuno-reactivity **(black dots);** cytoplasmic region containing dense-core vesicles (**DCVs**) is outlined with a **white dashed box** (Scale =1um).
(B) High-magnification images of **(i, ii)** dense-core vesicles and **(iii, iv)** multi-vesicular bodies, showing gold particle **(black dots)** stained for **DILP2 (10nm, closed arrow)** and **DILP5(5nm, open arrow)** (Scale bar=100nm).

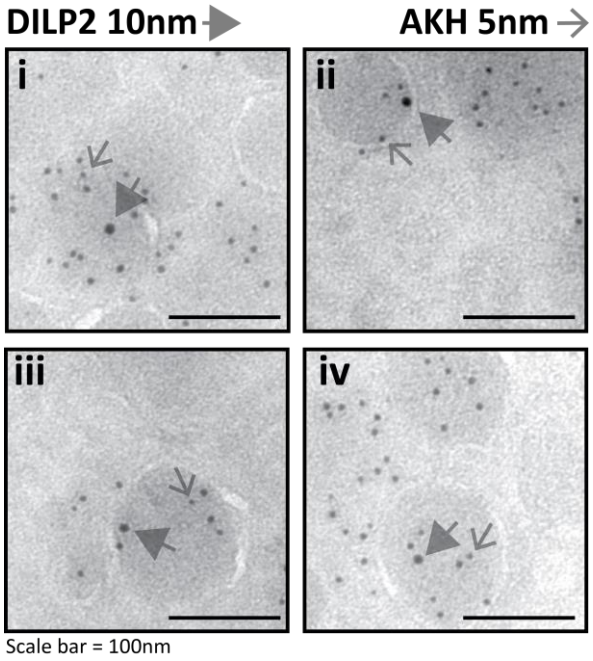

Figure 14. Vesicular co-localization of DILP2 and AKH in the Corpora Cardiaca.

Electron micrographs of immuno-gold staining of corpora cardiaca sections(70nm) of wild-type control (akh>w1118) larvae. High-magnification images of dense-core vesicles from multiple sections **(i-iv)**, showing gold particle **(black dots)** staining for **DILP2 (10nm, closed arrow)** and **AKH (5nm, open arrow)** (Scale bar =100nm)

3.1.4 Regulation of secretion of DILPs from the corpora cardiaca

In the previous section, I observed that DILP2 taken up in the CC cells is packed into the same secretory granules/DCVs as AKH, which suggested that DILP2 and AKH may be co-secreted from the CC. Larval starvation is known to induce AKH secretion from the CCs (Braco et al., 2012; Yamada, Habara, Kubo, & Nishimura, 2018); to maintain levels of circulating sugars during starvation, AKH breaks down energy stores such as glycogen in muscles (Yamada et al., 2018) and lipid stores in the fat body (Choi et al., 2015). Considering these facts together, I asked if stored DILPs 2 and 5 were secreted by the CC during larval starvation.

In order to measure DILPs in the CC upon starvation I used the experimental setup outlined in Figure 15. Briefly, 96-hour wild-type (akh>w1118) larvae were either allowed to feed normally or starved on agar. After 14 hours ring glands from the two groups of flies were fixed, stained for DILP5 and imaged on a laser confocal microscope. CC cells from starved larvae showed a significant loss of DILP5 compared to CC cells from those which fed normally (Figure 16A and 16C, left panel). This starvation-induced decrease in DILP5 in the CC might be due to a combination

of secretion and the inhibition of uptake, particularly since starvation induces inactivation and DILP retention in the IPCs (Géminard et al., 2009). To determine

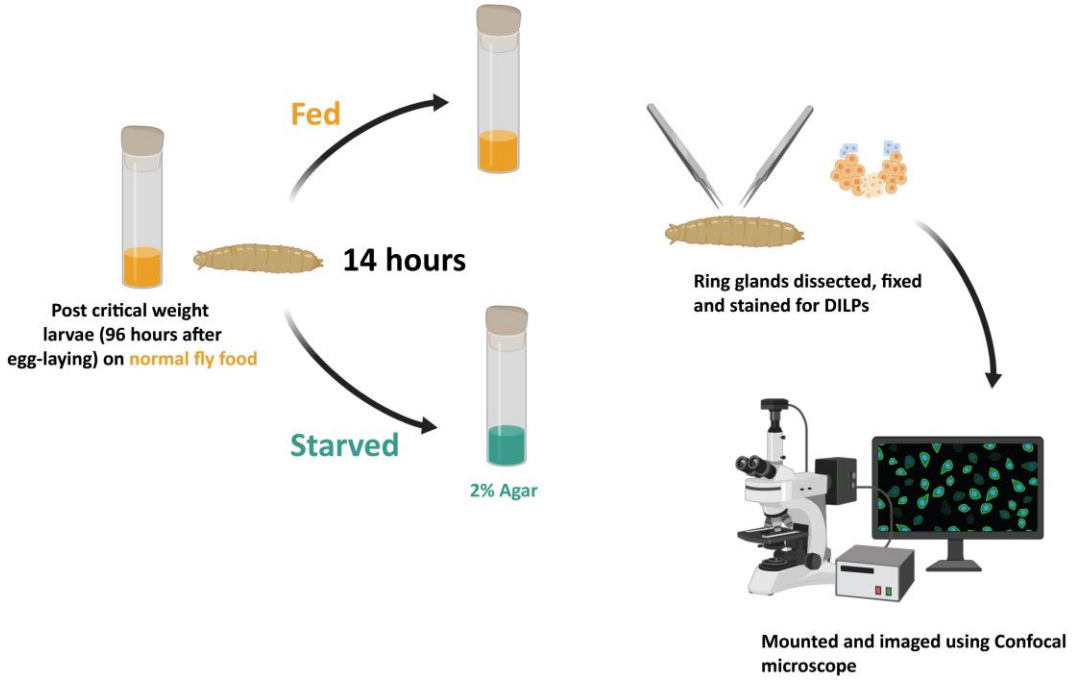

Figure 15. Experimental setup for *Drosophila* larval starvation.

Outline of experimental setup to measure effects of starvation. 96-hours old feeding L3 larvae are shifted to normal fly food or 2% agar for a 14-hour period. Subsequently, ring glands are dissected, fixed and stained for neuronal marker and DILP2 or DILP5. Ring glands are then mounted and the corpora cardiaca cells are imaged under a laser-scanning confocal microscope.

which process was responsible for the decrease in DILP5, I inactivated the CC cells by specifically expressing the human inward rectifying potassium channel Kir2.1 (Fakler, Brändle, Glowatzki, Zenner, & Ruppersberg, 1994) and repeated the experiment; CC cell inactivation prevents secretion but not uptake of DILP5. Inactivated CC cells (akh>Kir2.1) did not show a significant difference in DILP5 levels between fed and starved larvae (Figure 16B and 16C, right panel). Taken together, these data suggest that the DILP pool in the CC is secreted when the larvae are starved for 14 hours.

It remains unclear if the CC DILP pool signals in an endocrine or paracrine fashion. The CC cells make direct connections to the *Drosophila* aorta through axonal processes (Ikeya et al., 2002; Rulifson, 2002; Siegmund & Korge, 2001). To re-determine the CC connections in detail, I expressed fluorescently-labelled synaptotagmin 1 (SYT1-GFP) specifically in the CC (akh>SYT1-GFP). SYT1-GFP constructs have been routinely used to determine synaptic connections in *Drosophila* neurons (Andrews, Zhang, Trotta, & Broadie, 2002). Further, I fixed and stained RGs

for DILP2 and GFP, and observed terminal processes of the CC cells innervating the PG (Figure 17 A) with apparent central projections. Visualization of the volume of the

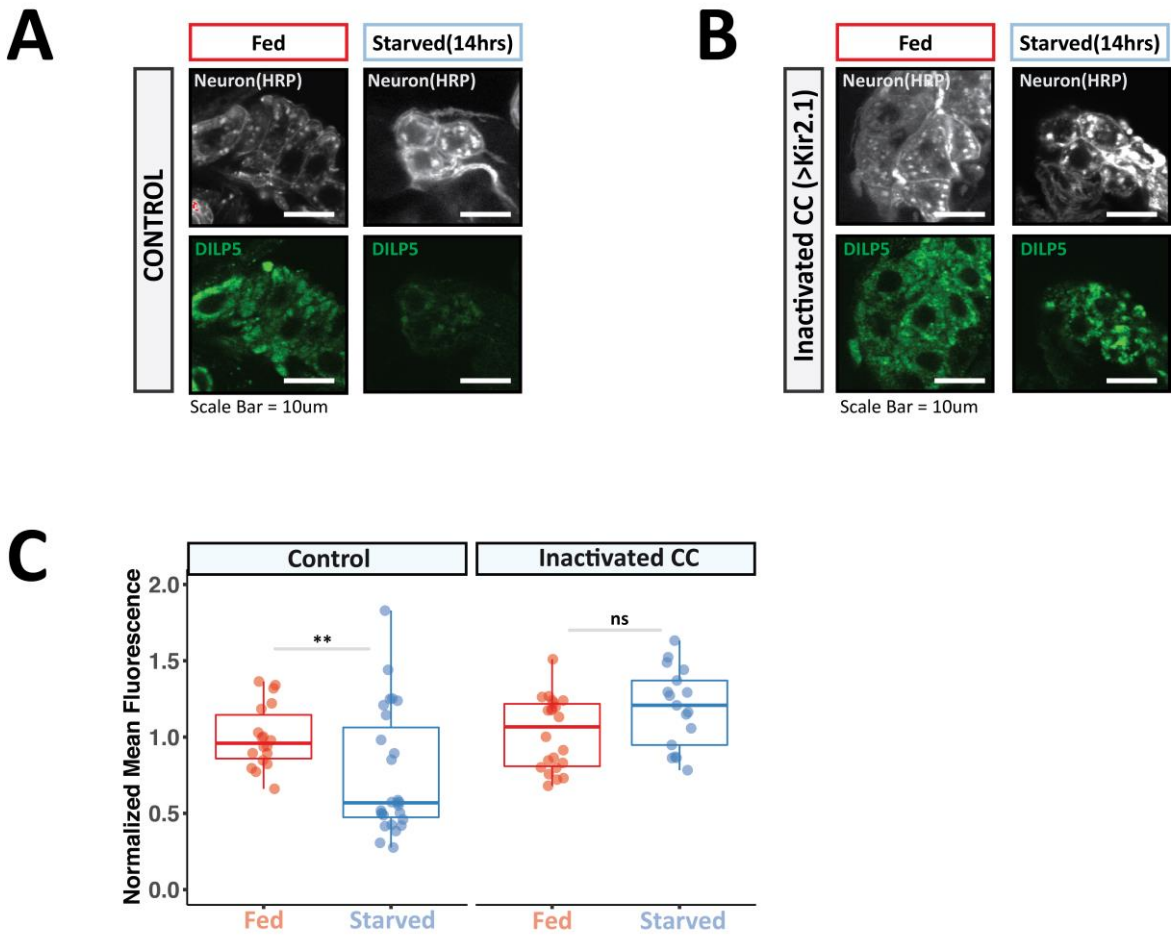

Figure 16. Secretion of Corpora Cardiaca DILP5 pool under starvation.

(A) Representative images showing a single medial plane of corpora cardiaca cell bodies (Scale bar = 10um) of **wild-type controls** (akh>w1118) under **fed** (left panel) or **starved** (right panel), stained for neuronal marker **HRP** (gray) and **DILP5** (green) (Scale bar = 10um).
(B) Representative images showing single medial plane of corpora cardiaca cell bodies (Scale bar = 10um) of **inactivated corpora cardiaca** (akh>**Kir2.1**) under **fed** (left panel) or **starved** (right panel), stained for neuronal marker **HRP** (gray) and **DILP5** (green) (Scale bar = 10um).
(C) Box plots show **DILP5** average fluorescence intensity values of **fed** and **starved** samples in **(A) wild-type controls** and **(B) inactivated corpora cardiaca**, normalized to **fed controls** (A, left panel). Each data point represents a single cell body. Multiple larvae (n>=3) used for each condition and genotype (**=p<0.01, Mann-Whitney U test).

RG in a YZ-plane clearly shows that the DILP2-containing processes do indeed run in between the PG cells (Figure 17B.i), and staining for SYT1 (GFP) (Figure 17B.ii) confirms that the projections originate from the CC. However, very little is known about how the structural organization of the PG cells accommodates the CC projections. The PG in *Drosophila* is conventionally known to be a group of tightly-packed glandular cells (Dai & Gilbert, 1991) which disintegrate during metamorphosis. Careful analysis of the whole RG electron micrographs (Figure 12A)

shows the presence of a lumen in the PG (Figure 17C). Additionally, processes containing DCVs can be seen in the PG lumen (Figure 17c, white arrows). Taken together, the above findings show that the CC project DILP2-containing processes into the PG lumen.

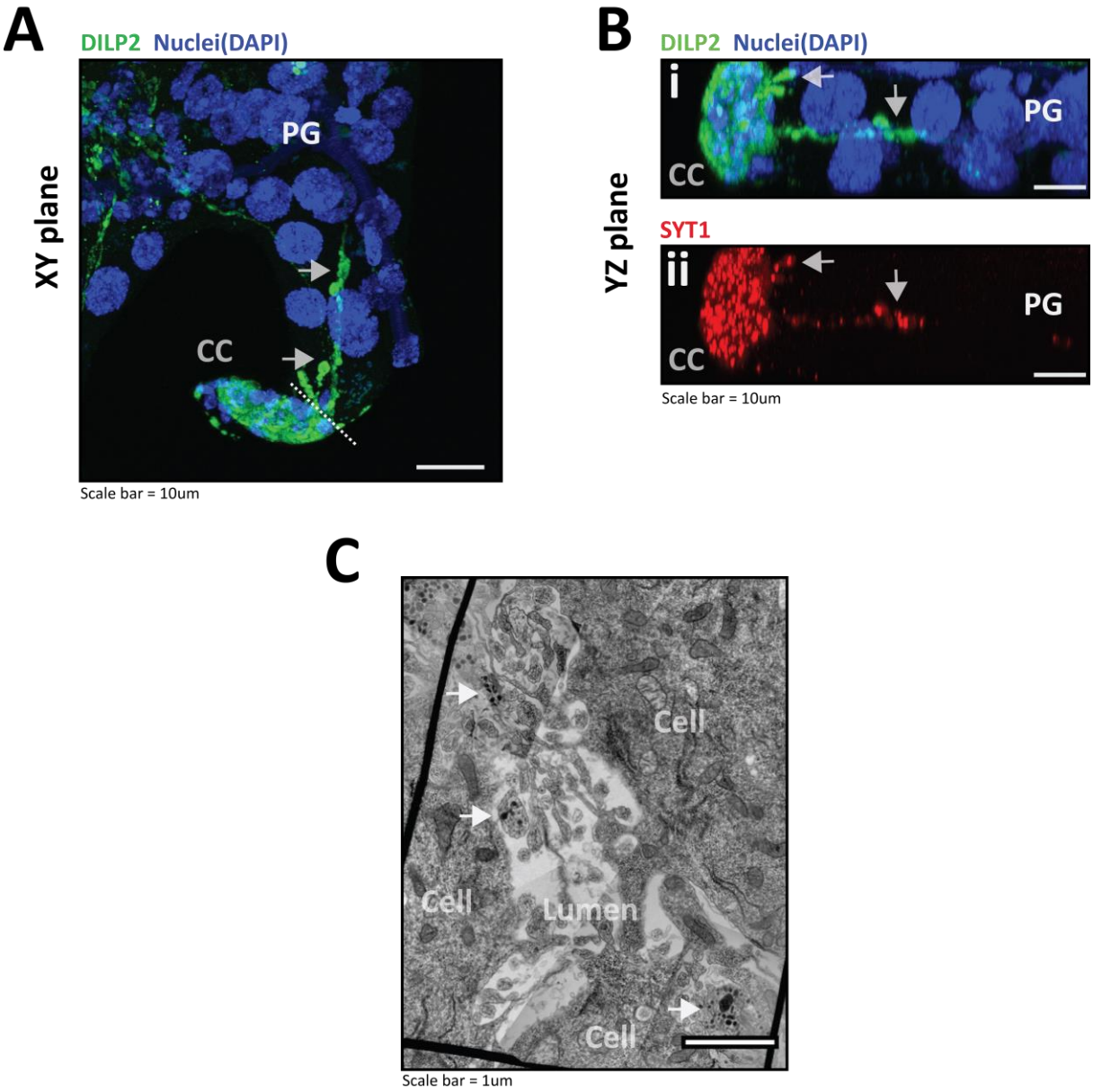

Figure 17. DILP2-positive terminal processes originating in Corpora Cardiaca innervate the Prothoracic Gland.

Maximum **(A)** z-projection or **(B)** x-projection of confocal stack of larval (akh>SYT1-GFP) ring gland (Scale bar = 10um) stained for **(A, B.i) DILP2** (green), **nuclei** (DAPI, blue) and **(B.ii) GFP** (red). Individual tissues are marked with adjoining initials – prothoracic gland (**PG, white**) and corpora cardiaca (**CC, gray**); **white arrows** mark terminal projections from corpora cardiaca.
(C) Electron micrograph showing prothoracic gland **cells**, obtained from ring gland sections (70nm) of wild-type control (akh>w1118) larvae; **white arrows** mark processes in the **lumen** containing dense-core vesicles (Scale bar = 1um)

The DILP-containing projection into the PG, together with the reduction of the DILP pool, suggests that CC signals to the PG in a paracrine fashion. To visualize CC signaling to the PG , I expressed a GFP-tagged atrial natriuretic factor (ANF-GFP) (Rao, Lang, Levitan, & Deitcher, 2001) specifically in the CC. Post critical-weight larvae (96-hour) expressing ANF-GFP in the CC were subjected to feeding or starvation for a period of 14 hours (Figure 15), following which the RGs were fixed and stained for GFP and DILP5. PG cells of fed larvae (Figure 18A.i) show a lower abundance of GFP and DILP5-positive puncta than the starved larvae (Figure 18A.ii). The corresponding quantification of GFP and DILP5-positive puncta is plotted in Figure 18B.i and 18B.ii respectively. Taken together, the results confirm that, during larval starvation, CC cells secrete up-taken DILP2 and 5 to the PG in a paracrine fashion. Moreover, the CC DILP pool is unaffected during larval feeding, indicating the importance of a novel signaling paradigm only during starvation.

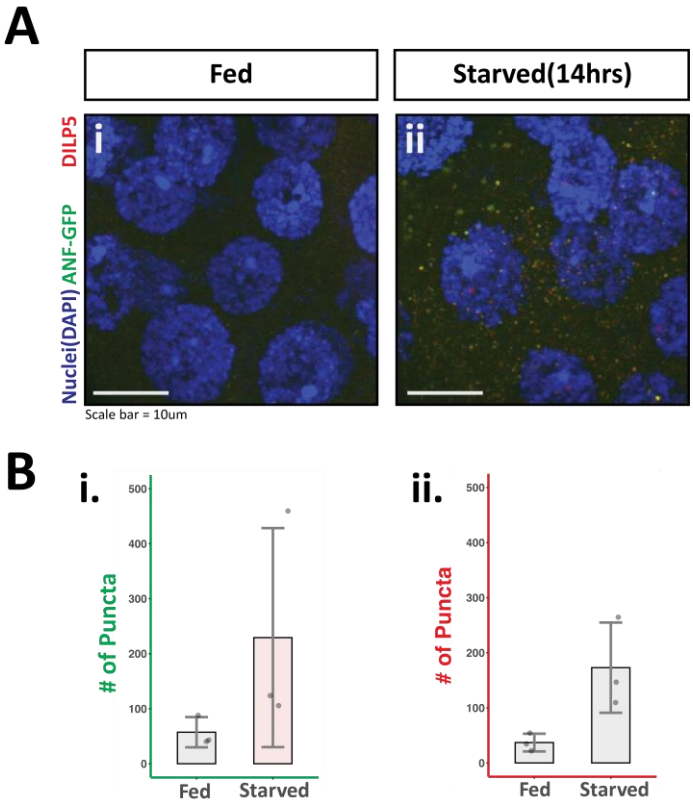

Figure 18. Corpora cardiaca signals to the prothoracic gland during larval starvation.

(A) Maximum z-projection of confocal stack of larval (akh>ANF-GFP) prothoracic gland in **(i) fed** and **(ii) starved** larvae, stained for **nuclei (blue)**, **GFP (green)** and **DILP5(red)** (Scale bar = 10um).
(B) Quantification of **(i) GFP** and **(ii) DILP5** puncta in a fixed volume of the prothoracic gland in **fed** or **starved** larvae (akh>ANF-GFP); each data point represents the number of puncta in a single prothoracic gland. Multiple larvae (n=3) used for each condition (Columns=mean; Error bars= mean+/- sd).

3.1.5 Role of corpora cardiaca DILPs in regulation of tissue size

Insulin-dependent growth of the PG cells regulates the pupariation timing and growth rate in *Drosophila* larvae (C. Mirth et al., 2005). Upregulating IIS specifically in the PG prepones pupariation, while downregulating it postpones it (C. Mirth et al., 2005); flies obtained from larvae with up- or down-regulated IIS in the PG during development have smaller or larger body size respectively (C. Mirth et al., 2005). However, the claim that observed difference in body size is primarily due to the change in pupariation time is debated. Colombani and colleagues showed that modulating IIS specifically in the PG significantly affected the rate of biomass accumulation in the larvae; upregulation of IIS in the PG resulted in slower larval growth, while downregulation increased growth rate in an ecdysone-dependent way (Colombani, 2005). In section 1.4, I observed that CC DILPs are directly secreted to the PG. I next asked if the absence of a CC pool of DILPs affects IIS activity in the PG and subsequently influences larval growth and developmental timing.

The CC-specific (akh-GAL4) RNAi-mediated knock-down of IMPL2 is a robust model to inhibit uptake of the CC pool of DILP2 and 5 without other physiological consequences, particularly compared to the harsh effects of dynamin inhibition, which ablates the CC. Hence, I reared CC-specific IMPL2 knock-down (akh>IMPL2 RNAi) larvae alongside appropriate controls (akh>w1118) and measured

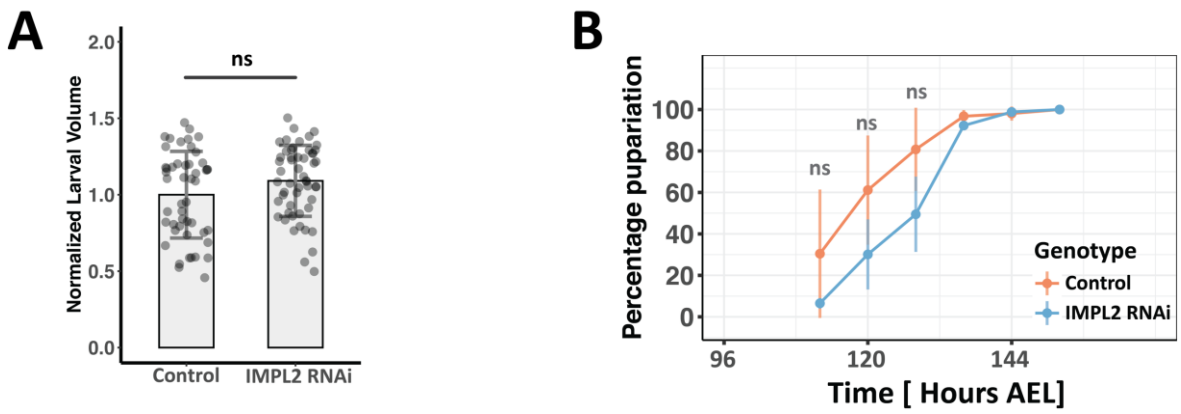

Figure 19. Effect of Corpora Cardiaca insulin pool on larval growth and developmental timing.

(A) Plot of **akh>IMPL2 RNAi** larval volume normalized to **control (akh>w1118)** at 96 hours after egg-laying. Each data point represents a single larva. (ns=p>0.05, Mann-Whitney test; Columns=mean; Error bars= mean+/- sd).
(B) Mean Percentage pupariation of **akh>IMPL2 RNAi (blue)** and **akh>w1118 (orange)** larvae plotted as a function of time (n=3,>50 larvae from each genotype). (ns=p>0.05, two-factor ANOVA; Error bars= mean+/- sd)

larval volume at a fixed timepoint (96 hours AEL). Larvae without a CC pool of DILP2 and 5 are not significantly different in size than control larvae (Figure 19A). I next measured pupariation timing in the IMPL2 knock-down and control larvae. CC DILP-absent larvae (i.e. IMPL2 knock-downs) appear to be slightly delayed to pupariation compared to the controls (Figure 19B), however the delay is not statistically significant (Figure 19B). Taken together, my data suggest that the absence of a CC pool of DILP2 and 5 does not have a significant effect on larval growth or developmental timing, at least under fed conditions. Consistent with my previous observations (Figure 18), it seems that the CC pool of DILPs do not signal to the PG during larval feeding.

Inhibiting DILP2 secretion through ablation of the IPCs has been shown to increase circulating sugar levels in the larval hemolymph (Broughton et al., 2008). Thus, I wanted to assess the contribution of the CC pool of DILPs in maintaining trehalose levels in the feeding larvae. If the CC-secreted DILPs represent a significant portion of the secreted DILPs in the larva, then absence of DILPs in the CC would result in an increase in trehalose levels. I measured trehalose concentration in 96-hour feeding larval hemolymph depleted of CC DILPs *(*akh>IMPL2 RNAi) and observed no significant difference compared to levels in control larvae *(*akh>w1118) (Figure 20). This result suggests that CC pool of DILPs does not regulate circulating sugar levels in the feeding larvae, however it might make a minor contribution to the secreted DILP level under fed conditions.

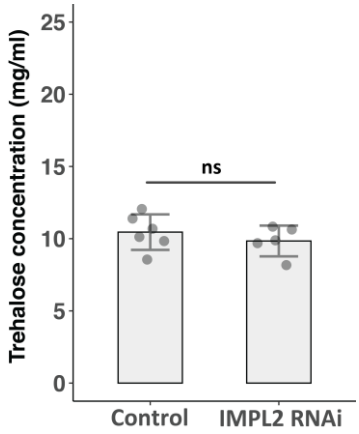

Figure 20. Effect of Corpora Cardiaca insulin pool on circulating sugar levels in larvae.

Concentration of trehalose (mg/ml) from 96-hour larval hemolymph extracts plotted for **akh>IMPL2 RNAi** and control (**akh>w1118**). Each data point represents pooled hemolymph samples from 8-12 larvae (ns=p>0.05, Mann-Whitney test; Columns=mean; Error bars= mean+/- sd).

Based on the data I have obtained so far, there does not seem to be a role for the CC DILP pool in regulating larval growth, developmental timing or circulating sugar levels. It is possible that CC DILPs regulate metabolic processes during pupal stages, so I next checked if absence of CC DILPs affects adult body size. To test this, I compared the weights of adult flies with and without CC DILPs (akh>IMPL2 RNAi v. (akh>IMPL2 RNAi) 2-3 days post eclosion. All adult flies examined had similar weights (Figure 21A). Thus, CC DILPs do not regulate final body size in adults under fed conditions.

CC DILPs were previously seen (Figure 18) to signal to the PG when starved from 96 hours AEL (post critical weight). Additionally, all of the larvae starved at 96 hours managed to pupariate and eclose into healthy adults, albeit with a smaller body size (data not shown) compared to fed larvae. Next, I asked if the CC DILPs enable growth during starvation after critical weight is reached. I starved larvae with (akh>w1118) and without (akh>IMPL2 RNAi) CC DILPs at 96 hours after egg-laying, as well as fed controls from each genotype were also reared. I collected adult flies corresponding to each genotype and treatment at 2-3 days after eclosion and measured wing areas as a readout of body size. Fed larvae (Figure 21B, red) with (left panel) or without (right panel) a CC pool of DILPs developed into adults with similar-sized wings. However, for the starved larvae (Figure 21B, blue), those without the CC pool of DILPs (right panel) developed into adults with significantly larger wings

compared to controls (left panel). In summary, the larvae lacking CC DILPs showed a smaller reduction in wing size (~18%) upon starvation compared to controls (~34%).

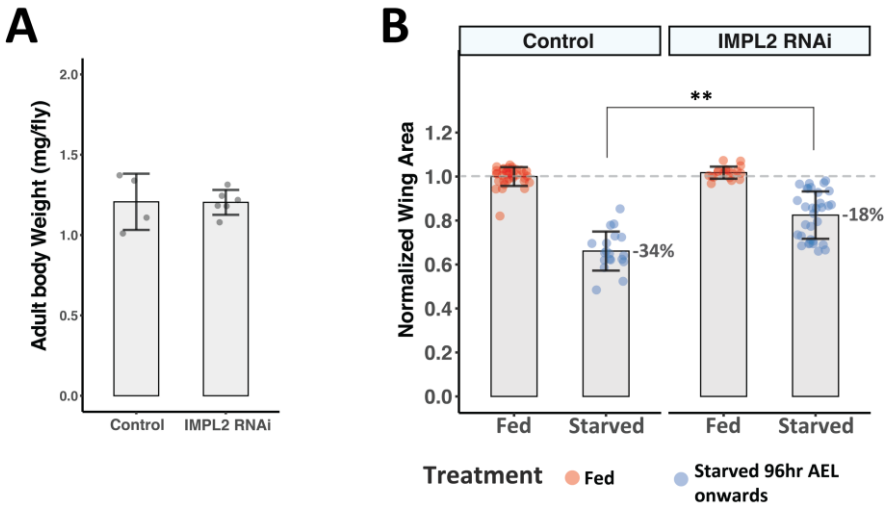

Figure 21. Effect of Corpora Cardiaca insulin pool on adult weight and organ size.

(A) Bar plot depicting weight of **akh>IMPL2 RNAi** and **control(akh>w1118)** single adult flies. Each data point represents the mean weight of a single cohort (9-10 flies). (Columns=mean; Error bars= mean+/- sd)
(B) Wing area normalized to fed controls (left panel, red). Larvae were starved from 96 hours onwards after egg-laying (AEL) until pupariation. Change in wing area is indicated as a percentage for both **akh>IMPL2 RNAi (right panel)** and **akh>w1118 (left panel)** upon **starvation (blue),** compared to **fed counterparts (red).** (**=p<0.01, Student t-test; Columns=mean; Error bars= mean+/- sd).

My results indicate that the absence of DILP secretion from the CC may down-regulate IIS in the PG and result in increased growth of tissues like the wing. Decreased IIS in the PG is known to accelerate larval growth through lessened 20E production (Colombani, 2005), however, the effect of an absent CC pool of DILP2 and 5 during starvation on pupariation timing, growth rate and circulating hemolymph sugar levels remains to be checked.

3.2 Analyzing the effects of growth temperature and insulin signaling on tissue size and shape

Tissue growth in *Drosophila* is tightly controlled through the exchange of systemic and tissue-autonomous signals during development(Géminard et al., 2006; Gokhale, Hayashi, Mirque, & Shingleton, 2016; Stieper, Kupershtok, Driscoll, & Shingleton, 2008). Like the majority of ectotherms, *Drosophila* grow faster at higher temperatures but develop into adults with smaller bodies under such conditions (Figure 22;Angilletta, Steury, & Sears, 2004), however this effect of growth temperature on body size cannot be solely explained by physical effects of temperature on enzyme kinetics and growth rate (A Clarke & Fraser, 2004; Andrew Clarke, 2003). It has been suggested that body size may be influenced by other physical factors such as oxygen availability (Frazier, Woods, & Harrison, 2001) or physiological

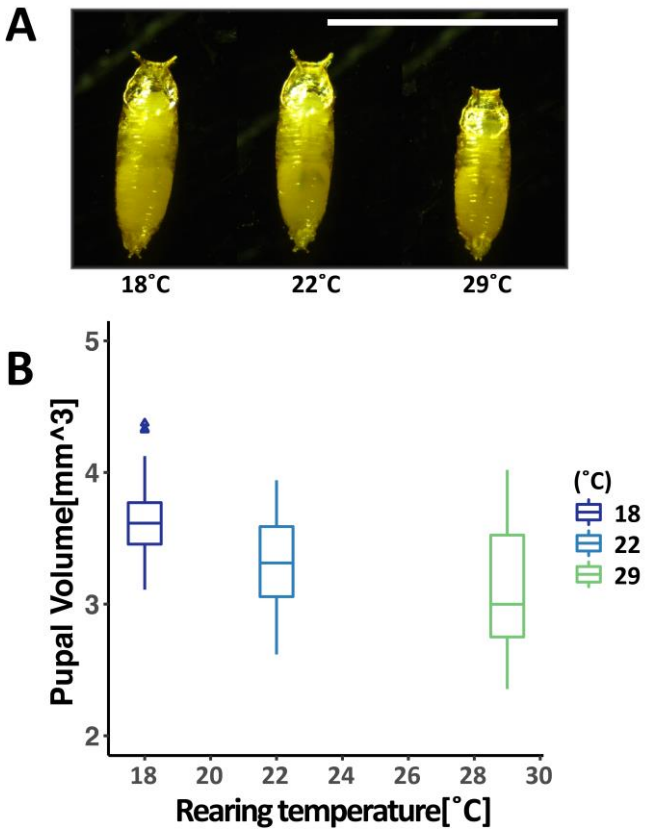

Figure 22. Effect of temperature on *Drosophila* body size.

Pupal size decreases as rearing temperature increases.
(A) Representative images; Female pupa from flies reared at 18˚C, 22˚C and 29˚C (left to right) (Scale bar= 1cm).
(B) Pupal volume calculated from flies reared under the same temperature as above (n=24 for each temperature).

adaptations like change in critical size (McDonald, Ghosh, Gascoigne, & Shingleton, 2018) (a growth-dependent checkpoint in larval development which self-adjusts to rearing temperature). While it is accepted that adjustments to critical size take place via cross-talk between growing larval tissues, no studies to date have focused on the **roles of signaling pathways in tissue size scaling according to growth temperature**.

Our lab and others have discovered multiple factors governing *Drosophila* adult wing shape and size control (Dye et al., 2017; Jülicher & Eaton, 2016; Sagner et al., 2012). Wing size and shape can be easily quantified as shown in Figure 23. Wing size is determined by drawing an outline around the wing blade region (Figure 23A). Wing shape is characterized by calculating the aspect ratio of an ellipse fitted on the wing outline (Figure 23B). As with the body, the adult wing size and shape scales with growth temperature (Figure 24). Thus, I used the adult wing as a model to **study the roles of specific signaling pathways in temperature-dependent control of tissue size.**

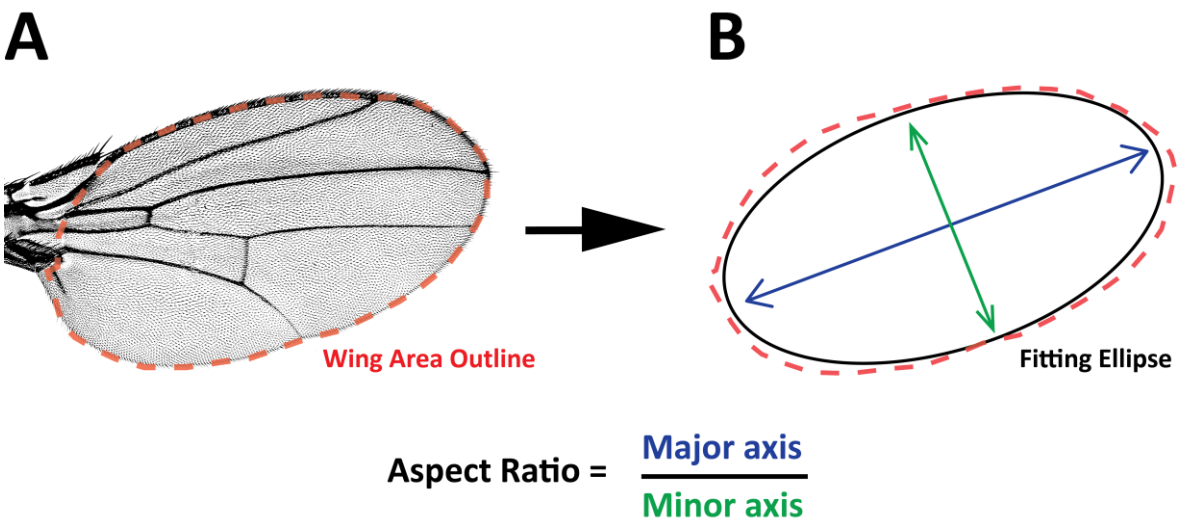

Figure 23. Quantifying *Drosophila* wing size and shape.

Dissected adult wings were mounted on glass slides and imaged.
(A) Wing size was determined by drawing an outline around the wing blade region using Fiji.
(B) Wing shape was determined by calculating the aspect ratio. An ellipse was fitted on the outlined region of individual wings and the aspect ratio expressed as the ratio of the major and minor axes.

The insulin/insulin-like growth factor signaling (IIS) pathway regulates development, growth and lifespan in *Drosophila* and other organisms. There are many examples of insulin/insulin-like signaling(IIS) regulating metabolism by controlling catabolic flux in tissues: systemic IIS regulates tissue size by coupling growth and nutrition in the developing *Drosophila* larvae (Koyama & Mirth, 2018; C. K. Mirth & Riddiford, 2007; C. K. Mirth & Shingleton, 2012). Local perturbation of IIS in wing imaginal discs (through tissue-specific expression of constitutively-active or

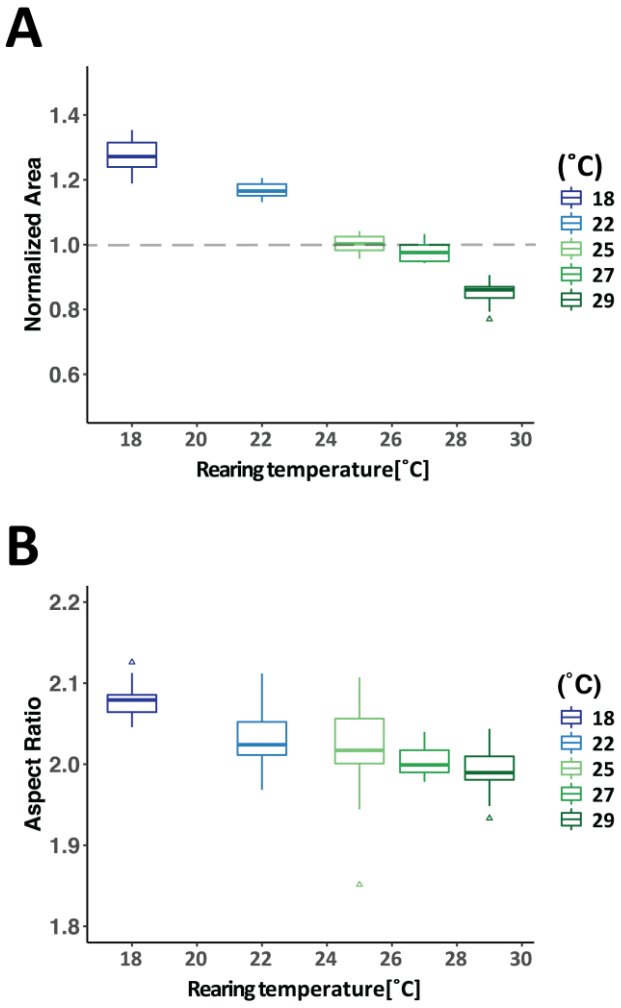

Figure 24. Effect of temperature on *Drosophila* wing size and shape.

Plots of wing size **(A)** and shape **(B)** versus rearing temperature show that wings become smaller and rounder with increasing temperature. All wing areas were normalized to the mean wing area of flies grown at optimum rearing temperature(25˚C).

dominant-negative forms of the insulin receptor) dramatically changes adult wing size and shape (Figure 25). Previous research in our lab (Brankatschk, Dunst, Nemetschke, & Eaton, 2014; Brankatschk et al., 2016) showed that a yeast-based diet confers elevated survival rate at a high growth temperature (29˚C) by upregulating a single insulin peptide, DILP2. It was also determined that genetic over-expression of DILP2 dramatically increases survival of animals eating a plant-based diet, which otherwise does not support growth or development at high temperatures. Taken together, these results present DILP2 as a key molecular player in supporting growth and development at high temperatures, and suggest insulin signaling as a possible mechanism through which diet may dictate temperature adaptation. In this chapter, I test the hypothesis that **insulin peptides DILP2 and DILP5 play an important role in temperature-mediated tissue size scaling.**

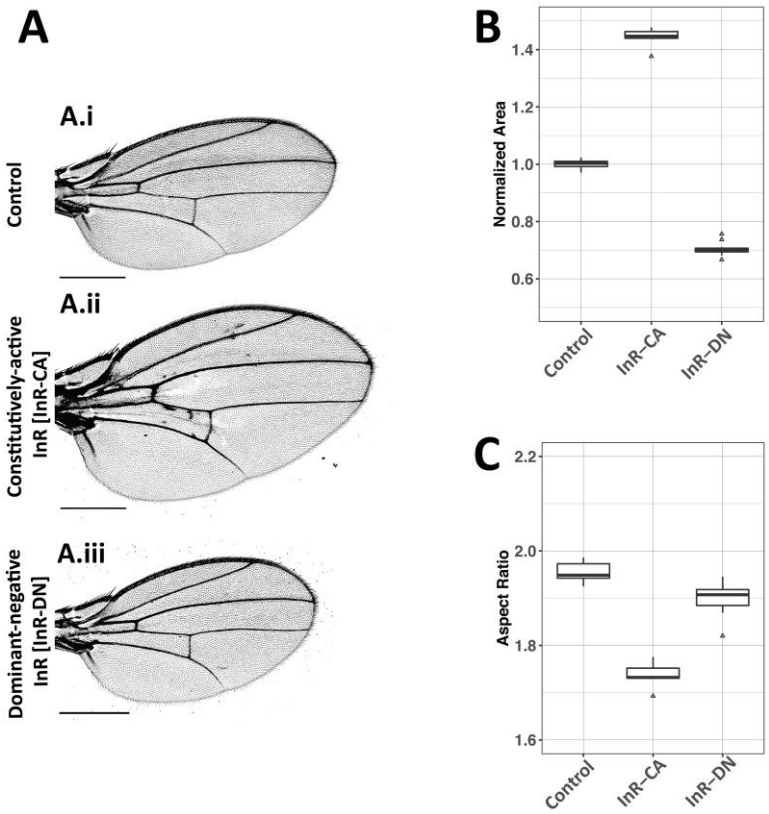

Figure 25. Local perturbation of IIS in wing imaginal discs changes wing size.

(A) Representative images of wings with **(A.ii)** constitutively active IIS (C765>**InR-CA**) and **(A.iii)** down-regulated IIS (C765>**InR-DN**) compared to **(A.i)** control wings (C765>w1118).
(B) Comparison of the wing blade area in control, InR-CA and InR-DN wings. All wing areas were normalized to the mean wing area of the control reared under same conditions.
(C) Wing aspect ratios of control, InR-CA and InR-DN flies.

3.2.1 DILP2 and DILP5 knock-out mutants show no changes in wing size scaling with temperature

Insulin peptides DILP2 , 3 and 5 are secreted from insulin-producing cells (IPCs) in the anterior larval brain (Ikeya et al., 2002). DILP3 is expressed towards the end of larval phase (Ikeya et al., 2002; Okamoto & Nishimura, 2015b), making DILP2 and 5 the major insulin peptides present during larval feeding stages. Triple mutants lacking DILP2, 3 and 5 show impaired growth and small body size, however, single DILP mutants do not show any defects in growth or size, suggesting possible redundancy between these peptides (Okamoto & Nishimura, 2015a).

In order to test whether DILP2 or DILP5 mediates a change in wing size with growth temperature, I reared DILP2 and DILP5 single knock-out flies at both 25˚C (optimal temperature) and 29˚C (high temperature). Wings of knock-out flies show similar temperature-dependent change in size as the wild-type control (Figure 26).

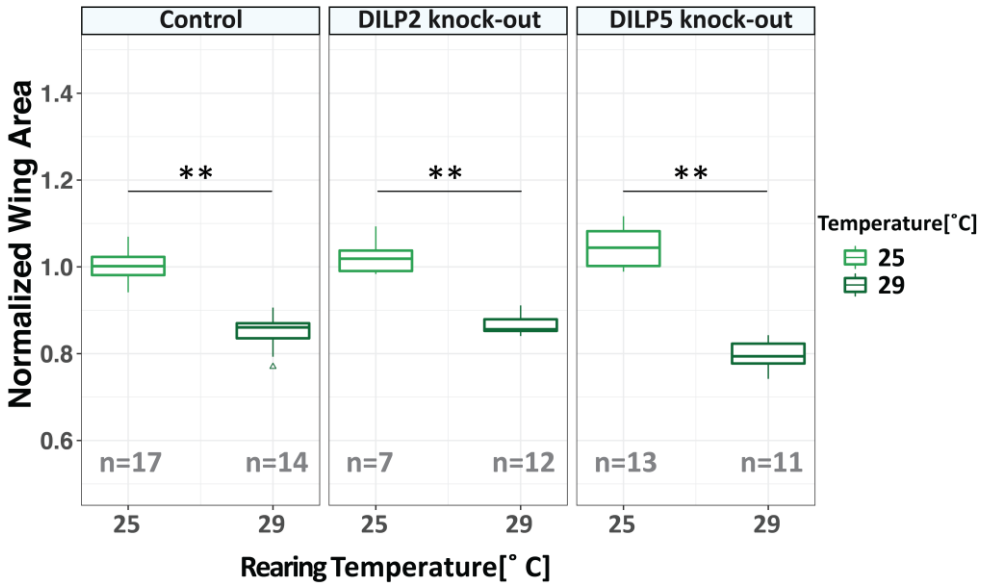

Figure 26. Temperature-dependent wing size change in DILP2 and 5 knock-out flies.

Normalized wing area versus rearing temperature for DILP2-knock-out (middle panel), DILP5-knock-out (right panel) and control (left panel) flies (** = p<0.01, Mann-Whitney U test).

Together, these results suggest that the neither the absence of DILP2 nor 5 affects the temperature-dependent scaling of wing size. It is possible that there is no significant difference because DILP2 and 5 are functionally redundant, but it is hard to design further experiments to test this hypothesis as a DILP 2/5 double knock-out mutant is larval lethal.

3.2.2 DILP2 over-expression abrogates wing and body size scaling with temperature

To determine if abundance of DILP2 or DILP5 has an effect on the scaling of wing size, I individually over-expressed DILP2 and DILP5 using an IPC-specific (dilp2-GAL4) driver. Each over-expressing line was reared at 25˚C and 29˚C along with respective control flies (Dilp2>w1118).

DILP2 over-expression (dilp2>DILP2) resulted in smaller wing size at 25˚C and no size difference at 29ºC (Figure 27A, middle panel). DILP5 over-expression (dilp2>DILP5) showed a significant reduction in wing size compared to the control only at 29˚C (Figure 27A, right panel). The smaller wing size in DILP2 over-expressing flies at 25˚C is probably due to the fact that they form smaller pupa (Figure 27C, middle panel). Similar to wing size, the pupal size also does not scale with temperature in the case of DILP2 over-expression. DILP5 over-expression does not show a change in pupal size or any temperature scaling compared to the controls (Figure 27C, right panel).

In addition to reduced wing size, DILP2 over-expression resulted in slightly rounder wings at 25˚C (reduced aspect ratio in Figure 27B, middle panel). Interestingly, temperature-dependent wing shape change showed the opposite effect (increased aspect ratio) in the case of DILP2 over-expression at 29ºC. No shape changes were observed at either growth temperature when DILP5 was over-expressed (Figure 27B). The changes in shape are small and statistically insignificant over a small temperature range, but nonetheless represent a potentially interesting trend.

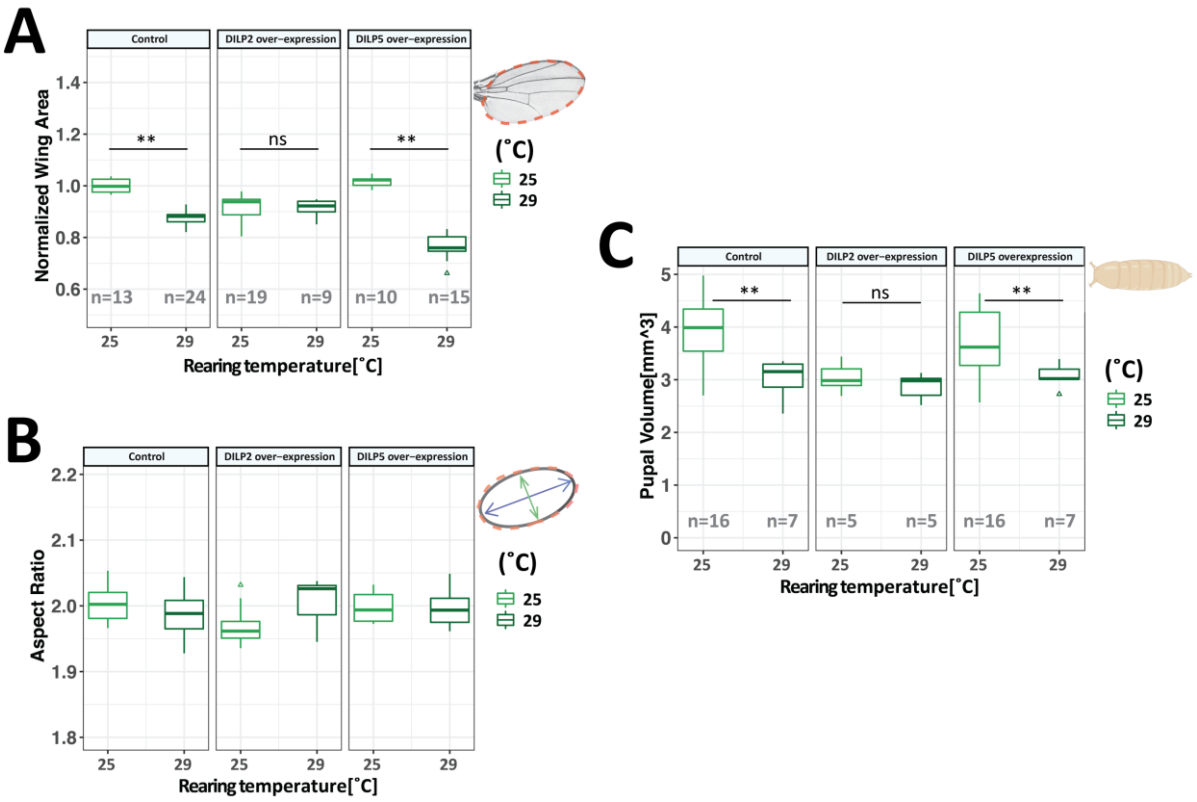

Figure 27. DILP2 over-expression reduces *Drosophila* wing and body size independent of rearing temperature.

(A) Normalized wing area versus rearing temperature for DILP2-over-expressing (middle panel), DILP-5 over-expressing (right panel) and control (left panel) flies.
(B) Wing shape versus rearing temperature for DILP2-over-expressing (middle panel), DILP-5 over-expressing (right panel) and control (left panel) flies.
(C) Pupal volume versus rearing temperature for DILP2-over-expressing (middle panel), DILP-5 over-expressing (right panel) and control (left panel) flies.
(** = p<0.01, Mann-Whitney U test).

Together these data suggest for the first time that an abundance of DILP2 mimics the wing and pupal size effects of higher rearing temperature (29˚C) at a relatively lower temperature (25˚C). Thus, I decided to investigate if there are convergent mechanisms through which both temperature and DILP2 over-expression results in smaller flies.

3.2.3 Insulin signaling in wing discs does not change with temperature or DILP2 overexpression.

Temperature affects *Drosophila* tissue size through regulation of cell size and number (French & Partridge, 1998). IIS controls tissue size in a similar way (Puig, Marr, Ruhf, & Tjian, 2003a; Scanga et al., 2000). IPCs secrete DILP2 and 5 into circulating hemolymph and they bind to insulin receptors on cells of target tissues; insulin receptors then activate the insulin pathway inside the cells through the

phosphorylation cascade involving chico and dAkt ; dAkt further phosphorylates dFOXO, retaining the latter in the cytoplasm and preventing its transcriptional response (Figure 28). The relative distribution of dFOXO between the nucleus and cytoplasm determines the insulin signaling state of the cell.

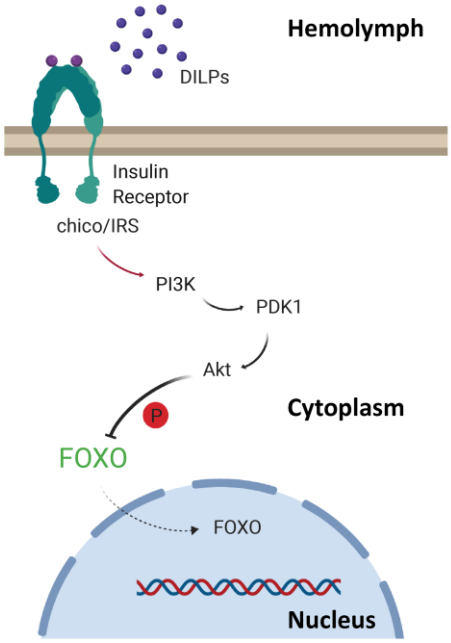

Figure 28. Schematic of the *Drosophila* insulin/insulin-like signaling pathway.

Circulating *Drosophila* insulin-like peptides (DILPs) are secreted into the circulating hemolymph from insulin-producing cells (IPCs) in the brain. DILPs bind to the *Drosophila* insulin receptor (dInR), which along with the receptor substrate chico activates the downstream enzyme, Phosphatidylinositol-3-kinase(PI3K). PI3K further phosphorylates *Drosophila* Akt which in turn phosphorylates the forkhead transcription factor FOXO. Phosphorylated dFOXO is retained in the cytoplasm; in the absence of insulin signaling, dFOXO dephosphorylates and localizes to the nucleus. In the nucleus, dFOXO activates genes required to maintain growth during starvation.

I wondered whether increased growth temperature and DILP2 over-expression result in smaller adult wings because of changes to IIS in the developing wing imaginal discs. To explore this hypothesis, I used a fly line where dFOXO was endogenously tagged with mCherry (Kakanj et al., 2016) to look at the effects of temperature and DILP2 over-expression separately.

First, I immuno-stained wing discs against mCherry from larvae grown at 3 different temperatures: 18˚C, 25˚C and 29˚C. I quantified the intensity ratio of dFOXO in the nucleus versus the cytoplasm in wing disc proper cells and observed no significant difference with growth temperature (Figure 29A, 29B and 29C). Next, I repeated the same experiment for DILP2 over-expressing larvae at 25˚C. Similarly, no significant difference in dFOXO localization was observed when DILP2 was over-

expressed (Figure 29D and 29E). Together these results suggest that there is no difference in IIS states caused by temperature or DILP2 over-expression in the developing wing disc.

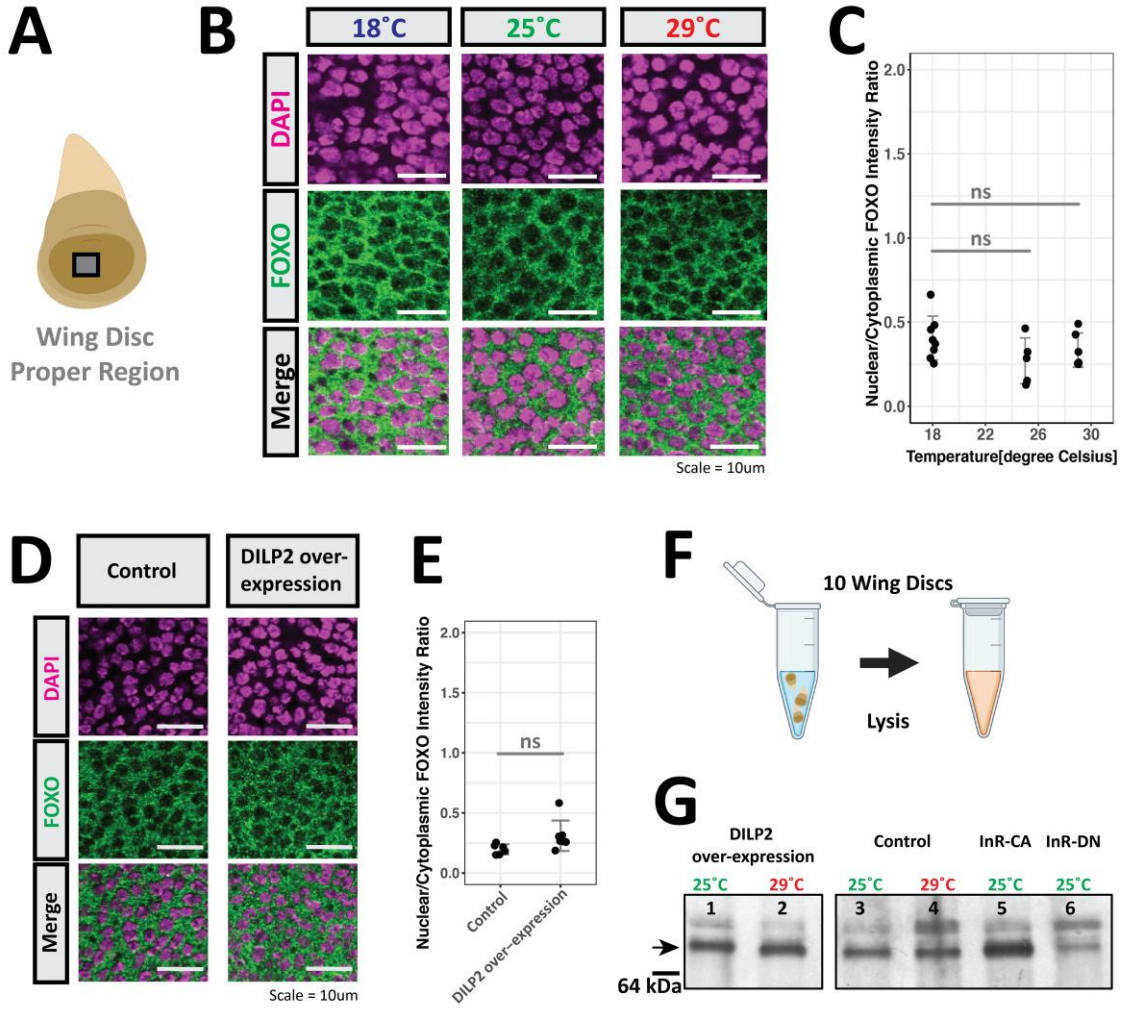

Figure 29. Insulin signaling in *Drosophila* wing discs does not change with temperature or DILP2 over-expression:

(A) Schematic cross-section of fly larva showing wing imaginal disc region. The box marks the part of the wing disc used to analyze dFOXO localization.
(B) Representative images of wing disc regions from larvae grown at 18˚C , 25˚C and 29˚C. DAPI staining shows the location of the nuclei.
(C) Quantification of the nuclear:cytoplasmic ratio of dFOXO in flies reared at the temperatures indicated. (Error bars = mean+/- sd; ns= p>0.01, Mann-Whitney U test)
(D) Representative images showing localization of dFOXO in control (left column) and DILP2 over-expressing flies (right column) reared at 25˚C.
(E) Quantification of localization results from (D); each dot represents a single wing disc from one larva. (Error bars = mean+/- sd; ns= p>0.01, Mann-Whitney U test)
(F) Schematic of western blot sample preparation. Cohorts of 10 similar-sized wing discs were lysed together from each sample condition and the whole lysate was used in western blot analysis. No total protein control was used.
(G) Western blot analysis of wing discs from DILP-2 over-expressing and control flies reared at 25 and 29°C (Lanes 1-4). Flies with wing-disc specific (C765-gal4) up-regulation (InR-CA) or down-regulation (InR-DN) of the insulin pathway serves as positive and negative controls (Lanes 5 & 6). The band corresponding to phosphorylated-Akt is indicated by the black arrow.

To confirm the previous observation, I measured phosphorylated dAkt levels in the wing disc as another indicator of IIS state. Freshly dissected L3 wing discs were snap- frozen in lysis buffer and lysed in cohorts of 10 discs (Figure 29F). I performed a western blot on the whole lysate using an antibody specific to the phosphorylated form of dAkt (Figure 29G) and used wing-specific up- and down-regulation of IIS as positive and negative controls respectively. The blot results confirmed that the level of phosphorylated dAkt did not change with DILP2 over-expression nor with growth temperature (Figure 29G).

3.2.4 DILP2 over-expression reduces larval growth but does not change developmental time.

Growth rate and developmental timing are the two ways in which body size can be set in flies (Nijhout, 2015). Temperature influences both of these, regulating body size in opposing ways: high rearing temperature increases growth rate but produces smaller flies by shortening developmental time (Angilletta et al., 2004).

I asked if DILP2 over-expression reduces body-size by slowing systemic growth or by regulating the developmental process. I reared larva at 25˚C or 29˚C until 96 hours after egg-laying (AEL) at which time I took out feeding larvae and used a dissection microscope to measure larval area by manual segmentation. Larvae in which DILP2 is over-expressed are significantly smaller than wildtype controls when grown at either temperature (Figure 30A and 30B). Thus, an abundance of DILP2 decreases larval size independently of rearing temperature.

Next, I measured percentage of pupariation as a function of time to determine rate of development. Animals grown at 29^{o}C reached a higher percentage of pupariation at earlier timepoints than those grown at 25˚C (Figure 30C.i). Larvae overexpressing DILP2 developed slightly faster at 25˚C (Figure 30C.ii) compared to wildtype controls at the same temperature (Figure 30C.i), but not at 29˚C. Also, animals over-expressing DILP2 did not show scaling of developmental rate with temperature (Figure 30C.ii).

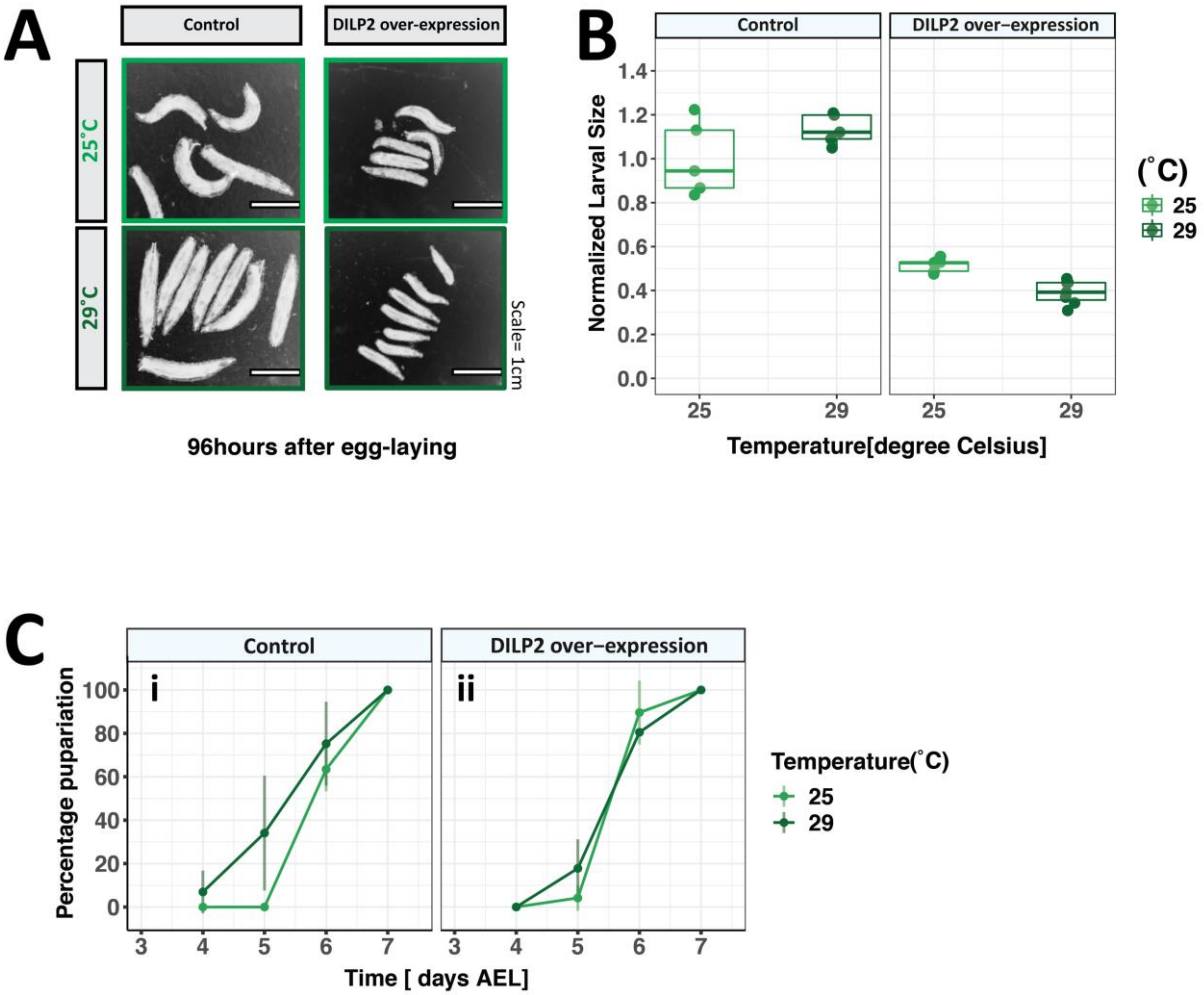

Figure 30. Larvae in flies over-expressing DILP2 grow more slowly, but show no change in pupariation timing.

(A) Representative images of control and DILP2-overexpressing larvae at 96 hours after egg-laying. Rows indicate rearing temperature (same colour) and columns indicate genotype.
(B) Larval volume of control (left panel) and DILP2 over-expressing flies (right panel) reared at 25 and 29°C.
(C) Plot of percentage pupariation versus time after egg laying (AEL) in control (**C.i**) and DILP2-overexpressing flies (**C.ii**) at two different rearing temperatures.

Together, the data suggest that DILP2 over-expression results in smaller tissues predominantly by slowing systemic growth and not via accelerating stages of development. Additionally, when grown at 29˚C, DILP2 over-expressing flies have a smaller final body size even though there is no change in developmental timing. Thus, the small acceleration in pupariation timing observed at 25˚C cannot account for the large change in resulting body size.

3.2.5 DILP2 over-expression selectively upregulates insulin signaling in the prothoracic gland

Reduced larval growth without a change in developmental time is observed with selective upregulation of IIS in the prothoracic gland (PG) (Colombani, 2005). Upregulation of IIS in the PG causes excess growth of PG cells, which leads to increased ecdysone production (Yamanaka et al., 2013). The higher levels of ecdysone restrict growth of larval tissues like the wing disc.

I wondered if DILP2 over-expression affected larval growth through selective signaling to the PG, in which case a reduced larval growth phenotype would be consistent with DILP2 over-expression. To test this hypothesis, I reared and dissected larva over-expressing DILP2 at 96hrs AEL and immuno-stained the PG using phospho-dAkt to indicate IIS pathway activity.

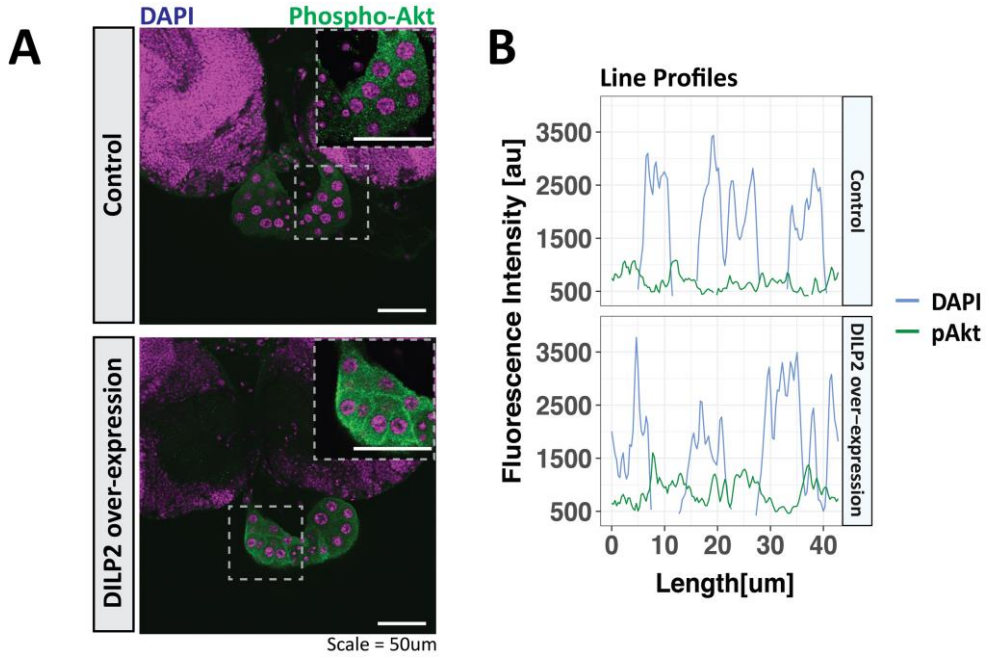

Figure 31. DILP2-over-expression upregulates the insulin pathway in the prothoracic gland.

(A) Representative images of the prothoracic gland (white dashed box, inset) of control (top) and DILP2 over-expressing larvae (bottom) at 96 hours AEL. Phosphorylated-Akt is shown in green and DAPI is shown in purple.
(B) Line profile quantification of respective prothoracic gland images shows almost two-fold higher intensity of phosphorylated-Akt in DILP2 over-expression compared to the controls. The cytoplasmic signal can be identified by the absence of DAPI intensity.

PG cells in larvae over-expressing DILP2 showed a higher amount of cytoplasmic phospho-dAkt compared to the wildtype control (Figure 31A; the nuclei are marked with DAPI to differentiate between nucleus and cytoplasm). The linear intensity profiles in Figure 31B show an almost a two-fold increase in the intensity of phospho-dAkt.

These data suggest that the reduced growth phenotype observed in flies over-expressing DILP2 is mediated through selective signaling in the PG. However, the findings in this chapter beg the following questions: Why does DILP2 but not DILP5 over-expression reduce growth, and what is the mechanism through which DILP2 might selectively signal to the PG?

3.3 Analyzing the effect of dietary lipids on insulin signaling

In order to survive and populate diverse environments, *Drosophila* adapts to different food resources (Holmbeck & Rand, 2015) in both behavior and physiology. Previous work in our lab (Brankatschk et al., 2018), has shown that the feeding preference of adult flies changes from yeast lipids to plant lipids at low ambient temperatures. In contrast, yeast lipids are preferred at high ambient temperatures. Feeding on plant or yeast lipids has a profound effect on the number of carbons and degree of unsaturation in the side chains of phospholipid fatty acids. Furthermore, flies fed on plant lipids show decreased membrane order at low temperatures (Brankatschk et al., 2018).

Unpublished data from colleagues (Brankatschk et al., 2016) showed that feeding on yeast lipids during larval stages, confers better survival to flies living at higher temperatures compared to feeding on plant lipids. Feeding on yeast lipids was shown to up-regulate DILP2 - one of the major insulin-like peptides in *Drosophila*. Insulin-producing cells (IPCs), which produce DILP2, are activated when larvae feed on yeast lipids (Brankatschk et al., 2014). DILP2 gain-of-function flies show improved survival when feeding on plant lipids even when maintained at a higher temperature. Conversely, larval survival at high temperature was compromised in DILP2 knock-out larvae feeding on yeast lipids (Brankatschk et al., 2016). These previous studies have focused only on organism-level function of DILP2 in mediating effects of dietary lipids. It is currently not understood **how dietary lipids regulate insulin secretion and signaling to target tissues in feeding larvae**. Our group has already generated a temporal and spatial lipidome resource for plant and yeast-lipid diet in the larvae (Carvalho et al., 2012) – a useful resource to establish a causal relationship between tissue lipid composition and IIS activity.

In this chapter, **I test the effect of plant and yeast lipids on insulin/insulin-like growth factor signaling (IIS) in developing larval tissues such as the wing imaginal disc.**

3.3.1 Survival of plant- and yeast-lipid fed larvae at high temperature is independent of DILP2

Brankatschk and colleagues proposed that a yeast-lipid (YF) diet ensured pupariation at high temperatures (30˚C) through the upregulation of DILP2 expression. Flies lacking DILP2 don't pupariate at high temperature as successfully as do wild-type controls, and developmental success at high temperature is low in flies reared on a plant-lipid diet (PF) (Brankatschk et al., 2016, unpublished).

To further this investigation, I decided to reproduce the results obtained by Brankatschk and colleagues. First, I reared wild-type Oregon R larvae on PF or YF media at 25ºC and measured pupariation timing. Consistent with previous observations (Brankatschk et al., 2014), PF fed larvae showed slower development compared to larvae on a YF diet (Figure 32A); the PF-fed larvae pupariation is delayed by 48 hours compared to YF-fed counterparts.

Second, I reared DILP2 knock-out larvae along with controls on PF or YF media at 30˚C to measure pupariation as an indicator of developmental success. Both PF and YF fed controls (w1118) showed a high percentage of pupariation and were not significantly different from each other (Figure 32B, left panel). Surprisingly, DILP2 knock-out larvae successfully developed both on PF- and YF-diets (Figure 32A, right panel). No effect of dietary lipids was observed on pupariation or survival at a high rearing temperature.

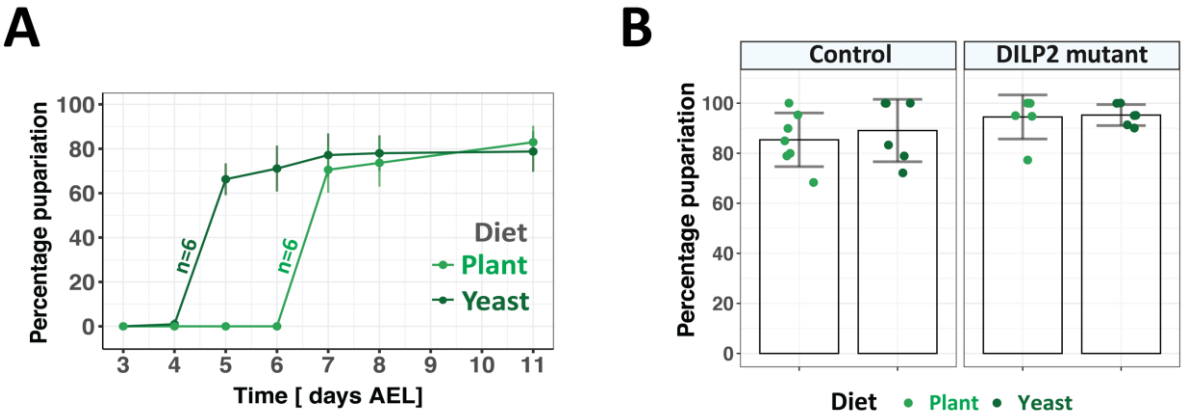

Figure 32. Effect of diet on high temperature survival in DILP2 knock-out mutants.

(A) A plot of pupariation versus time AEL for **PF-(light green)** and **YF-fed(dark green) wild-type larvae** reared at high temperature**.** (n=6, 120 larvae/diet; Error bars = mean +/- sd).
(B) Comparison of final percentage pupariation of control and DILP2 knock out flies fed PF- or YF-diets. (Columns = mean; Error bars = mean +/- sd).

Taken together, my results contradict previous reports (Brankatschk et al., 2016, 2018); they suggest that yeast lipids do not enable higher developmental success than do plant lipids at a rearing temperature of 30˚C and that DILP2 is not required for survival at high temperatures.

3.3.2 Dietary lipids do not affect insulin signaling in wing discs *in-vivo*

Organism-wide IIS upregulation through genetic perturbation increases developmental rate (Walkiewicz & Stern, 2009). We have seen that PF-fed flies show a decreased developmental rate compared to YF-fed counterparts (Figure 32A). It has been hypothesized that this slow development might be due to the presence of different sterols in the PF and YF diets (Carvalho et al., 2012, 2010), however, Brankatschk et al., 2014 showed that a YF diet activates IPC neurons in the larval brain significantly more than a PF diet does. Furthermore, YF-fed larvae have higher levels of circulating DILP2 in the hemolymph, and larval tissues like the salivary glands in YF-fed larvae also show higher insulin signaling activity (Brankatschk et al., 2014).

Given the apparent irreproducibility of data reported in Brankatschk et al., 2016, I wanted to confirm the diet-dependent upregulation of insulin signaling in larval tissues such as the wing disc. Since YF- and PF- fed larvae show different developmental rates, it was key to compare their IIS activity at a similar developmental stage. To accomplish this, I staged 0-3hr wandering L3 larvae from each diet, ignoring the time taken to reach the wandering stage. Additionally, I visually compared wing imaginal discs of similar size from each of the respective diets (Figure 33A) and assumed that any decrease in systemic DILP levels would be reflected in insulin-pathway activity in discs of similar size. I then used the ratio of nuclear:cytoplasmic localization of dFOXO to quantitatively compare the IIS state of wing discs from flies on different diets (see previous chapter for method details). Wing discs from larvae feeding on a PF diet showed no significant difference in dFOXO localization compared to the those fed a YF diet (Figure 33B). These results are orthogonal to previously reported findings that YF diet upregulates insulin signaling in larval tissues like the salivary glands and fat body (Brankatschk et al., 2014). Imaginal and larval tissues might respond differently to circulating DILPs.

The results shown here indicate that a YF diet speeds up growth and development compared to a PF diet without affecting the IIS pathway in the wing

disc, as measured by dFOXO localization. When circulating levels of DILPs are low, dFOXO translocation to the nucleus upregulates the expression of *Drosophila* Insulin Receptor (dInR) (Puig et al., 2003b). This type of feedback regulation ensures fly growth and proliferation through binding of DILPs to the increased number of insulin receptors. It also requires increased dFOXO in the nucleus to maintain high expression of dInR. Surprisingly, that is not what I directly observe in the wing imaginal discs of PF- or YF-fed larvae. Rather, at first glance, the data presented here suggest that there is no difference in circulating DILP levels in larvae fed the different diets.

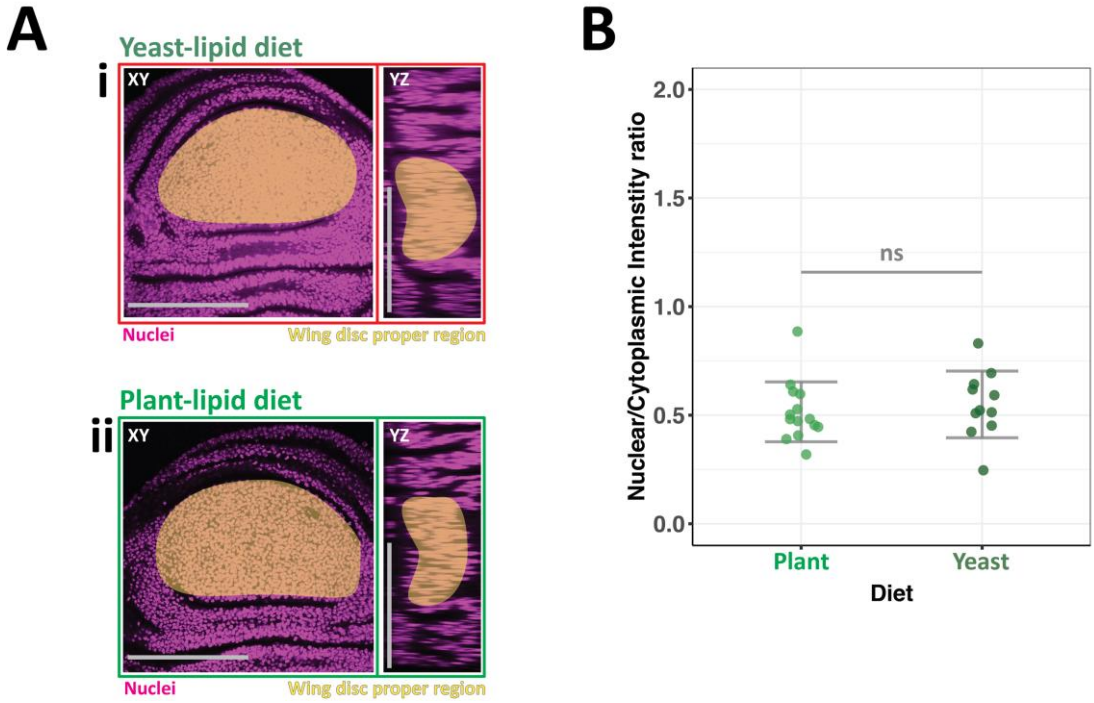

Figure 33. Diet does not affect insulin signaling in the wing disc.

(A) Single representative slices of wing discs in the XY and YZ plane. dFOXO localization was measured in discs of similar size from **(A.i)** YF-fed or **(A.ii)** PF-fed wandering larvae. The nuclei were stained with DAPI(magenta) and the wing disc proper region is marked in yellow.
(B) Quantification of **dFOXO** nuclear to cytoplasmic intensity ratio in wing disc cells of larvae fed on PF or YF diet (ns = p>0.01, Mann-Whitney U test; Error bars = mean +/- sd).

3.3.3 Quantification of insulin sensitivity using wing disc explant culture

In the previous section, we saw that wing discs from PF and YF-fed larvae show similar insulin pathway activity determined by dFOXO localization in the nucleus and cytoplasm. This similarity in insulin pathway activity could be the result of one of two scenarios - **similar levels of circulating DILPs in flies fed both diets** or a **diet-dependent change to insulin sensitivity in target tissues**. It is unlikely

to be the first scenario as it was previously shown that YF-fed larvae have higher levels of circulating DILP2 than their PF-fed counterparts (Brankatschk et al., 2014). Elaborating on the second scenario, similar pathway activity or dFOXO localization of in a tissue may arise due to a combination of different amounts of circulating insulin between diets and corresponding change in insulin sensitivity.

Lipidomic analysis done in our lab (Carvalho et al., 2012) showed that diet influences the composition of membrane lipids in larval tissues, including the wing imaginal disc. Recent evidence from cell lines shows that activation of the membrane-embedded insulin receptor and its tyrosine-kinase domain is dependent on the membrane lipid environment (Mariniello et. al., 2019). Additionally, sterols were found to regulate the degree of insulin receptor auto-phosphorylation through formation of ordered domains in HEK 293T cells (Delle Bovi, Kim, Suresh, London, & Miller, 2019). In flies, Carvalho and colleagues also reported substantial changes in sterol composition, fatty acid side-chain length and degree of saturation in wing discs derived from larvae reared on PF or YF diets. Thus, I wanted to determine if membrane lipid composition influences insulin sensitivity of wing imaginal disc by modulating insulin receptor activation.

In order to accurately determine the insulin sensitivity of PF- and YF-derived wing discs, it was important to tightly control the concentration of insulin ligands. Although genetic tools in *Drosophila* are advanced, controlling the concentration of circulating DILPs *in-vivo* with micromolar precision is nearly impossible. To overcome this challenge, I modified the wing disc explant culture system developed by Dye et. al., 2017. Initially optimized to study tissue growth and cellular rearrangements over a long period of time, this protocol can be easily adapted to study the effects of ligands such as insulin/DILPs over a short, 2-hour time period (Figure 34A). After 2 hours of incubation, wing discs were fixed and stained for dFOXO. Similar to the method used in previous sections, insulin pathway activity was determined by quantifying the dFOXO intensity in the nucleus and cytoplasm.

The next step was to determine if DILPS 2 and 5 were able to activate the insulin pathway in cultured wing discs. It is important to note that DILPs 2 and 5 have not yet been synthesized on a large scale and so have limited use in explant tissue culture experiments. Instead, a saturating concentration of bovine insulin (5ug/ml) can be used to activate insulin pathway in wing disc culture (supplementary information; Dye et. al., 2017). I obtained a small aliquot of synthesized DILPs 2 and 5 from the Tatar lab (Post et al., 2018) and incubated wing discs in supplemented

Graces medium (5% FBS and 20nM 20-hydroxy-ecdysone) with either 100nM DILP2, 100nM DILP5 or bovine insulin for 2 hours. Wing discs cultured without any hormone were used as a negative control. Wing disc proper cells in which DILP2, DILP5 and bovine insulin were added showed similar ratios of nuclear to cytoplasmic dFOXO localization (Figure 34B and 34C). Discs cultured without any insulin showed both high variability in dFOXO localization and an increase in nuclear:cytoplasmic localization (Figure 34B,C). This suggests that discs cultured without insulin have reduced insulin pathway activity.

The similar effects of DILPs and bovine insulin on dFOXO localization in wing discs suggest that bovine insulin might be used as an alternative to synthesized DILPs. Additionally, different concentrations of bovine insulin can now be used to generate a dosage curve for activation of the insulin pathway measured by dFOXO localization. Dosage curves obtained from wing discs of larvae reared on YF and PF diets might help us to determine diet-dependent changes in tissue insulin sensitivity.

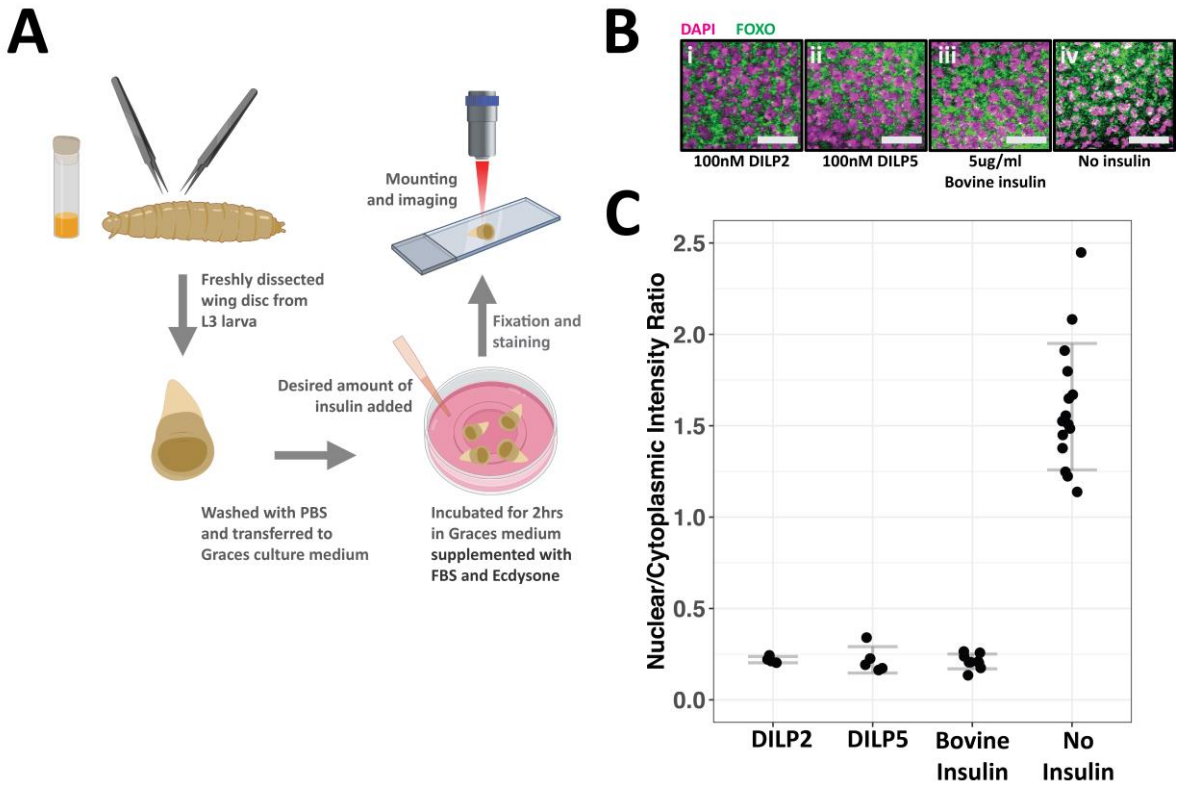

Figure 34. Ex-vivo wing disc insulin sensitivity assay.

(A) Schematic of the wing disc culture system modified from Dye et. al. 2017.
(B) Representative images of wing disc proper cells with **nuclei (DAPI, magenta)** and **dFOXO (green)** labelled. Discs were either incubated with **(B.i)** 100nM DILP2, **(B.ii)** 100nM DILP5 , **(B.iii)** 5ug/ml bovine insulin or **(B.iv)** no hormone for 2 hrs.
(C) Quantification of dFOXO nuclear to cytoplasmic intensity ratio in wing disc cells under each of the above treatments. (Error bars = mean +/- sd).

3.3.4 Dietary lipids change insulin sensitivity of wing discs.

At present, we do not have a clear understanding on the effect of tissue lipid composition on underlying cell signaling systems such as the insulin pathway. To date, the effects of membrane lipids on the insulin pathway have only been tested in cell culture (Delle Bovi et al., 2019) - never at a tissue level. The assay optimized in the previous section enables me to accomplish tissue-specific effects of membrane lipid composition on insulin sensitivity of the wing imaginal disc. Furthermore, this assay gives me the ability to modulate the lipid composition of tissues in a physiologically relevant manner (*i.e.* through diet).

In order to generate an insulin dosage curve for YF or PF-derived wing discs, it was essential to choose an appropriate incubation period, that would accurately reflect the steady-state insulin pathway activity. To determine that incubation time, I dissected wing discs from PF or YF-fed larvae and cultured them without insulin for periods of 15 , 30, 45, 60 and 120 minutes. I fixed and immuno-stained discs from each time point for dFOXO as a readout of insulin pathway activity. Freshly dissected uncultured wing discs were used as positive controls. Both PF- and YF-derived wing discs showed stable dFOXO localization by 60 minutes; no further change in localization was observed after 120 minutes (Figure 35A). Compared to YF-derived wing discs (Figure 35A.ii), PF-derived wing discs showed a larger variation in dFOXO localization from 15-45 minutes of incubation (Figure 35A.i). This variation can be easily seen by in a plot of variance versus incubation time (Figure 35B). YF-derived wing discs only showed considerable initial variation at the 15 minutes timepoint (Figure 35A.ii and 35B.ii).

Taken together, these results suggest that, independent of diet, dFOXO localization in wing discs reaches a steady state after 1-hour of incubation with insulin, and does not change until at least 2 hours of incubation time. Therefore, the 2 hour incubation period can be safely used to determine insulin sensitivity of wing discs. These observations point towards previous findings (Puig et al., 2003b), which show that in the absence of insulin dFOXO translocation to the nucleus is necessary for insulin receptor expression, and that this in turn upregulates activity of the insulin pathway. High nuclear localization of dFOXO at 15 minutes followed by subsequent cytoplasmic localization suggests feedback regulation (as proposed by the authors of the previous study) either through dInR auto-activation or the action of residual quantities of insulin present in media components (FBS) . Interestingly,

dFOXO localization seems to stabilize more quickly in YF-derived wing discs than in PF-derived ones.

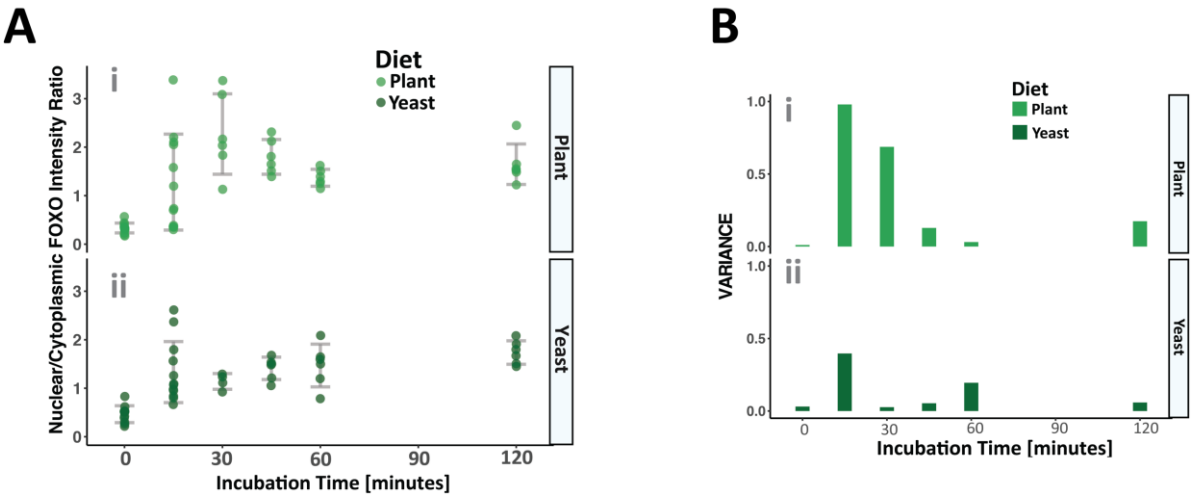

Figure 35. Steady-state of wing disc insulin activity.

(A) dFOXO nuclear:cytoplasmic intensity ratios from **yeast(dark green)** or **plant(light green)** lipid diet-derived wing discs plotted against incubation time in culture without insulin (Error bars = mean +/- sd).
(B) Plot of dFOXO intensity ratio variance from (A) at each incubation timepoint.

Having determined the assay conditions for wing disc insulin sensitivity assay, I performed the experiment with four non-saturating of concentrations bovine insulin – 10, 100, 200 and 500 ug/ml – and a no hormone control. All treatments were incubated for two hours, after which discs were fixed and immuno-stained for dFOXO. YF-derived discs showed greater cytoplasmic dFOXO localization compared to PF-derived discs at all concentrations of bovine insulin, while no significant differences were observed between the PF- and YF-derived discs in the no-hormone controls (Figure 36A). These data suggest that YF-derived discs have higher insulin pathway activity compared to PF-derived discs at same concentrations of insulin ligands. The increased insulin sensitivity of YF-derived discs can be better visualized in a dosage response curve using logarithmic values of ligand concentration (Figure 36B). Smooth fitting the curve to the dFOXO intensity ratio values shows that PF- and YF-derived discs might have similar insulin pathway activation at very low concentrations (<10ng/ml), but clearly diverge as insulin concentration increases (Figure 36B). Taken together, the results in this section suggest a dietary lipid-dependent change in sensitivity of wing discs to insulin. However, this experiment needs to be repeated with a larger sample number to determine an EC50 value of bovine insulin for wing discs derived from the respective diets. Diet may impact the

expression of insulin pathway components including the insulin receptor, but further experiments are required to understand such effects.

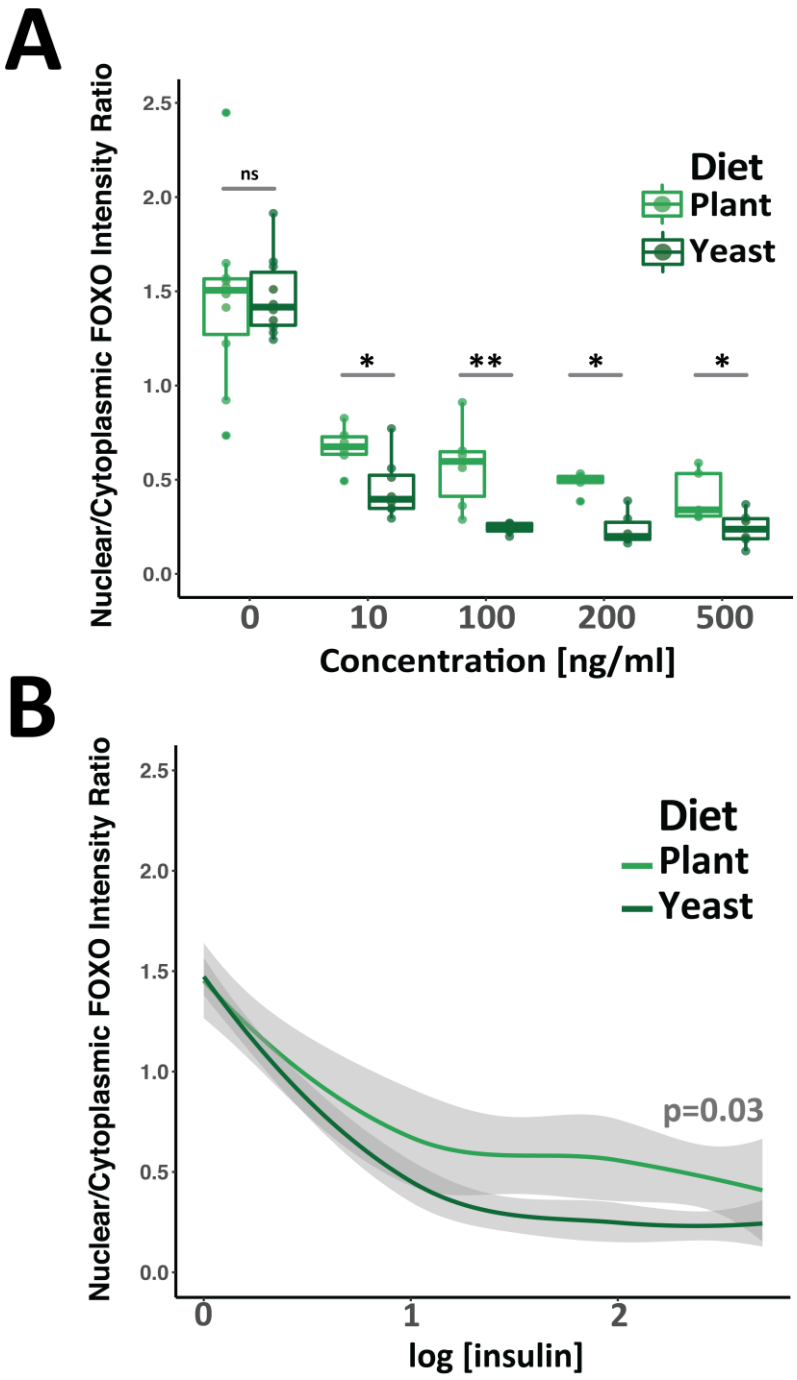

Figure 36. Diet-dependent insulin sensitivity in wing imaginal discs.

(A) Boxplot showing dFOXO nuclear:cytoplasm intensity ratio for **YF-(dark green)** and **PF-derived(light green)** wing discs incubated with various concentrations of bovine insulin in culture for 2 hours (**=p<0.01,*=p<0.05, Mann-Whitney U test).
(B) Logarithmic concentration values plotted against dFOXO intensity ratio; data points obtained in**(A)** were smoothed (y ~x) for each diet (p-value from two-way ANOVA of means; confidence intervals = s.e.)

4. Discussion

4.1 A novel insulin relay mechanism regulating *Drosophila* growth and development

Drosophila insulin-like peptide (DILP) 2 was first observed in the corpora cardiaca (CC) when insulin-producing cells (IPCs) were discovered in the larval brain (Rulifson, 2002). In the same year, another group studying the nutrient-dependent expression of DILPs 2,3 and 5, revealed the presence of extensive IPC projections to the CC (Ikeya et al., 2002). However, neither of these studies was able to detect mRNA expression of any DILPs in the CC. This raised questions about the mechanism of how DILPs are localized to the CC. The CC-IPC function is homologous to beta-alpha cell function in the mammalian pancreas (Wang et al., 2007), but insulin localization to the alpha cells has never been observed. Over the past 18 years, the roles of IPCs, DILPs and CC-produced glucagon-like adipo-kinetic hormone (AKH) in growth, development and metabolism have been extensively studied (reviewed in Droujinine & Perrimon, 2016); like insulin and glucagon in mammals, IPC-produced DILPs and CC-produced AKH have been shown to be functionally antagonistic in *Drosophila*. However, the seemingly paradoxical observation of DILPs localization to the CC has not been explored. One of the aims of my thesis is to understand the relevance of the aforementioned phenomenon in *Drosophila* growth and development.

4.1.1 The curious case of insulin in the *Drosophila* corpora cardiaca

The observation here of insulin localization to the alpha-cell homolog corpora cardiaca (CC) in *Drosophila* is novel across all studied organisms. In one previous study, mice pancreatic alpha-cells were shown to express both glucagon and insulin when 'trans-differentiating' into beta-cells upon extreme beta-cell loss (Thorel et al., 2010). However, the bi-hormonal expression in the alpha-cell is only transient as glucagon expression is lost upon full differentiation into a beta-cell (Thorel et al., 2010). Other non-beta-cells (such as delta-cells), also differentiate into insulin-producing beta-cells during insulin insufficiency caused by beta-cell loss (Chera et al., 2014; Cigliola, Thorel, Chera, & Herrera, 2016). In contrast, the *Drosophila* CC

contains nutrition-dependent DILPs 2 and 5 throughout stages of larval development.

4.1.2 Mechanism of IMPL2-mediated insulin uptake

I have further shown that CC cells do not express insulin but specialize in taking up insulin using IMPL2, a homolog of vertebrate IGF-binding protein 7 (Honegger et al., 2008). DILPs 2 and 5 are known to bind to IMPL2 in addition to the dInR (Andersen et al., 2000; Roed et al., 2018). IMPL2 is known to be secreted into circulation (Honegger et al., 2008) and function to inhibit IIS in developing larval tissues; competitive binding by IMPL2 reduces the availability of DILPs in the hemolymph (Honegger et al., 2008; G. J. Lee et al., 2018). However, IMPL2 has not been shown to be involved in DILP uptake, although DILP2 and 5 localize intracellularly in IMPL2-producing neurons in the larval brain. Recent structural analysis of IMPL2 does not reveal the presence of membrane domains in the protein (Roed et al., 2018). Hence, the role of IMPL2 as a receptor to mediate DILP uptake is unclear.

My data presented in section 3.1.2 shows that the absence of the dInR does not affect DILP uptake in the CC, an IMPL2-producing neuroendocrine tissue. The data further suggest that IMPL2 might act independently of dInR in taking up DILPs 2 and 5. This is in contrast to a previously published study that proposed a model of insulin uptake involving the cooperative action of IMPL2 and dInR (Bader et al., 2013). Bader and colleagues also suggested that IMPL2 increases IIS activity in neuronal cells, but the effect of IMPL2 inhibition on IIS activity in the CC cells remains to be investigated.

4.1.3 Sorting of up-taken insulin in corpora cardiaca

The fate of DILPs in IMPL2-producing neurons is not well understood. Bader and colleagues (Bader et al., 2013) have proposed that DILPs are degraded upon IMPL2-mediated uptake. Using electron microscopy, I have shown that DILPs 2 and 5 are sorted into dense secretory vesicles in the CC. Additionally, DILPs are co-packaged into secretory vesicles containing AKH (a CC-specific hormone). Thus, the DILPs are sorted for secretion rather than being completely degraded. The presence of DILPs in multi-vesicular bodies (MVBs) raises the possibility that they may be secreted from the CC through transcytosis (Von Bartheld, 2004). Alternatively, a fraction of DILPs involved in IIS in the CC, may be taken up through binding to the dInR. This ligand-

receptor complex might be undergoing lysosomal degradation in order to maintain IIS activity in the CC (Krämer, 2002).

As shown in section 3.1.2, DILPs in the CC are taken up through clathrin-mediated endocytosis (CME), yet the proteins involved in sorting DILPs from the resulting endocytic vesicles into secretory granules remain uncharacterized. In order to identify them, the library of endogenously-tagged *Drosophila* Rab proteins generated by our group (Dunst et al., 2015) can be exploited. Also, it is unclear whether whole IMPL2-DILP2/5 complexes undergo sorting into vesicles or IMPL2 molecules are recycled. Preliminary electron micrographs (Figure 37) indicate that some dense-core vesicles (DCVs) located in the CC soma do contain both IMPL2 and DILP2/5 molecules. It is possible that DILPs are secreted in a complex with IMPL2. Roed and colleagues showed that the *in-vitro* binding between purified DILP5 and IMPL2 is highly sensitive to ionic strength of the solution (Roed et al., 2018). One can speculate that following secretion from the CC, the IMPL2-DILP2/5 complex dissociates upon encountering the hemolymph due to difference in ionic strength, and in the process release free DILP2/5 for binding to the dInR and enabling IIS in target tissues.

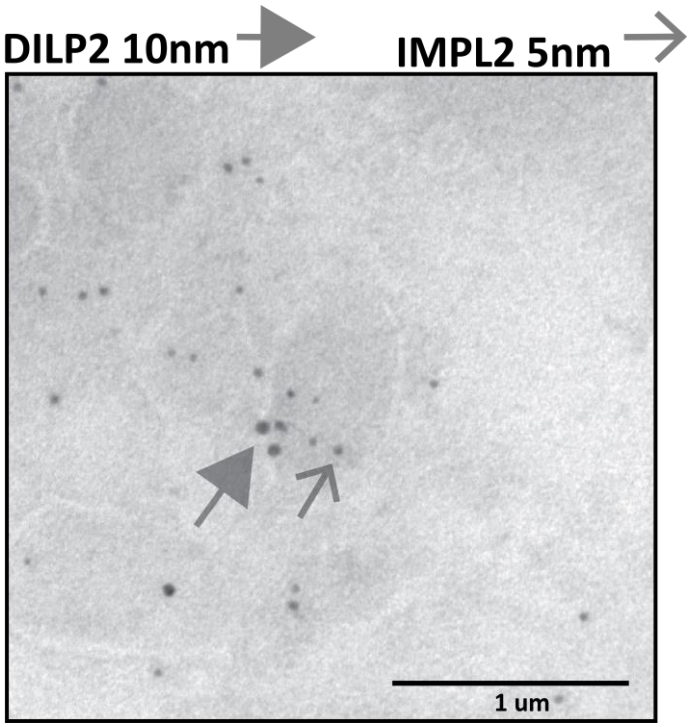

Figure 37. Colocalization of IMPL2 and DILP2.

Immuno-gold labelling in the corpora cardiaca cells; stained for DILP2 (10nm particles, closed arrowhead) and IMPL2 (5nm particles, open arrowhead). Scale = 1um.

4.1.4 Paracrine insulin signaling to the prothoracic gland

CCs innervate the larval prothoracic gland (PG) and the aorta through axon-like projections (G. Lee & Park, 2004; Siegmund & Korge, 2001). My data clearly show that CC projections to the PG are structurally reminiscent of pre-synaptic boutons that form at neuro-muscular junctions (Broadie & Bate, 1993; Zito, Parnas, Fetter, Isacoff, & Goodman, 1999). The fact that these CC projections contain DILPs2 and 5 suggests anterograde transport of secretory vesicles containing insulin. Brain-derived neurons containing the prothoracicotropic hormone (PTTH) also innervate the PG (McBrayer et al., 2007; Zitnan, Sehnal, & Bryant, 1993), but the current understanding of PG tissue morphology fails to account for such neuronal projections (G. J. Lee et al., 2018; Texada, Malita, & Rewitz, 2019). Ultra-structural analysis reveals that the PG consists of a central lumen innervated with DCV-filled neuronal processes, rather than the long-standing model of tightly-packed cells (Dai & Gilbert, 1991).

In data presented in section 3.1.3, co-packaging of AKH and DILPs in DCVs suggests co-secretion from the CC. It is known that CCs secrete AKH upon larval starvation (G. Lee & Park, 2004). Predictably, I observed a reduction in CC DILP levels upon starvation; starvation-induced secretion of DILPs was stopped by inactivation of CC neurons.

I further showed that CC signal directly to the PG only during larval starvation and not during feeding. This change in steady-state DILP intensity in the PG might be a result of low receptor-ligand turnover rates as a response to low IIS activity induced by starvation (Sorkin & Von Zastrow, 2002, 2009).

4.1.5 Function of corpora cardiaca-prothoracic gland insulin signaling axis in *Drosophila* growth and development

Removing DILPs in the CC in well-fed larvae does not seem to impact growth or development. The absence of a phenotype for IMPL2 knockdown larvae (which lack a CC DILP 2,5 pool) under normal rearing conditions (section 3.1.4) and the fact that

trehalose levels remain unchanged are consistent with the CC-secretion/exocytosis assay discussed in the previous section.

Past studies have shown that when larvae are reared under fed conditions, even over-expressing AKH in the CC does not have an effect on circulating sugars (G. Lee & Park, 2004). This in turn indicates that CC cells in fed larvae are in a state of low secretory activity. Thus, larval feeding may account for retention of CC-DILPs and subsequently, no effects on growth or development is observed in its absence.

Ecdysone biosynthesis by the PG regulates development and body size in *Drosophila* (reviewed in Shingleton, Das, Vinicius, & Stern, 2005). The PG cells couple nutrition to development by producing ecdysone in an insulin-dependent manner (Colombani, 2005; C. K. Mirth et al., 2014; C. Mirth et al., 2005). Colombani and colleagues observed that down-regulation of IIS specifically in the PG cells produces flies with larger body and wings, without delaying pupariation (Colombani, 2005). They and others have concluded that IIS-dependent ecdysone production in the PG is inversely proportional to larval growth (Colombani, 2005; C. K. Mirth et al., 2014; C. Mirth et al., 2005; Yuan et al., 2020). On the other hand, a number of *in-vivo* studies (Herboso et al., 2015; Moeller et al., 2017) and one *ex-vivo* study from our group (Dye et al., 2017) suggest that low levels of ecdysone is required for imaginal disc growth and proliferation. Thus, the debate on the effect of ecdysone on tissue growth in *Drosophila* continues. The inconsistency in the effect of ecdysone reported in literature arises due to the fact that the growth response of imaginal tissues may be biphasic in nature. However, there is no solid evidence for such a conclusion yet.

In the absence of CC DILPs, starved larvae produce adult flies with larger wings compared to wild-type counterparts (Figure 21). Consistent with previous observations, increased tissue growth suggests low IIS activity and ecdysone synthesis in the PG during starvation. I hypothesize that CC cells secrete stored DILPs to the PG upon larval starvation in order to maintain IIS activity and ecdysone synthesis in the PG cells. A recent study showed that ecdysone levels increased when L3 larvae were starved (G. J. Lee et al., 2018) and indirectly suggested that during starvation, the PG cells must require a different source of insulin to increase ecdysone production, particularly as the IPCs retain DILP secretion (Géminard et al., 2009) (Figure 38A). The CC pool of up-taken DILPs may serve this purpose. A working model of the hypothesis is represented in Figure 38.

Further experimental evidence is required to define the precise role(s) of CC DILPs in development under starvation. Currently it is not known how IIS activity is affected in the PG during starvation and whether it depends on the DILPs secreted by the CC. To directly address this, a direct readout of IIS activity from the PG in the absence of a CC insulin pool should be measured. If CC DILPs are found to be signaling to the PG and regulating ecdysone production during starvation, then their absence is expected to result in lower levels of circulating ecdysone, although this remains to be tested.

Working Model

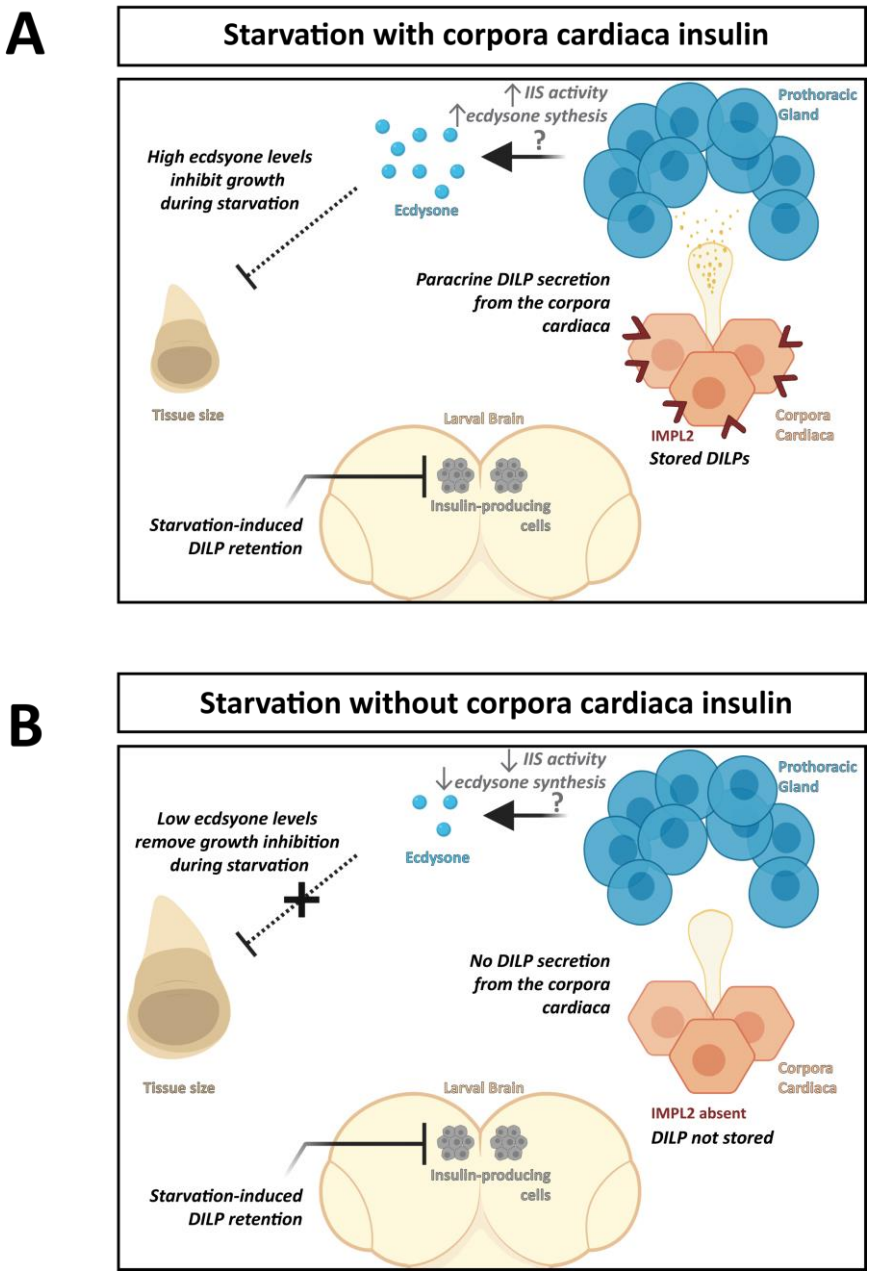

Figure 38.Working model and experimental outlook.

Hormonal regulation underlying growth during starvation in **(A)**wild-type larvae vs. **(B)** larvae devoid of insulin(DILPs) in the corpora cardiaca. Experimental outlook (gray,italic) as mentioned in the section 4.1.5

4.2 *Drosophila* insulin-like peptides do not mediate the effects of growth temperature on tissue size and shape

Results obtained in section 3.2.1 suggest that the nutrition-dependent DILPs 2 and 5 do not have a temperature-dependent role in reducing tissue size. Even though perturbing IIS can cause changes in wing size, temperature might not affect just a single growth pathway, but instead have more widespread and complex effects. My initial hypothesis connecting IIS and effects of growth temperature was based on indirect but aligned observations; previous reports have suggested that an organism's ability to increase metabolic rate with increasing temperature dictates its survival (A Clarke, 2004; A Clarke & Fraser, 2004; Cruz et al., 2012), and insulin signaling is known to be one of the most important pathways influencing metabolic rate in cells (reviewed in Saltiel & Kahn, 2001). Our lab previously observed that high insulin activity in *Drosophila* larvae was essential for survival at high temperature (Brankatschk et al., 2016). Oddly, the results obtained by Brankatschk and colleagues were irreproducible and eventually discarded (discussed below in section 4.3.1 ; compare Brankatschk et al., 2016, 2018). Thus, there remains no reason to consider a role for IIS in regulation of growth at different temperatures.

In section 3.2.5, I showed that DILP2 over-expression selectively increases IIS activity in the PG. While it remains unclear why overexpression of only DILP2 (and not DILP5) reduces growth, reduction in larval growth observed in DILP2 over-expressing larvae with no change to developmental timing is consistent with previous observations (Colombani, 2005; C. K. Mirth et al., 2014; C. Mirth et al., 2005; Yuan et al., 2020). Like DILP2 over-expression, up-regulation of IIS in the PG resulted in flies with smaller bodies and wings due to ecdysone-mediated growth inhibition (Colombani, 2005). This uncoupling of size and growth temperature in DILP2 over-expressing flies might be due to the fact that larvae develop to the minimum viable size even at lower temperatures. While, it is not clear why over-expression of DILP2 selectively affects the PG, I suspect that the novel insulin relay mechanism discussed in section 4.1, plays a role. In short, excess DILP2 produced by the IPCs in the brain might be taken up by the CC and secreted, changing the steady-state IIS activity in the PG cells. It remains to be seen if over-expression of DILP2 in the IPCs change the amount of DILPs secreted by the CC in a fed state. Further, if DILP2 is over-

expressed ectopically in the CC, would there be a similar up-regulation of IIS activity in the PG?

4.3 Relationship between dietary lipids, insulin signaling and high temperature survival in *Drosophila* larvae

A yeast-lipid based diet was shown to upregulate IIS in developing *Drosophila* larvae through activation of IPCs and subsequent secretion of DILP2 (Brankatschk et al., 2014). Conversely, a plant-lipid based diet showed IIS downregulation due to lower activation of IPCs (Brankatschk et al., 2014). Additionally, larvae feeding on yeast-lipids survived better in high ambient temperatures than plant-lipid fed counterparts (Brankatschk et al., 2018). Further study of the mechanism behind these observations revealed that yeast lipids improve high temperature survival by increasing IIS activity (Brankatschk et al., 2016). This suggests that upregulation of IIS facilitates increased survival of larvae at high temperatures independently of diet. Several experiments done during the course of this thesis were unable to reproduce the data reported by Brankatschk and colleagues (Brankatschk et al., 2016, 2018). In this section I discuss the most fundamental contradictions to the conclusions drawn in the aforementioned publications.

4.3.1 Neither dietary lipids nor DILP2 affect larval survival at high rearing temperature

In the section 3.3.1 , I discovered that larval survival at high rearing temperatures is independent of dietary lipid composition. This finding directly contradicts published work by Brankatschk and colleagues (Brankatschk et al., 2018) as I did not observe yeast lipids to provide any selective advantage to larval growth at high temperatures. Further, unpublished work implicated DILP2 in mediating the effect of yeast lipids (Brankatschk et al., 2016). In my data, survival of DILP2 knock-out flies does not seem to be affected at high temperatures by either plant or yeast-lipid diets. Experiments done in parallel with the lead author of the previous studies (Dr. Marko Brankatschk) revealed similar results. Thus, DILP2 was not considered to be involved in high temperature survival.

Brankatschk and colleagues also showed up-regulation of IIS across various larval tissues when fed a yeast-lipid diet (Brankatschk et al., 2014). In section 3.3.2,

IIS activity in the wing disc *in-vivo* seemed to be indistinguishable when measured at the level of dFOXO localization. It should be noted that the authors used a different readout for IIS activity in the original study (Brankatschk et al., 2014), suggesting that the reported effect of yeast-lipid diet on IIS in larval tissues needs to be further investigated.

4.3.2 Tissue lipid composition affects insulin sensitivity

Dietary lipids do not change IIS in target tissues *in-vivo,* but change the sensitivity to insulin (Section 3.3.4). Tissue sensitivity to insulin might be dictated by membrane lipid and/or sterol composition (Delle Bovi et al., 2019). It has been shown that dietary lipids do in fact change both sterol composition and the length and degree of unsaturation of phospholipid side sidechains in the larval wing imaginal tissue (Carvalho et al., 2012). Several experiments in the past have suggested that membrane lipids control endocytosis and intracellular signaling through changing membrane curvature, binding of adaptor proteins or formation of sterol-enriched microdomains (reviewed in Doherty & McMahon, 2009). However, the exact mechanism through which IIS activity is differentially controlled in wing discs is hard to dissect, primarily because dietary lipids simultaneously change multiple lipid species and sterol composition of the plasma membrane. In order to dissect out individual effects of sterols and lipid unsaturation on insulin sensitivity, food with defined lipid composition is required. Protocols to generate accurately defined lipid and sterol for *Drosophila* larvae have already been developed in the lab (Carvalho et al., 2012, 2010). In the future, such protocols coupled with the assay optimized in this thesis can be used to ask how membrane lipid composition governs insulin sensitivity in tissues.

4.4 Conclusions and implications

In conclusion, the CC-PG insulin signaling axis presents a novel paradigm in hormonal signaling (discussed in Section 4.1). A non-insulin-producing tissue (corpora cardiaca) takes up circulating insulin (DILP2/5) using a non-canonical insulin-binding protein (IMPL2), and stores it when nutrition is abundant. Upon starvation the stored insulin is directly secreted to a target tissue (prothoracic gland) to facilitate the timely production of a developmental hormone (ecdysone). This represents a new type of hormonal signaling, wherein the cell type which secretes the hormone does not produce it. Moreover, secretion of a general endocrine hormone is adequately specific in time and space, thereby, ensuring coordination of development through controlled secretion of other hormones. The CC-PG insulin axis induced during starvation is distinct from known models of endocrine, exocrine, autocrine and juxtacrine hormonal signaling.

In humans, insulin transcytosis occurs across endothelial cells in the blood-brain-barrier(BBB) and is essential for maintaining our cognitive function (Gray & Barrett, 2018 ; Yazdani et al. 2019). The mechanism through which insulin travels across the BBB is not clearly understood and serves as an impediment in determining insulin dosage in diabetic patients (Lee & Klip, 2016; Yazdani et al. 2019). Hopefully, studying DILP transcytosis in *Drosophila* will help us unravel those mechanisms.

The effect of dietary lipids on insulin action have been observed yet not clearly understood at an organism scale. This is primarily because dietary lipids have diverse effects on different tissues in the body. Side-chain saturation affects tissue insulin sensitivity directly but has complex interactions with gut microbes and the immune system (Caesar, Tremaroli, Kovatcheva-Datchary, Cani, & Bäckhed, 2015; Storlien et al., 1996; Tschöp & Thomas, 2006). Thus, it is crucial to develop an isolable model system. The wing disc insulin sensitivity assay coupled with better control diet can be used as a model to test the effects of specific lipid species/types.

5. Materials and methods

5.1 Electron microscopy

Epon embedding: Dissected brain-ring gland complexes were initially fixed in PBS with 2%PFA and 1% glutaraldehyde for 2 hours at room temperature followed by overnight incubation at 4˚C. Then the samples were post-fixed with 1% OsO_4 and 1.5% potassium ferrocyanide in water on ice for 1 hour. En bloc stain was done in the dark with 1% UA in water on ice. Following infiltration and embedding, 70nm sections were made and picked up with slot grids. All samples were then post-stained with 1% UA in water for 10 minutes and 0.04% lead citrate for 5 minutes. Electron micrographs were obtained at ~80kV using Morgan FEI (EM sys camera) and ~100kV using Tecnai (TMPS camera) electron microscopes.

Tokayasu method: Dissected brain-ring gland complexes were initially fixed in PBS with 4% PFA and 0.05% glutaraldehyde for 20 minutes at room temperature. Post-fixation was done in 1:1 dilution of the initial fixative overnight at 4˚C. Ring glands were then embedded using 12% gelatin in PBS and infiltrated with 2.3M sucrose overnight at 4˚C. Following infiltration and embedding, 70nm sections were made and picked up with slot grids. Samples were stained with both secondary gold- and fluorophore-conjugated antibodies. Correlative fluorescence imaging on Zeiss W9 microscope was done to locate regions of interest in individual sections. Electron micrographs were generated at ~80kV using Morgan FEY (EMsys camera) microscope.

5.2 Western blotting

Wing discs were freshly dissected in cold PBS and collected in cohorts of 10 discs into 20ul of RIPA buffer supplemented with protease inhibitor (Roche). After collection, each cohort was lysed and stored at -80˚C. Prior to loading the SDS-PAGE gel (10%), 5ul of 5x loading dye was added to the lysate and boiled for 5 minutes at 95˚C. Following which the whole volume (25ul) was loaded in a single well in the gel. Instead of milk, 4% bovine serum albumin in PBS was used as a blocking agent and to dilute antibodies. Primary antibody solution was incubated overnight at 4˚C and secondary (HRP-labelled) antibody for 3 hours at room temperature. Detection was

done on X-ray films (Amersham;#28906835) using a chemiluminescence detection kit (Amersham ECL;#RPN2109).

5.3 Immunofluorescence

Freshly dissected tissue in PBS was fixed with 4% paraformaldehyde (Sigma) for 20-25 minutes. After fixation, tissues were thoroughly washed 3-4 times with PBS.

Brain and ring gland: Tissues were permeabilized with PBS containing 0.2%(v/v) Triton X-100(Sigma) for 2 hours at room temperature with shaking. Primary incubation with antibody was done overnight in incubation buffer- PBS with 0.1% Triton X-100 (PBST) and 1mg/ml bovine serum albumin (BSA). Incubation was followed by 3x15 minute washes with the same incubation buffer without antibodies. Secondary incubation was done in incubation buffer supplemented with 4%(v/v) normal goat serum (NGS) for 2-3 hours. Tissues were then washed 3X15 minutes in 0.1%PBST and mounted on glass slides using VectaShield H-1000 mounting medium.

Wing discs: Discs were permeabilized with PBS containing 0.05%(v/v) Triton X-100(Sigma) supplemented with 1mg/ml bovine serum albumin (BSA) and 250mM NaCl for 3X10 minutes at room temperature with shaking. Primary incubation with antibody was done overnight in incubation buffer- PBS with 0.05% Triton X-100 (PBST) and 1mg/ml bovine serum albumin (BSA). Incubation was followed by 3x15 minute washes with the same incubation buffer without antibodies. Secondary incubation was done in incubation buffer supplemented with 4%(v/v) normal goat serum (NGS) for 2-3 hours. Wing discs were then washed 3X15 minutes in 0.1%PBST and mounted on glass slides using VectaShield H-1000 mounting medium.

5.3.1 List of antibodies/dyes

Antibody	Host	Dilution	Source
DILP2	Rat	1:500	Leopold lab, Institut Curie
DILP5	Rat	1:1000	Self-made
DILP5	Rabbit	1:500	Leopold lab, Institut Curie
AKH	Rabbit	1:800	Leopold lab,

			Institut Curie
IMPL2	Rabbit	1:1000	Stocker lab, ETH Zurich
EcR(DDA2.7)	Mouse	1:500	DSHB
GFP(monoclonal)	Mouse	1:500	Santa Cruz Biotechnology
mCherry	Rabbit	1:500	Thermo Fisher
Drosophila phospho-Akt(Ser505)	Rabbit	1:250(IF)/1:1000(WB)	Cell Signaling Technology
DAPI	-	1:2000(4mg/ml stock)	Roche

5.4 Fluorescence intensity quantification

Whole cell intensity: Individual cells from multiple samples were manually segmented and mean intensity was measured using Fiji/ImageJ (Schindelin et al., 2012).

Nuclear and cytoplasmic intensity ratio: Regions of interested were manually drawn on respective tissues. Nuclear to cytoplasmic intensity ratio was then calculated using a Fiji/ImageJ macro developed by Volker Baecker at Montpellier RIO Imaging (www.mri.cnrs.fr).

Line profiles: Using Fiji/ImageJ (Schindelin et al., 2012), a line was manually drawn across a tissue field and raw intensities were measured.

5.5 Fly weight measurements

Cohorts of 10-15 cold-anesthetized flies were weighed in pre-weighed micro-centrifuge tubes using a fine balance (Metler-Toledo). Care was taken to remove food particles or liquid sticking to the fly. In order to prevent damage to the appendages, a soft brush was used to transfer flies to the pre-weighed tubes.

5.6 Size determination

Wing Area: Newly eclosed adults were collected and stored in isopropanol. Prior to dissection, flies were transferred to a cavity dissection-glass. Care was taken to keep flies submerged in adequate isopropanol at all times. One wing from each fly was

dissected using fine forceps (Dumont 5-SA) and transferred to a glass slide along with a small amount of isopropanol (in forceps due to capillary action). It is important to keep wings flat on the slide surface. This can be achieved by repeatedly moistening the wings with isopropanol, using forceps. Once the desired number of wings were obtained, 30ul of Euparal (Roth #7356.1) was pipetted on the slide. Next, a glass coverslip (22mm/22mm/17um) was placed covering the entire area on the slide occupied by wings. To ensure absence of air bubbles and minimum displacement in the wings, it is important to place the coverslip starting from one edge. Following mounting, the slides were left to dry for 2 hours prior to imaging. Single wing images were taken using Zeiss Sv11 dissection scope fitted with a CCD camera (Jenoptik ProgRes C10). Images were segmented and analyzed using a Fiji macro script developed in the lab.

Pupal volume: Pupae (24-30-hours APF) were collected using a wet brush. Following which, they were washed with PBS to dislodge attached food and glue particles. Each pupa was then transferred to a single well of a transparent 24-well plate and imaged using Zeiss Sv11 dissection scope fitted with a CCD camera (Jenoptik ProgRes C10). Sex determination was done post-eclosion and only females were taken for analysis. Using Fiji, an ellipse was fitted to the pupa. Volume was calculated by using the value of the minor radius as the height. Volume = 0.75π*(major-axis)*(minor-axis)^2.

Larval volume: Feeding L3 larvae (96-hours AEL) were collected by washing food with PBS. Following which, they were cold-anesthetized and washed 3 times with cold PBS. Then larvae (~20) in PBS were transferred to micro-centrifuge tubes and treated with a brief (10min) heat shock (98˚C). This step causes larvae to fully extend out, thus reducing variability in size. Only female larvae were taken for imaging. Imaging and size analysis were done as mentioned above (pupal volume).

5.7 Wing disc explant culture

Wing disc explants were cultured according to a protocol developed in the lab (Dye 2017). In brief, freshly dissected L3 discs were cultured in Grace's Insect medium (Sigma G9771) supplemented with 5% Fetal Bovine Serum (FBS, ThermoFisher/Invitrogen 10270098) and Penicillin-Streptomycin (Sigma P4333,

100x). 20-hydroxyecdysone (20E) (Sigma H5142) was added as a 1:1000 dilution from a stock solution made in ethanol. The final concentration of 20E in the culture media was 20nM.

5.8 Pupariation timing assay

Fly crosses were fed fresh yeast paste and allowed to lay eggs for 3 hours on apple-juice agar plates. Following egg-laying, the plates were stored at 25˚C. After 18-24 hours of incubation, freshly hatched L1 larvae were collected in PBS every 2 hours. In order to prevent overcrowding, 20-30 larvae were then transferred into a single food vial using a micropipette. Vials were stored at respective temperatures. Number of pupae, including white pre-puparium, were counted at fixed hourly or daily intervals starting on the fourth day (96 hours) after egg-laying. Counting was stopped once there was no increase in the number of new pupae for 3-4 consecutive time points.

5.9 Larval starvation assay

Freshly hatched L1 larvae from respective crosses were transferred using the same method as pupariation timing assay (see above). At 96 hours after egg-laying, the food was washed with PBS and individual L3 larvae were transferred to vials containing 2% agar in PBS. Fed controls were transferred to fresh food vials. To prevent over-crowding, no more than 20-25 larvae were transferred into each vial. Upon end of starvation period, larvae were collected individually and dissected for tissue of interest. For body and tissue size estimations, both starved and fed-control vial were left undisturbed and larvae were allowed to pupariate.

5.10 List of flies

Genotype	Source	Identifier	Reference	Comments
w1118	Bloomington	#5905	Ryder et. al., 2004	isogenic strain
OregonR	MPI-CBG	-	-	-
w; Dilp2-Gal4/Cyo, act-GFP	MPI-CBG	-	Rulifson et. al., 2002	-
yw, Akh-Gal4;;	Tennessen lab	#72	Lee et. al., 2004	-
w,hsflp;;C765-Gal4/TM6b	MPI-CBG	FRF20	-	made by Falko Riedel
w; {TI} DILP2[1]	Bloomington	#30881	Gronke et. al., 2010	ends out

				replacement with [w+]
w; {TI} DILP5[1]	Bloomington	#30884	Gronke et. al., 2010	ends out replacement with [w+]
yv; DILP5-RNAi [TRiP]	Bloomington	#31378	Perkins et. al., 2015	expresses dsRNA
yv; dInR-RNAi[TRiP]	Bloomington	#31037	Perkins et. al., 2015	expresses dsRNA
y sc v sev; IMPL2-RNAi[TRiP]	Bloomington	#64936	Perkins et. al., 2015	expresses dsRNA
w1118; UAS-rpr	Bloomington	#5824	Aplin and Kaufman, 1997	-
yw;; UAS-shibirets1	Bloomington	#		
w;UAS-Kir2.1GFP	Bloomington	#6596	Hardie et. al., 2001	-
w1118; UAS-EcR-RNAi	Bloomington	#9326	Colombani et. al., 2005	
w; UAS-SYT1-GFP	Bloomington	#6926	Zhang and Broadie, 2003	-
yw, UAS-preproANF-GFP	Bloomington	#7001	Rao et. al., 2001	-
w1118; UAS-InR-A1325D	Bloomington	#8265	Exelixis Inc.	Constitutively-active
y w1118; UAS-InR-K1409A	Bloomington	#8252	Exelixis Inc.	Dominant-negative
w;; Foxo-mCherry	Partridge Lab	-	Kakanj et. al., 2016	Endogenous-tagging
yw; UAS-DILP2	Marko Brankatschk	-	Brankatschk et. al., 2016	-
yw; UAS-DILP5	Marko Brankatschk	-	Brankatschk et. al., 2016	-

5.11 Fly food

All experiments were done on standard fly food medium containing cornmeal, molasses, agar and yeast extract, unless explicitly mentioned. Plant-lipid based food(PF) and yeast-lipid-based food(YF) were developed in the lab (Carvalho et al., 2012). The recipes are listed below-

Plant-lipid based food (PF)- 1 litre		**Yeast-lipid-based food (YF)-1 litre**	
Agar	7g	Yeast Extract	20g
Soy	76g	Peptone	20g
Cornmeal	160g	Sucrose	30g
Malt	160g	Glucose	30g
Vegetable oil	0.4g	Brewer' Yeast	80g
Treacle	44g	Nipagin	2.61g
Propionic acid	12.6ml		
Nipagin	2.61g		

5.12 Temperature control

All flies were reared in at 25˚C unless explicitly mentioned. Incubators (Snijders Scientific) were set to 12-hour day/night cycle. For induction of temperature-sensitive lines, entire vials were transferred to a water bath set at 29˚C.

5.13 Hemolymph trehalose assay

96-hour-AEL larvae were extracted from the food and washed thoroughly with PBS. Then they were surface sterilized by briefly washing with 70% ethanol, followed by 3x PBS washes to remove residual ethanol. In order to immobilize the larvae, they were transferred to cold PBS in a dish. From this step onwards, the hemolymph extraction took place in the cold room (4˚C). Cohorts of 8-12 larvae were dried on soft tissues and placed on each well of glass cavity slide. The epidermis was then punctured under a dissection microscope using a fine needle. To ensure maximum bleeding, larvae were allowed to rest for 5 minutes. 2ul of hemolymph was collected from each cohort and diluted in 98ul of PBS. Hemocytes and tissue fragments were removed by centrifugation at 10,000 rpm for 15 minutes. Trehalose was measured using Megazyme trehalose assay kit (K-TREH). Trehalose concentration of each cohort was averaged over 3 technical replicates.

Cartoons and schematics in this thesis were generated using Adobe Illustrator CS5.1 and BioRender.com.

6. References

Andersen, A. S., Hansen, P. H., Schäffer, L., & Kristensen, C. (2000). A new secreted insect protein belonging to the immunoglobulin superfamily binds insulin and related peptides and inhibits their activities. *Journal of Biological Chemistry*, *275*(22), 16948–16953. https://doi.org/10.1074/jbc.M001578200

Andrews, H. K., Zhang, Y. Q., Trotta, N., & Broadie, K. (2002). Drosophila Sec10 is required for hormone secretion but not general exocytosis or neurotransmission. *Traffic*, *3*(12), 906–921. https://doi.org/10.1034/j.1600-0854.2002.31206.x

Angilletta, M. J., Steury, T. D., & Sears, M. W. (2004). Temperature, growth rate, and body size in ectotherms: Fitting pieces of a life-history puzzle. *Integrative and Comparative Biology*, *44*(6), 498–509. https://doi.org/10.1093/icb/44.6.498

Arrese, E. L., Flowers, M. T., Gazard, J. L., & Wells, M. A. (1999). Calcium and cAMP are second messengers in the adipokinetic hormone- induced lipolysis of triacylglycerols in Manduca sexta fat body. *Journal of Lipid Research*, *40*(3), 556–564.

Bader, R., Sarraf-Zadeh, L., Peters, M., Moderau, N., Stocker, H., Kö hler, K., … Hafen, E. (2013). The IGFBP7 homolog Imp-L2 promotes insulin signaling in distinct neurons of the Drosophila brain. *Journal of Cell Science*, *126*(12), 2571–2576. https://doi.org/10.1242/jcs.120261

Baumbach, J., Xu, Y., Hehlert, P., & Kühnlein, R. P. (2014). Gαq, Gγ1 and Plc21C control drosophila body fat storage. *Journal of Genetics and Genomics*, *41*(5), 283–292. https://doi.org/10.1016/j.jgg.2014.03.005

Bharucha, K. N., Tarr, P., & Zipursky, S. L. (2008). A glucagon-like endocrine pathway in Drosophila modulates both lipid and carbohydrate homeostasis. *Journal of Experimental Biology*, *211*(19), 3103–3110. https://doi.org/10.1242/jeb.016451

Böhni, R., Riesgo-Escovar, J., Oldham, S., Brogiolo, W., Stocker, H., Andruss, B. F., … Hafen, E. (1999). Autonomous control of cell and organ size by CHICO, a Drosophila homolog of vertebrate IRS1-4. *Cell*, *97*(7), 865–875. https://doi.org/10.1016/S0092-8674(00)80799-0

Braco, J. T., Gillespie, E. L., Alberto, G. E., Brenman, J. E., & Johnson, E. C. (2012). Energy-dependent modulation of glucagon-like signaling in Drosophila via the AMP-activated protein kinase. *Genetics*, *192*(2), 457–466. https://doi.org/10.1534/genetics.112.143610

Brankatschk, M., Dunst, S., Nemetschke, L., & Eaton, S. (2014). Delivery of circulating lipoproteins to specific neurons in the Drosophila brain regulates systemic insulin signaling. *ELife*, *3*, 1–19. https://doi.org/10.7554/eLife.02862

Brankatschk, M., Gutmann, T., Grzybek, M., Brankatschk, B., Coskun, U., & Eaton, S. (2016). A temperature-dependent shift in dietary preference alters the viable temperature range of Drosophila. https://doi.org/10.1101/059923

Brankatschk, M., Gutmann, T., Knittelfelder, O., Palladini, A., Prince, E., Grzybek, M., … Eaton, S. (2018). A Temperature-Dependent Switch in Feeding Preference Improves Drosophila Development and Survival in the Cold. *Developmental Cell*, *46*(6), 781-793.e4. https://doi.org/10.1016/j.devcel.2018.05.028

Broadie, K. S., & Bate, M. (1993). Development of the embryonic neuromuscular synapse of Drosophila melanogaster. *Journal of Neuroscience*, *13*(1), 144–166. https://doi.org/10.1523/jneurosci.13-01-00144.1993

Brogiolo, W., Stocker, H., Ikeya, T., Rintelen, F., Fernandez, R., & Hafen, E. (2001). An evolutionarily conserved function of the drosophila insulin receptor and insulin-like peptides in growth control. *Current Biology*, *11*(4), 213–221. https://doi.org/10.1016/S0960-9822(01)00068-9

Broughton, S., Alic, N., Slack, C., Bass, T., Ikeya, T., Vinti, G., … Partridge, L. (2008). Reduction of DILP2 in Drosophila triages a metabolic phenotype from lifespan revealing redundancy and compensation among DILPs. *PLoS ONE*, *3*(11), 3–11. https://doi.org/10.1371/journal.pone.0003721

Buch, S., Melcher, C., Bauer, M., Katzenberger, J., & Pankratz, M. J. (2008). Opposing Effects of Dietary Protein and Sugar Regulate a Transcriptional Target of Drosophila Insulin-like Peptide Signaling. *Cell Metabolism*, *7*(4), 321–332. https://doi.org/10.1016/j.cmet.2008.02.012

Bussolati, G., Capella, C., Vassallo, G., & Solcia, E. (1971). Histochemical and ultrastructural studies on pancreatic A cells. Evidence for glucagon and non-glucagon components of the α granule. *Diabetologia*, *7*(3), 181–188. https://doi.org/10.1007/BF01212551

Caesar, R., Tremaroli, V., Kovatcheva-Datchary, P., Cani, P. D., & Bäckhed, F. (2015). Crosstalk between gut microbiota and dietary lipids aggravates WAT inflammation through TLR signaling. *Cell Metabolism*, *22*(4), 658–668. https://doi.org/10.1016/j.cmet.2015.07.026

Carvalho, M., Sampaio, J. L., Palm, W., Brankatschk, M., Eaton, S., & Shevchenko, A. (2012). Effects of diet and development on the Drosophila lipidome. *Molecular Systems Biology*, *8*(600), 1–17. https://doi.org/10.1038/msb.2012.29

Carvalho, M., Schwudke, D., Sampaio, J. L., Palm, W., Riezman, I., Dey, G., … Eaton, S. (2010). Survival strategies of a sterol auxotroph. *Development (Cambridge, England)*, *137*(21), 3675–3685. https://doi.org/10.1242/dev.044560

Chanaday, N. L., & Kavalali, E. T. (2018). Time course and temperature dependence of synaptic vesicle endocytosis. *FEBS Letters*, *592*(21), 3606–3614. https://doi.org/10.1002/1873-3468.13268

Chera, S., Baronnier, D., Ghila, L., Cigliola, V., Jensen, J. N., Gu, G., … Herrera, P. L. (2014). Diabetes recovery by age-dependent conversion of pancreatic δ-cells into insulin producers. *Nature*, *514*(7253), 503–507. https://doi.org/10.1038/nature13633

Choi, S., Lim, D. S., & Chung, J. (2015). Feeding and Fasting Signals Converge on the LKB1-SIK3 Pathway to Regulate Lipid Metabolism in Drosophila. *PLoS Genetics*, *11*(5), 1–19. https://doi.org/10.1371/journal.pgen.1005263

Cigliola, V., Thorel, F., Chera, S., & Herrera, P. L. (2016). Stress-induced adaptive islet cell identity changes. *Diabetes, Obesity and Metabolism*, *18*(April), 87–96. https://doi.org/10.1111/dom.12726

Clarke, A. (2004). Is there a universl temperature dependence of metabolism? *Functional Ecology*, *18*, 252–256. https://doi.org/10.1111/j.0269-8463.2004.00842.x

Clarke, A, & Fraser, K. P. P. (2004). Why does metabolism scale with temperature ?, 243–251.

Clarke, Andrew. (2003). Costs and consequences of evolutionary temperature adaptation. *Trends in Ecology and Evolution*, *18*(11), 573–581. https://doi.org/10.1016/j.tree.2003.08.007

Colombani, J. (2005). Antagonistic Actions of Ecdysone and Insulins Determine Final Size in Drosophila. *Science*, *310*(5748), 667–670. https://doi.org/10.1126/science.1119432

Corrigan, L., Redhai, S., Leiblich, A., Fan, S. J., Perera, S. M. W., Patel, R., … Wilson, C. (2014). BMP-regulated exosomes from Drosophila male reproductive glands reprogram female behavior. *Journal of Cell Biology*, *206*(5), 671–688. https://doi.org/10.1083/jcb.201401072

Cruz, A. L. B., Hebly, M., Duong, G., Wahl, S. A., Pronk, J. T., Heijnen, J. J., … Gulik, W. M. Van. (2012). Similar temperature dependencies of glycolytic enzymes : an evolutionary adaptation to temperature dynamics ? *BMC Systems Biology*, *6*(1), 1. https://doi.org/10.1186/1752-0509-6-151

Cryer, P. E. (2001). Hypoglycemia-associated autonomic failure in diabetes. *American Journal of Physiology-Endocrinology And Metabolism*, *281*(6), E1115-E1121.

Cryer, P. E. (2012). Minireview: Glucagon in the pathogenesis of hypoglycemia and hyperglycemia in diabetes. *Endocrinology*, *153*(3), 1039–1048. https://doi.org/10.1210/en.2011-1499

Dai, J., & Gilbert, L. I. (1991). Corpora Allata:Prothoracic Gland, *326*, 1–18. Retrieved from papers://2d48c847-ccb0-4836-a68e-3902ed2765d3/Paper/p6221

De Camilli, P., Takei, K., & McPherson, P. S. (1995). The function of dynamin in

endocytosis. *Current Opinion in Neurobiology*, *5*(5), 559–565. https://doi.org/10.1016/0959-4388(95)80059-X

Delle Bovi, R. J., Kim, J. H., Suresh, P., London, E., & Miller, W. T. (2019). Sterol structure dependence of insulin receptor and insulin-like growth factor 1 receptor activation. *Biochimica et Biophysica Acta - Biomembranes*, *1861*(4), 819–826. https://doi.org/10.1016/j.bbamem.2019.01.009

Dimitriadis, G., Mitron, P., Lambadiari, V., Maratou, E., & Raptis, S. A. (2011). Insulin effects in muscle and adipose tissue. *Diabetes Research and Clinical Practice*, *93*(SUPPL. 1), 52–59. https://doi.org/10.1016/S0168-8227(11)70014-6

Doherty, G. J., & McMahon, H. T. (2009). Mechanisms of Endocytosis. *Annual Review of Biochemistry*, *78*(1), 857–902. https://doi.org/10.1146/annurev.biochem.78.081307.110540

Droujinine, I. A., & Perrimon, N. (2016a). Interorgan communication pathways in physiology: focus on Drosophila. *Annual Review of Genetics*, *50*, 539–570. https://doi.org/10.1146/annurev-genet-121415-122024

Droujinine, I. A., & Perrimon, N. (2016b). Interorgan communication pathways in physiology: focus on Drosophila. *Annual Review of Genetics*. https://doi.org/10.1146/annurev-genet-121415-122024

Dunst, S., Kazimiers, T., von Zadow, F., Jambor, H., Sagner, A., Brankatschk, B., … Brankatschk, M. (2015). Endogenously Tagged Rab Proteins: A Resource to Study Membrane Trafficking in Drosophila. *Developmental Cell*, *33*(3), 351–365. https://doi.org/10.1016/j.devcel.2015.03.022

Duvanel, C. B., Fawer, C. L., Colling, J., Hohlfeld, P., & Matthieu, J. M. (1999). Long-term effects of neonatal hypoglycemia on brain growth and psychomotor development in small-for-gestational-age preterm infants. *Journal of Pediatrics*, *134*(4), 492–498. https://doi.org/10.1016/S0022-3476(99)70209-X

Dye, N. A., Popović, M., Spannl, S., Etournay, R., Kainmüller, D., Ghosh, S., … Eaton, S. (2017). Cell dynamics underlying oriented growth of the *Drosophila* wing imaginal disc. *Development*, (October), dev.155069. https://doi.org/10.1242/dev.155069

Estes, P. S., Roos, J., Van Der Bliek, A., Kelly, R. B., Krishnan, K. S., & Ramaswami, M. (1996). Traffic of dynamin within individual Drosophila synaptic boutons relative to compartment-specific markers. *Journal of Neuroscience*, *16*(17), 5443–5456. https://doi.org/10.1523/jneurosci.16-17-05443.1996

Fakler, B., Brändle, U., Glowatzki, E., Zenner, H. P., & Ruppersberg, J. P. (1994). Kir2.1 inward rectifier K+ channels are regulated independently by protein kinases and ATP hydrolysis. *Neuron*, *13*(6), 1413–1420. https://doi.org/10.1016/0896-6273(94)90426-X

French, V., & Partridge, L. (1998). Body size and cell size in Drosophila : the

developmental response to temperature, *44*, 1081–1089.

Galikova, M., Diesner, M., Klepsatel, P., Hehlert, P., Xu, Y., Bickmeyer, I., … K??hnlein, R. P. (2015). Energy homeostasis control in drosophila adipokinetic hormone mutants. *Genetics*, *201*(2), 665–683. https://doi.org/10.1534/genetics.115.178897

Garofalo, R. S., & Rosen, O. M. (1988). Tissue localization of Drosophila melanogaster insulin receptor transcripts during development. *Molecular and Cellular Biology*, *8*(4), 1638–1647. https://doi.org/10.1128/mcb.8.4.1638

Géminard, C., Arquier, N., Layalle, S., Bourouis, M., Slaidina, M., Delanoue, R., … Léopold, P. (2006). Control of metabolism and growth through insulin-like peptides in Drosophila. *Diabetes*, *55*(SUPPL. 2), 5–8. https://doi.org/10.2337/db06-S001

Géminard, C., Rulifson, E. J., & Léopold, P. (2009). Remote Control of Insulin Secretion by Fat Cells in Drosophila. *Cell Metabolism*, *10*(3), 199–207. https://doi.org/10.1016/j.cmet.2009.08.002

Gokhale, R. H., Hayashi, T., Mirque, C. D., & Shingleton, A. W. (2016). Intra-Organ Growth Coordination in Drosophila Is Mediated By Systemic Ecdysone Signaling. *Developmental Biology*. https://doi.org/10.1016/j.ydbio.2016.07.016

Gottlieb, S., & Ruvkun, G. (1994). daf-2, daf-16 and daf-23: Genetically interacting genes controlling dauer formation in Caenorhabditis elegans. *Genetics*, *137*(1), 107–120.

Gray, S. M., & Barrett, E. J. (2018). Insulin transport into the brain. *American Journal of Physiology - Cell Physiology*, *315*(2), C125–C136. https://doi.org/10.1152/ajpcell.00240.2017

Grönke, S., Clarke, D.-F., Broughton, S. J., Andrews, T. D., & Partridge, L. (2010). Molecular Evolution and Functional Characterization of Drosophila Insulin-Like Peptides. *PLoS Genetics*, *6*(2), 18. https://doi.org/10.1371/journal.pgen.1000857

Grönke, S., Müller, G., Hirsch, J., Fellert, S., Andreou, A., Haase, T., … Kühnlein, R. P. (2007). Dual lipolytic control of body fat storage and mobilization in Drosophila. *PLoS Biology*, *5*(6), 1248–1256. https://doi.org/10.1371/journal.pbio.0050137

Gustavsson, N., Wei, S. H., Hoang, D. N., Lao, Y., Zhang, Q., Radda, G. K., … Han, W. (2009). Synaptotagmin-7 is a principal Ca2+ sensor for Ca2+ -induced glucagon exocytosis in pancreas. *Journal of Physiology*, *587*(6), 1169–1178. https://doi.org/10.1113/jphysiol.2008.168005

Herboso, L., Oliveira, M. M., Talamillo, A., Pérez, C., González, M., Martín, D., … Barrio, R. (2015). Ecdysone promotes growth of imaginal discs through the regulation of Thor in D. melanogaster. *Scientific Reports*, *5*(June), 1–14. https://doi.org/10.1038/srep12383

Holmbeck, M. a., & Rand, D. M. (2015). Dietary Fatty Acids and Temperature Modulate Mitochondrial Function and Longevity in Drosophila. *The Journals of Gerontology Series A: Biological Sciences and Medical Sciences*, (16), 1–12. https://doi.org/10.1093/gerona/glv044

Honegger, B., Galic, M., Köhler, K., Wittwer, F., Brogiolo, W., Hafen, E., & Stocker, H. (2008). Imp-L2, a putative homolog of vertebrate IGF-binding protein 7, counteracts insulin signaling in Drosophila and is essential for starvation resistance. *Journal of Biology*, *7*(3). https://doi.org/10.1186/jbiol72

Huang, J. S., Lee, T. A., & Lu, M. C. (2007). Prenatal programming of childhood overweight and obesity. *Maternal and Child Health Journal*, *11*(5), 461–473. https://doi.org/10.1007/s10995-006-0141-8

Ikeya, T., Galic, M., Belawat, P., Nairz, K., Hafen, E., & Zu, C.-. (2002). Nutrient-Dependent Expression of Insulin-like Peptides from Neuroendocrine Cells in the CNS Contributes to Growth Regulation in Drosophila, *12*(02), 1293–1300.

Johnson, W. G., & Wildman, H. E. (1983). Influence of external and covert food stimuli on insulin secretion in obese and normal persons. *Behavioral Neuroscience*, *97*(6), 1025–1028. https://doi.org/10.1037/0735-7044.97.6.1025

Jülicher, F., & Eaton, S. (2016). Emergence of tissue shape changes from collective cell behaviours. *Seminars in Cell and Developmental Biology*. https://doi.org/10.1016/j.semcdb.2017.04.004

Kakanj, P., Moussian, B., Grönke, S., Bustos, V., Eming, S. A., Partridge, L., & Leptin, M. (2016). Insulin and TOR signal in parallel through FOXO and S6K to promote epithelial wound healing. *Nature Communications*, *7*, 12972. https://doi.org/10.1038/ncomms12972

Karsenty, G., & Olson, E. N. (2016). Bone and Muscle Endocrine Functions: Unexpected Paradigms of Inter-organ Communication. *Cell*, *164*(6), 1248–1256. https://doi.org/10.1016/j.cell.2016.02.043

Kaplan, M., Kauli, R., Lubin, E., Grunebaum, M., & Laron, Z. (1978). Ectopic thyroid gland: a clinical study of 30 children and review. *The Journal of pediatrics*, *92*(2), 205-209.

Kelly, L. E., & Suzuki, D. T. (1974). The effects of increased temperature on electroretinograms of temperature-sensitive paralysis mutants of Drosophila melanogaster. *Proceedings of the National Academy of Sciences of the United States of America*, *71*(12), 4906–4909. https://doi.org/10.1073/pnas.71.12.4906

Kim, J., & Neufeld, T. P. (2015). Dietary sugar promotes systemic TOR activation in Drosophila through AKH-dependent selective secretion of Dilp3. *Nat Commun*, *6*, 6846. https://doi.org/10.1038/ncomms7846

Koenig, J. H., & Ikeda, K. (1996). Synaptic vesicles have two distinct recycling pathways. *Journal of Cell Biology*, *135*(3), 797–808.

https://doi.org/10.1083/jcb.135.3.797

Koyama, T., & Mirth, C. K. (2018). Unravelling the diversity of mechanisms through which nutrition regulates body size in insects. *Current Opinion in Insect Science*, *25*, 1–8. https://doi.org/10.1016/j.cois.2017.11.002

Koyama, T., Rodrigues, M. A., Athanasiadis, A., Shingleton, A. W., & Mirth, C. K. (2014). Nutritional control of body size through FoxO-Ultraspiracle mediated ecdysone biosynthesis. *ELife*, *3*, 1–20. https://doi.org/10.7554/eLife.03091

Krämer, H. (2002). Sorting out signals in fly endosomes. *Traffic*, *3*(2), 87–91. https://doi.org/10.1034/j.1600-0854.2002.030201.x

Lang, J. (1999). Molecular mechanisms and regulation of insulin exocytosis as a paradigm of endocrine secretion. *European Journal of Biochemistry*, *259*(1–2), 3–17. https://doi.org/10.1046/j.1432-1327.1999.00043.x

Layalle, S., Arquier, N., & Léopold, P. (2008). The TOR Pathway Couples Nutrition and Developmental Timing in Drosophila. *Developmental Cell*, *15*(4), 568–577. https://doi.org/10.1016/j.devcel.2008.08.003

Lee, G. J., Han, G., Yun, H. M., Lim, J. J., Noh, S., Lee, J., & Hyun, S. (2018). Steroid signaling mediates nutritional regulation of juvenile body growth via IGF-binding protein in Drosophila. *Proceedings of the National Academy of Sciences of the United States of America*, *115*(23), 5992–5997. https://doi.org/10.1073/pnas.1718834115

Lee, G., & Park, J. H. (2004). Hemolymph sugar homeostasis and starvation-induced hyperactivity affected by genetic manipulations of the adipokinetic hormone-encoding gene in Drosophila melanogaster. *Genetics*, *167*(1), 311–323. https://doi.org/10.1534/genetics.167.1.311

Lee, W. L., & Klip, A. (2016). Endothelial transcytosis of insulin: Does it contribute to insulin resistance? *Physiology*, *31*(5), 336–345. https://doi.org/10.1152/physiol.00010.2016

Liu, S., Alexander, R. K., & Lee, C. H. (2014). Lipid metabolites as metabolic messengers in inter-organ communication. *Trends in Endocrinology and Metabolism*, *25*(7), 356–363. https://doi.org/10.1016/j.tem.2014.05.002

Loeken, M. R. (2005). Current perspectives on the causes of neural tube defects resulting from diabetic pregnancy. *American Journal of Medical Genetics - Seminars in Medical Genetics*, *135 C*(1), 77–87. https://doi.org/10.1002/ajmg.c.30056

Malone, E. A., & Thomas, J. H. (1994). A screen for nonconditional dauer-constitutive mutations in Caenorhabditis elegans. *Genetics*, *136*(3), 879–886.

McBrayer, Z., Ono, H., Shimell, M. J., Parvy, J. P., Beckstead, R. B., Warren, J. T., … O'Connor, M. B. (2007). Prothoracicotropic Hormone Regulates Developmental

Timing and Body Size in Drosophila. *Developmental Cell*, *13*(6), 857–871. https://doi.org/10.1016/j.devcel.2007.11.003

McDonald, J. M. C., Ghosh, S. M., Gascoigne, S. J. L., & Shingleton, A. W. (2018). Plasticity Through Canalization: The Contrasting Effect of Temperature on Trait Size and Growth in Drosophila. *Frontiers in Cell and Developmental Biology*, *6*(November), 1–7. https://doi.org/10.3389/fcell.2018.00156

Mirth, C. K., & Riddiford, L. M. (2007). Size assessment and growth control: How adult size is determined in insects. *BioEssays*, *29*(4), 344–355. https://doi.org/10.1002/bies.20552

Mirth, C. K., & Shingleton, A. W. (2012). Integrating body and organ size in Drosophila: Recent advances and outstanding problems. *Frontiers in Endocrinology*, *3*(APR), 1–13. https://doi.org/10.3389/fendo.2012.00049

Mirth, C. K., Tang, H. Y., Makohon-Moore, S. C., Salhadar, S., Gokhale, R. H., Warner, R. D., … Shingleton, A. W. (2014). Juvenile hormone regulates body size and perturbs insulin signaling in Drosophila. *Proceedings of the National Academy of Sciences of the United States of America*, *111*(19), 7018–7023. https://doi.org/10.1073/pnas.1313058111

Mirth, C., Truman, J. W., & Riddiford, L. M. (2005). The Role of the Prothoracic Gland in Determining Critical Weight for Metamorphosis in Drosophila melanogaster, *15*, 1796–1807. https://doi.org/10.1016/j.cub.2005.09.017

Moeller, M. E., Nagy, S., Gerlach, S. U., Soegaard, K. C., Danielsen, E. T., Texada, M. J., & Rewitz, K. F. (2017). Report Warts Signaling Controls Organ and Body Growth through Regulation of Ecdysone. *Current Biology*, 1–8. https://doi.org/10.1016/j.cub.2017.04.048

Moore, T. R. (2010). Fetal exposure to gestational diabetes contributes to subsequent adult metabolic syndrome. *American Journal of Obstetrics and Gynecology*, *202*(6), 643–649. https://doi.org/10.1016/j.ajog.2010.02.059

Nijhout, H. F. (2015). Big or fast: Two strategies in the developmental control of body size. *BMC Biology*, *13*(1), 1–4. https://doi.org/10.1186/s12915-015-0173-x

Oh, Y., Lai, J. S.-Y., Mills, H. J., Erdjument-Bromage, H., Giammarinaro, B., Saadipour, K., … Suh, G. S. B. (2019). A glucose-sensing neuron pair regulates insulin and glucagon in Drosophila. *Nature*, *574*(7779), 559–564. https://doi.org/10.1038/s41586-019-1675-4

Okamoto, N., & Nishimura, T. (2015a). Signaling from Glia and Cholinergic Neurons Controls Nutrient-Dependent Production of an Insulin-like Peptide for Drosophila Body Growth. *Developmental Cell*, *35*(3), 295–310. https://doi.org/10.1016/j.devcel.2015.10.003

Okamoto, N., & Nishimura, T. (2015b). Signaling from Glia and Cholinergic Neurons Controls Nutrient-Dependent Production of an Insulin-like Peptide for

Drosophila Body Growth. *Developmental Cell*, *35*(3), 295–310. https://doi.org/10.1016/j.devcel.2015.10.003

Okamoto, N., & Yamanaka, N. (2015). Nutrition-dependent control of insect development by insulin-like peptides. *Current Opinion in Insect Science*, *11*, 21–30. https://doi.org/10.1016/j.cois.2015.08.001

Okamoto, N., & Yamanaka, N. (2020). Steroid Hormone Entry into the Brain Requires a Membrane Transporter in Drosophila Report Steroid Hormone Entry into the Brain Requires a Membrane Transporter in Drosophila. *Current Biology*, 1–8. https://doi.org/10.1016/j.cub.2019.11.085

Osterbur, D. L., Fristrom, D. K., Natzle, J. E., Tojo, S. J., & Fristrom, J. W. (1988). Genes expressed during imaginal discs morphogenesis: IMP-L2, a gene expressed during imaginal disc and imaginal histoblast morphogenesis. *Developmental Biology*, *129*(2), 439–448. https://doi.org/10.1016/0012-1606(88)90391-0

Parvy, J. P., Wang, P., Garrido, D., Maria, A., Blais, C., Poidevin, M., & Montagne, J. (2014). Forward and feedback regulation of cyclic steroid production in drosophila melanogaster. *Development (Cambridge)*, *141*(20), 3955–3965. https://doi.org/10.1242/dev.102020

Petryk, A., Warren, J. T., Marqués, G., Jarcho, M. P., Gilbert, L. I., Kahler, J., … O'Connor, M. B. (2003). Shade is the Drosophila P450 enzyme that mediates the hydroxylation of ecdysone to the steroid insect molting hormone 20-hydroxyecdysone. *Proceedings of the National Academy of Sciences of the United States of America*, *100*(SUPPL. 2), 13773–13778. https://doi.org/10.1073/pnas.2336088100

Post, S., Karashchuk, G., Wade, J. D., Sajid, W., De Meyts, P., & Tatar, M. (2018). Drosophila insulin-like peptides DILP2 and DILP5 differentially stimulate cell signaling and glycogen phosphorylase to regulate longevity. *Frontiers in Endocrinology*, *9*(MAY), 1–16. https://doi.org/10.3389/fendo.2018.00245

Puig, O., Marr, M. T. M., Ruhf, M. L., & Tjian, R. (2003a). Control of cell number by Drosophila FOXO : downstream and feedback regulation of the insulin receptor pathway. *Genes & Development*, *17*(16), 2006–2020. https://doi.org/10.1101/gad.1098703.messengers

Puig, O., Marr, M. T., Ruhf, M. L., & Tjian, R. (2003b). Control of cell number by Drosophila FOXO: Downstream and feedback regulation of the insulin receptor pathway. *Genes and Development*, *17*(16), 2006–2020. https://doi.org/10.1101/gad.1098703

Ramaswami, M., Krishnan, K. S., & Kelly, R. B. (1994). Intermediates in synaptic vesicle recycling revealed by optical imaging of Drosophila neuromuscular junctions. *Neuron*, *13*, 363–375. https://doi.org/10.1016/0896-6273(94)90353-

o

Rao, S., Lang, C., Levitan, E. S., & Deitcher, D. L. (2001). Fast track: Visualization of neuropeptide expression, transport, and exocytosis in Drosophila melanogaster. *Journal of Neurobiology*, *49*(3), 159–172. https://doi.org/10.1002/neu.1072

Roed, N. K., Viola, C. M., Kristensen, O., Schluckebier, G., Norrman, M., Sajid, W., … Brzozowski, A. M. (2018). Structures of insect Imp-L2 suggest an alternative strategy for regulating the bioavailability of insulin-like hormones. *Nature Communications*, *9*(1). https://doi.org/10.1038/s41467-018-06192-3

Rosenbloom, A. L., Grgic, A., & Frias, J. L. (1974). Diabetes mellitus, short stature and joint stiffness—a new syndrome. *Pediatric Research*, *8*(4), 441-441.

Rulifson, E. J. (2002). Ablation of Insulin-Producing Neurons in Flies: Growth and Diabetic Phenotypes. *Science*, *296*(5570), 1118–1120. https://doi.org/10.1126/science.1070058

Sagner, A., Merkel, M., Aigouy, B., Gaebel, J., Brankatschk, M., Jülicher, F., & Eaton, S. (2012). Establishment of global patterns of planar polarity during growth of the drosophila wing epithelium. *Current Biology*, *22*(14), 1296–1301. https://doi.org/10.1016/j.cub.2012.04.066

Saltiel, A. R., & Kahn, C. R. (2001). Glucose and Lipid Metabolism, *414*(December), 799–806.

Scanga, S. E., Ruel, L., Binari, R. C., Snow, B., Stambolic, V., Bouchard, D., … Manoukian, a S. (2000). The conserved PI3'K/PTEN/Akt signaling pathway regulates both cell size and survival in Drosophila. *Oncogene*, *19*, 3971–3977. https://doi.org/10.1038/sj.onc.1203739

Scharrer, A. (1967). Peptidergic Neurons :

Schindelin, J., Arganda-Carreras, I., Frise, E., Kaynig, V., Longair, M., Pietzsch, T., … Cardona, A. (2012). Fiji: An open-source platform for biological-image analysis. *Nature Methods*, *9*(7), 676–682. https://doi.org/10.1038/nmeth.2019

Shingleton, A. W., Das, J., Vinicius, L., & Stern, D. L. (2005). The Temporal Requirements for Insulin Signaling During Development in Drosophila, *3*(9). https://doi.org/10.1371/journal.pbio.0030289

Siegmund, T., & Korge, G. (2001). Innervation of the ring gland of drosophila melanogaster. *Journal of Comparative Neurology*, *431*(4), 481–491. https://doi.org/10.1002/1096-9861(20010319)431:4<481::AID-CNE1084>3.0.CO;2-7

Sorkin, A., & Von Zastrow, M. (2002). Signal transduction and endocytosis: Close encounters of many kinds. *Nature Reviews Molecular Cell Biology*, *3*(8), 600–614. https://doi.org/10.1038/nrm883

Sorkin, A., & Von Zastrow, M. (2009). Endocytosis and signalling: Intertwining

molecular networks. *Nature Reviews Molecular Cell Biology*, *10*(9), 609–622. https://doi.org/10.1038/nrm2748

Stieper, B. C., Kupershtok, M., Driscoll, M. V., & Shingleton, A. W. (2008). Imaginal discs regulate developmental timing in Drosophila melanogaster. *Developmental Biology*, *321*(1), 18–26. https://doi.org/10.1016/j.ydbio.2008.05.556

Storlien, L. H., Pan, D. A., Kriketos, A. D., O'Connor, J., Caterson, I. D., Cooney, G. J., … Baur, L. A. (1996). Skeletal muscle membrane lipids and insulin resistance. *Lipids*, *31*(1), S261–S265. https://doi.org/10.1007/bf02637087

Talbot, W. S., Swyryd, E. A., & Hogness, D. S. (1993). Drosophila tissues with different metamorphic responses to ecdysone express different ecdysone receptor isoforms. *Cell*, *73*(7), 1323–1337. https://doi.org/10.1016/0092-8674(93)90359-X

Taniguchi, C. M., Emanuelli, B., & Kahn, C. R. (2006). Critical nodes in signalling pathways: Insights into insulin action. *Nature Reviews Molecular Cell Biology*, *7*(2), 85–96. https://doi.org/10.1038/nrm1837

Texada, M. J., Malita, A., & Rewitz, K. (2019). Autophagy regulates steroid production by mediating cholesterol trafficking in endocrine cells. *Autophagy*, *15*(8), 1478–1480. https://doi.org/10.1080/15548627.2019.1617608

Thorel, F., Népote, V., Avril, I., Kohno, K., Desgraz, R., Chera, S., & Herrera, P. L. (2010). Conversion of adult pancreatic α-cells to B-cells after extreme B-cell loss. *Nature*, *464*(7292), 1149–1154. https://doi.org/10.1038/nature08894

Tschöp, M., & Thomas, G. (2006). Fat fuels insulin resistance through Toll-like receptors. *Nature Medicine*, *12*(12), 1359–1361. https://doi.org/10.1038/nm1206-1359

Van De Goor, J., Ramaswami, M., & Kelly, R. (1995). Redistribution of synaptic vesicles and their proteins in temperature-sensitive shibirets1 mutant Drosophila. *Proceedings of the National Academy of Sciences of the United States of America*, *92*(12), 5739–5743. https://doi.org/10.1073/pnas.92.12.5739

Van Der Bliek, A. M., & Meyerowrtz, E. M. (1991). Dynamin-like protein encoded by the Drosophila shibire gene associated with vesicular traffic. *Nature*, *351*(6325), 411–414. https://doi.org/10.1038/351411a0

Von Bartheld, C. S. (2004). Axonal Transport and Neuronal Transcytosis of Trophic Factors, Tracers, and Pathogens. *Journal of Neurobiology*, *58*(2), 295–314. https://doi.org/10.1002/neu.10315

Vroemen, S. F., Van Marrewijk, W. J. A., Schepers, C. C. J., & Van Der Horst, D. J. (1995). signal transduction of adipokinetic hormones involves Ca2+ fluxes and depends on extracellular Ca2+ to potentiate cAMP-induced activation of glycogen phosphorylase. *Cell Calcium*, *17*(6), 459–467. https://doi.org/10.1016/0143-4160(95)90092-6

Walkiewicz, M. A., & Stern, M. (2009). Increased insulin/insulin growth factor signaling advances the onset of metamorphosis in Drosophila. *PLoS ONE*, *4*(4). https://doi.org/10.1371/journal.pone.0005072

Wang, S., Tulina, N., Carlin, D. L., & Rulifson, E. J. (2007). The origin of islet-like cells in Drosophila identifies parallels to the vertebrate endocrine axis. *Proceedings of the National Academy of Sciences of the United States of America*, *104*(50), 19873–19878. https://doi.org/10.1073/pnas.0707465104

Westgaard, R. H. (1917). Exocytosis-Endocytosis Coupling in the Pancreatic Beta Cell curs concomitantly , and consequently Predator-Prey Interactions in Continuous Culture, (3), 561–562.

Weinstein, I., Klausner, H. A., & Heimberg, M. (1973). The effect of concentration of glucagon on output of triglyceride, ketone bodies, glucose, and urea by the liver. *Biochimica et Biophysica Acta (BBA)-Lipids and Lipid Metabolism*, *296*(2), 300-309.

Yamada, T., Habara, O., Kubo, H., & Nishimura, T. (2018). Fat body glycogen serves as a metabolic safeguard for the maintenance of sugar levels in *Drosophila*. *Development*, *145*(6), dev158865. https://doi.org/10.1242/dev.158865

Yamanaka, N., Rewitz, K. F., & O'Connor, M. B. (2013). Ecdysone Control of Developmental Transitions: Lessons from *Drosophila* Research. *Annual Review of Entomology*, *58*(1), 497–516. https://doi.org/10.1146/annurev-ento-120811-153608

Yazdani, S., Jaldin-Fincati, J. R., Pereira, R. V., & Klip, A. (2019). Endothelial cell barriers: Transport of molecules between blood and tissues. *Traffic*, *20*(6), 390-403.

Yuan, D., Zhou, S., Liu, S., Li, K., Zhao, H., Long, S., & Liu, H. (2020). The AMPK-PP2A axis in insect fat body is activated by 20-hydroxyecdysone to antagonize insulin / IGF signaling and restrict growth rate. https://doi.org/10.1073/pnas.2000963117

Ziegler, R., Jasensky, R. D., & Morimoto, H. (1995). Characterization of the adipokinetic hormone receptor from the fat body of Manduca sexta. *Regulatory Peptides*, *57*(3), 329–338. https://doi.org/10.1016/0167-0115(95)00046-E

Zitnan, D., Sehnal, F., & Bryant, P. J. (1993). Neurons producing specific neuropeptides in the central nervous system of normal and pupariation-delayed Drosophila. *Developmental Biology*. https://doi.org/10.1006/dbio.1993.1063

Zito, K., Parnas, D., Fetter, R. D., Isacoff, E. Y., & Goodman, C. S. (1999). Watching a synapse grow: Noninvasive confocal imaging of synaptic growth in Drosophila. *Neuron*, *22*(4), 719–729. https://doi.org/10.1016/S0896-6273(00)80731-X